U.S. Department of the Interior
U.S. Geological Survey

U.S. ENVIRONMENTAL PROTECTION AGENCY REGION 1
WASTE MANAGEMENT DIVISION

Construction and Calibration of Numerical Ground-Water-Flow Models of the Western Half of the Milford-Souhegan Glacial-Drift Aquifer, Milford, New Hampshire

By Philip T. Harte, Robert H. Flynn, *and* Thomas J. Mack

Open-File Report 99-462

Pembroke, New Hampshire
1999

U.S. DEPARTMENT OF THE INTERIOR
BRUCE BABBITT, Secretary

U.S. GEOLOGICAL SURVEY
Charles G. Groat, Director

For additional information write to:

District Chief
U.S. Geological Survey
New Hampshire/Vermont District
361 Commerce Way
Pembroke, NH 03275-3718

or through our website at
http://nh.water.usgs.gov

Copies of this report can be purchased from:

U.S. Geological Survey
Information Services
Box 25286
Federal Center
Denver, CO 80225

CONTENTS

PLATES

FIGURES

TABLES

CONVERSION FACTORS, VERTICAL DATUM, AND ABBREVIATIONS

Multiply	By	To obtain
inch (in.)	25.4	millimeter
foot (ft)	0.3048	meter
mile (mi)	1.609	kilometer
square mile (mi^2)	2.590	square kilometer
cubic foot (ft^3)	0.02832	cubic meter
gallon (gal)	3.785	liter
million gallons (Mgal)	3.785	cubic meter
inch per month (in/m)	25.4	millimeter per month
inch per year (in/yr)	25.4	millimeter per year
foot per mile (ft/mi)	0.3048	meter per mile
cubic foot per second (ft^3/s)	0.02832	cubic meter per second
cubic foot per second per square mile [$(ft^3/s)/mi^2$)]	0.01093	cubic meter per second per square kilometer
gallon per minute (gal/min)	0.06308	liter per second
million gallons per day (Mgal/d)	0.04381	cubic meter per second
million gallons per day (Mgal/d)	1.547	cubic foot per second
foot per day (ft/d)	0.3048	meter per day
square foot per second (ft^2/s)	0.0929	square meter per second
square foot per day (ft^2/day)	0.09290	square meter per day

Vertical Datum: In this report "sea level" refers to the National Geodetic Vertical Datum of 1929 (NGVD of 1929)—a geodetic datum derived from a general adjustment of the first-order level nets of both the United States and Canada, formerly called Sea Level Datum of 1929.

ABBREVIATIONS USED IN THIS REPORT

PCE tetrachloroethylene

PVC polyvinyl chloride

ppb parts per billion

ft/ft foot per foot

Construction and Calibration of Numerical Ground-Water-Flow Models of the Western Half of the Milford-Souhegan Glacial-Drift Aquifer, Milford, New Hampshire

By Philip T. Harte, Robert H. Flynn, *and* Thomas J. Mack

Abstract

The Milford-Souhegan glacial-drift (MSGD) aquifer, in southcentral New Hampshire, is an important source of water for industrial, commercial, and domestic use that provides more than 2.7 million gallons of water per day in 1994. A large plume of volatile-organic compounds (approximately 0.5 square miles in area) covers a large part of the western half of the MSGD aquifer and threatens existing ground-water usage. The plume area has been designated a superfund site and named after a former municipal water-supply well (Savage Well) that was discontinued because of contamination.

A 3-year study by the U.S. Geological Survey and the U.S. Environmental Protection Agency began in January 1994 to examine the temporal variability of ground-water flow in the contaminant plume and adjacent areas of the western half of the MSGD aquifer. This report summarizes construction and evaluation of three-dimensional, steady state and transient numerical ground-water-flow models that will be used to help design a remediation plan for containing volatile organic contaminants.

The results of the steady-state simulation of average-flow conditions from June 1994 to June 1995 show a close comparison between model-computed heads and observed heads at more than 70 wells. Most heads are within 1.5 feet of observed heads. The standard-mean-head error is -0.12 feet, indicating that computed heads are slightly lower than observed heads. The absolute-mean-head error is 0.59 feet, and the root-mean-square error is 0.89 feet.

The results of the transient model of seasonal-flow conditions also show a close comparison between computed-head fluctuations and observed-head fluctuations for the same wells. The largest difference in computed and observed heads occurs for the fall of 1994 (standard-mean-head error of 0.29 feet).

Computed variations in direction and slope of maximum hydraulic gradients compare well with observed variations for most areas of the model. The analysis, however, identified several areas of the model where further testing is suggested. These areas include those (1) near the source area of contaminants, (2) in the northcentral part of the plume, and (3) at the northern leading edge of contaminants near the confluence of two rivers.

INTRODUCTION

The Milford-Souhegan glacial-drift (MSGD) aquifer, in southcentral New Hampshire (fig. 1), is an important source of water for industrial, commercial, and domestic use, providing for more than 2.7 Mgal/d in 1994. Until it was found to contain high concentrations of volatile organic compounds (VOC's) in the early 1980's, the aquifer was also an important source of drinking water. Two former municipal supply wells (the Savage and Keyes wells) were shut down in 1983 after withdrawn waters were found to contain elevated concentrations of VOC's. Subsequently, local, State, and Federal agencies initiated geohydrologic studies to characterize the glacial-drift river-valley aquifer and delineate the extent of contamination. In 1989, during an investigation of the Savage well, a large VOC plume composed primarily of tetrachloroethylene

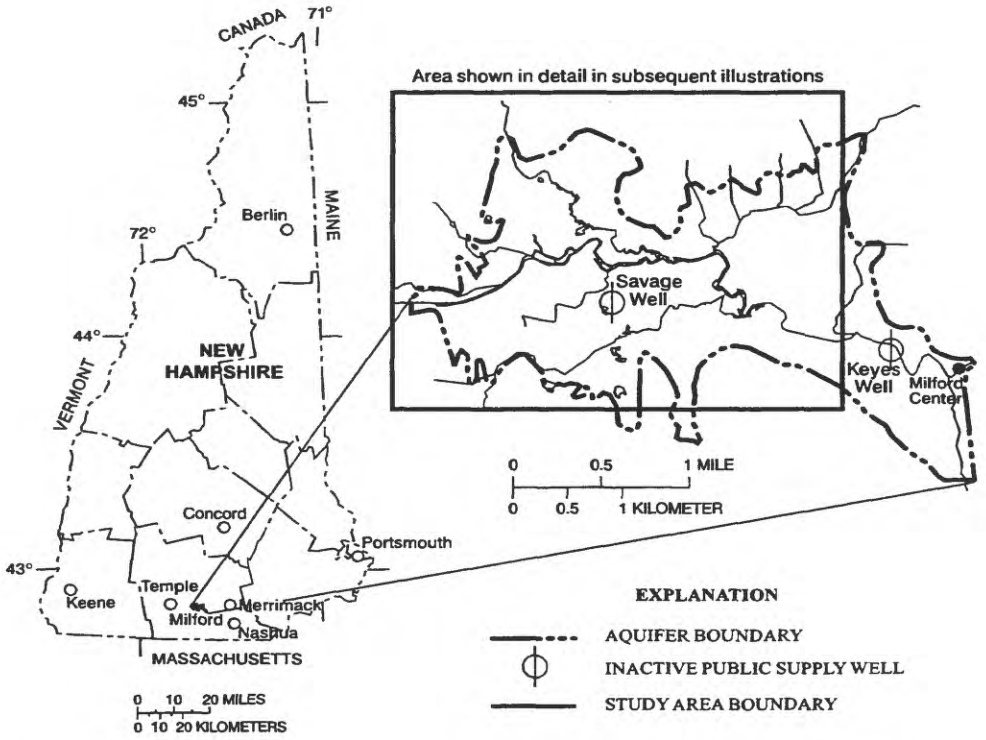

Figure 1. Location of the Milford-Souhegan glacial-drift aquifer, Milford, New Hampshire.

(PCE) was found to underlie the southwestern part of the MSGD aquifer (HMM Associates, 1989, 1991). The primary source of contamination is a former, discontinued, tool company (fig. 2) that discharged solvents into the subsurface for many years until the early 1980's. Although discharges have ceased, the underlying contaminant soaked sediments, and immiscible solvents continue to contaminate ground water flowing underneath the site. Currently (1999), this large plume continues to threaten existing ground-water usage at State and commercial fish hatcheries, and restricts the full beneficial use of this resource.

An initial study of ground-water flow in the MSGD aquifer was done in the late 1980's and early 1990's by the U.S. Geological Survey (USGS) (Harte and Mack, 1992). The focus of that study was the delineation of well capture zones to the two former municipal wells (Savage and Keyes well) under average annual conditions.

Subsequent (unpublished) work by the primary author since the initial study found that the advective transport of contaminated ground water from the primary source area under the assumption of static or long-term steady-state conditions significantly underestimated the lateral extent of contaminated ground waters. Furthermore, the primary factor contributing to the inability of the model to simulate the plume configuration was the transient variability of the aquifer, which was not addressed by Harte and Mack (1992).

A 3-year study by the USGS and the U.S. Environmental Protection Agency (USEPA) began in January 1994 to increase the understanding of transient hydrologic conditions in the aquifer. The primary objective of this study is to evaluate the effects of temporal changes in recharge, discharge, and ground-water withdrawals on contaminant flow. Specific objectives include:

1. Determine the temporal variability of ground-water-flow directions in the plume area.
2. Determine the temporal variability of surface and ground-water interactions between the Souhegan River and the glacial-drift aquifer.
3. Construct detailed numerical ground-water-flow models to use as predictive tools in remedial and monitoring well network design.
4. Identify flow paths to extraction wells by use of ground-water-flow models and supportive chemical data collected in the field.

Previous studies include analysis of effects of ground-water withdrawals on advective transport of contaminated ground waters (Harte and Willey, 1997), transient hydrological data (Harte and others, 1997), and effects of model discretization on low-pumping rate wells (Harte and Mack, 1996).

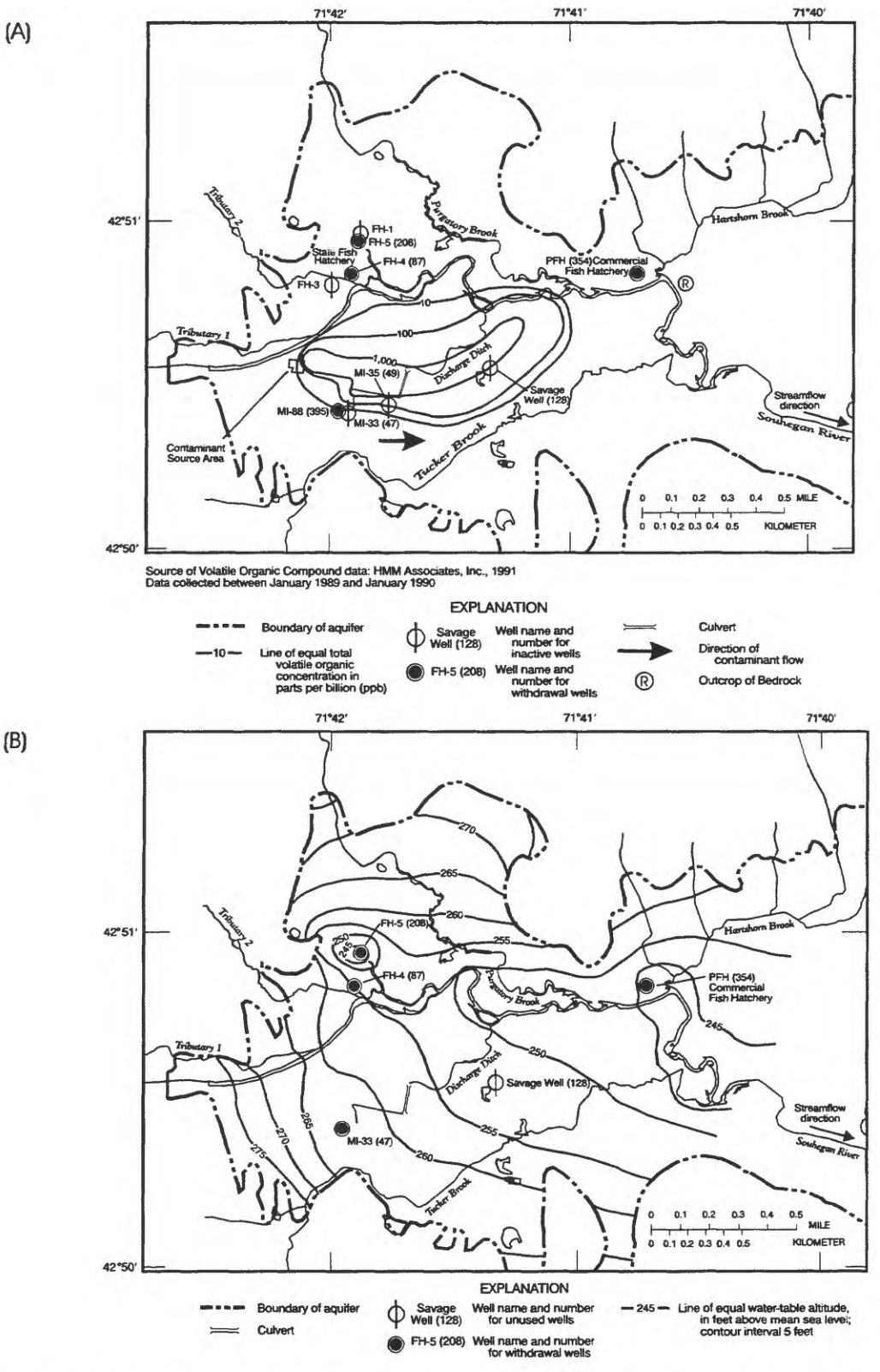

Figure 2. Extent of contaminant plume (as defined by 10 parts per billion [ppb] line of equal concentration) of total volatile organic compounds in 1989 (A), and altitude of water-table surface, in feet above mean sea level in April 1994 (B), in the Milford-Souhegan glacial-drift aquifer, Milford, New Hampshire. (Modified from Harte and others, 1997)

Purpose and Scope

This report summarizes the construction and calibration of both steady-state and transient finite-difference numerical ground-water-flow models of the western half of the Milford-Souhegan glacial-drift aquifer. Model simulations focused on simulating hydrologic stresses during 1994-95.

Model performance is evaluated by comparing ground-water levels (heads) and river seepages from data collected from April 1994 to September 1995 (Harte and others, 1997). Other data also were used to evaluate model performance including data from 1988 and 1990 (Harte and Mack, 1992; and Olimpio and Harte, 1994). A comparison also is made between advective transport of ground-water particles and the movement of contaminated ground water between 1989 and 1994.

Hydrogeologic Setting

The MSGD aquifer (fig. 1) is defined as the entire sequence of unsaturated and saturated alluvium, glacial drift, and other unconsolidated deposits above the bedrock surface in the Souhegan River valley in Milford, N.H. The aquifer consists primarily of stratified sand and gravel with some basal till, and is overlain in places by recent alluvium. The maximum saturated thickness of the aquifer exceeds 100 ft in the eastern part of the aquifer, but generally ranges from 0 to 60 ft. Laterally, the aquifer is bounded by till-covered bedrock uplands.

Two bedrock types have been identified in rock cores and include a white to pink, medium to coarse-grained granite and a gray biotite rich diorite gneiss (HMM Associates Inc., 1989, 1991). Lyons and others (1997) identifies two bedrock formations in the Milford area, the Massabesic Gneiss Complex of Late Proterozoic Age and an intrusive gray biotite granite of Permian Age. A high-angle strike-slip fault called the Camp Hill Fault traverses the area.

Till forms the basal unit of glacial drift in the MSGD and discontinuously overlies bedrock from the Massabesic-Merrimack-Rye terrane (Harte and Mack, 1992; Lyons and other, 1997). The till consists of a sandy to silty matrix.

Stratified-drift deposits represent the most transmissive units in the MSGD. Stratified drift was deposited as ice-contact materials, glacial-lake deposits, fluvial deltas, and outwash materials (Koteff, 1970). During the late stages of glaciation, a west to east drainage pattern, similar to present drainage patterns, caused coarser sediments to be deposited in the western part of the valley. Specifically, glacial drainage occurred through the channel occupied by Purgatory Brook and through the channel occupied by the Souhegan River west of the contaminant source area. These glacial drainage channels transported coarse-grained sediments into the present day Souhegan valley.

The river valley in the study area slopes gently at 12 ft/mi along the river. Land-surface elevations range from 230 to 280 ft in the study area. The land is drained by the Souhegan River and its tributaries (fig. 2), including Tucker, Purgatory, Great (not shown on map), and Hartshorn Brooks, and a number of small, unnamed streams. A discharge ditch drains processed waters from several manufacturing companies in the southwestern part of the study area.

Land use is predominantly industrial in the southwestern part of the study area, agricultural in the central and northwestern areas, and residential to commercial elsewhere. The contaminant plume (fig. 2) underlies a large agricultural area in the center of the study area (not shown on any figures) and abuts a commercial-industrial area to the south.

Current ground-water withdrawals are primarily used for commercial and industrial purposes. Withdrawal wells (table 1) include two wells for the State Fish Hatchery in the northwestern part of the study area (well numbers 87 and 208; fig. 2), a well at a private fish hatchery in the eastern part of the study area (well number 354; fig. 2), and a well for an industrial and manufacturing complex in the southwestern part of the study area (well number 395; fig. 2).

Acknowledgments

The study of the Milford-Souhegan glacial-drift aquifer is a collaborative effort between Federal, State, and local governments, and private companies and individuals. The authors wish to express thanks to Richard Goehlert and Richard Willey of the U.S. Environmental Protection Agency, Region 1, and Wayne Ives of the New Hampshire Department of Environmental Services (NHDES) for their interest. Test drilling, water-level data, well construction, and

Table 1. Ground-water withdrawals from currently used commercial and industrial water-supply wells, Milford, New Hampshire

Well name	Well number used in report (figure 2)	Depth of well, in feet below land surface	Average daily withdrawals in 1994, in millions of gallons per day	Average daily withdrawals in 1995, in millions of gallons per day
State of New Hampshire Fish Hatchery well #5	208	65	1.05	1.10
State of New Hampshire Fish Hatchery well #4	87	42	1.26	1.19
Commercial Production well MI-88	395	42	0.25	0.25
[1]Commercial Production well MI-33	47	60	0.0	0.0
Private Fish Hatchery well	354	40	0.22	0.14

[1] This well is a backup to well MI-88.

water-budget information were collected with the help of NHDES, Environmental Science and Engineering, Inc., and Camp, Dresser, and McKee, Inc., for the superfund remedial investigations and design phases of investigations. Estimates of ground-water recharge and baseflow were done with the help of Forest Lyford and Albert Rutledge of the USGS.

CONSTRUCTION OF NUMERICAL MODELS

A block-centered, finite-difference ground-water-flow model (McDonald and Harbaugh, 1988), called MODFLOW, was used to simulate steady state and transient ground-water flow in the Milford-Souhegan glacial-drift aquifer. Construction of steady-state and transient ground-water-flow models for the aquifer included compiling certain geologic and hydrologic data (from wells, field observations, and available literature) for use in the model. Aquifer properties were assigned to each cell of the model and represent an integrated value over the cell area. In addition to aquifer properties, riverbed conductance, river stage, recharge from precipitation and lateral inflow, and discharge from ground-water withdrawals were also included at appropriate cells.

Steady-state and transient-seasonal models of flow were constructed to simulate 1994 and 1995 hydrologic conditions on the basis of ground-water level and river-leakage field data available for this period. This period was considered acceptable for steady-state simulations of average annual conditions because precipitation during 1994-95 approximated the long-term average precipitation (Harte and others, 1997) and changes in net ground-water storage in the aquifer were negligible. Starting and ending water levels for the period were within 0.27 ft, or less than 4 percent of historical fluctuations at long-term observation well MOW-36 (located in the southwest part of the aquifer), also called MI-18 (Coakley and others, 1997). This period is also considered acceptable for transient-seasonal simulations because fluctuations in ground-water levels exceeded 5 ft in parts of the aquifer because of seasonal changes in recharge, withdrawals, and river stage (Harte and others, 1997, table 7).

A list of computer-model files for the steady-state and transient-seasonal models are provided in appendix 1. Also listed are model files for the transient-historical model by Harte and Willey (1997). Model files are archived at the USGS office in Pembroke, N.H. and are available upon request. Model-input files require about 8 megabytes (MB) of storage. Model-output files require considerably more space if cell-by-cell flows are stored.

Grid Design

The model area is 1.65 mi^2 and includes 165,375 model cells. The number of active model cells is 70,517 cells and they are limited to the lateral extent and thickness of the MSGD aquifer (fig. 3).

Model orientation is aligned with the primary longitudinal axis of the contaminant plume (figs. 2 and 3) in a slightly southwest to northeast trend. It is

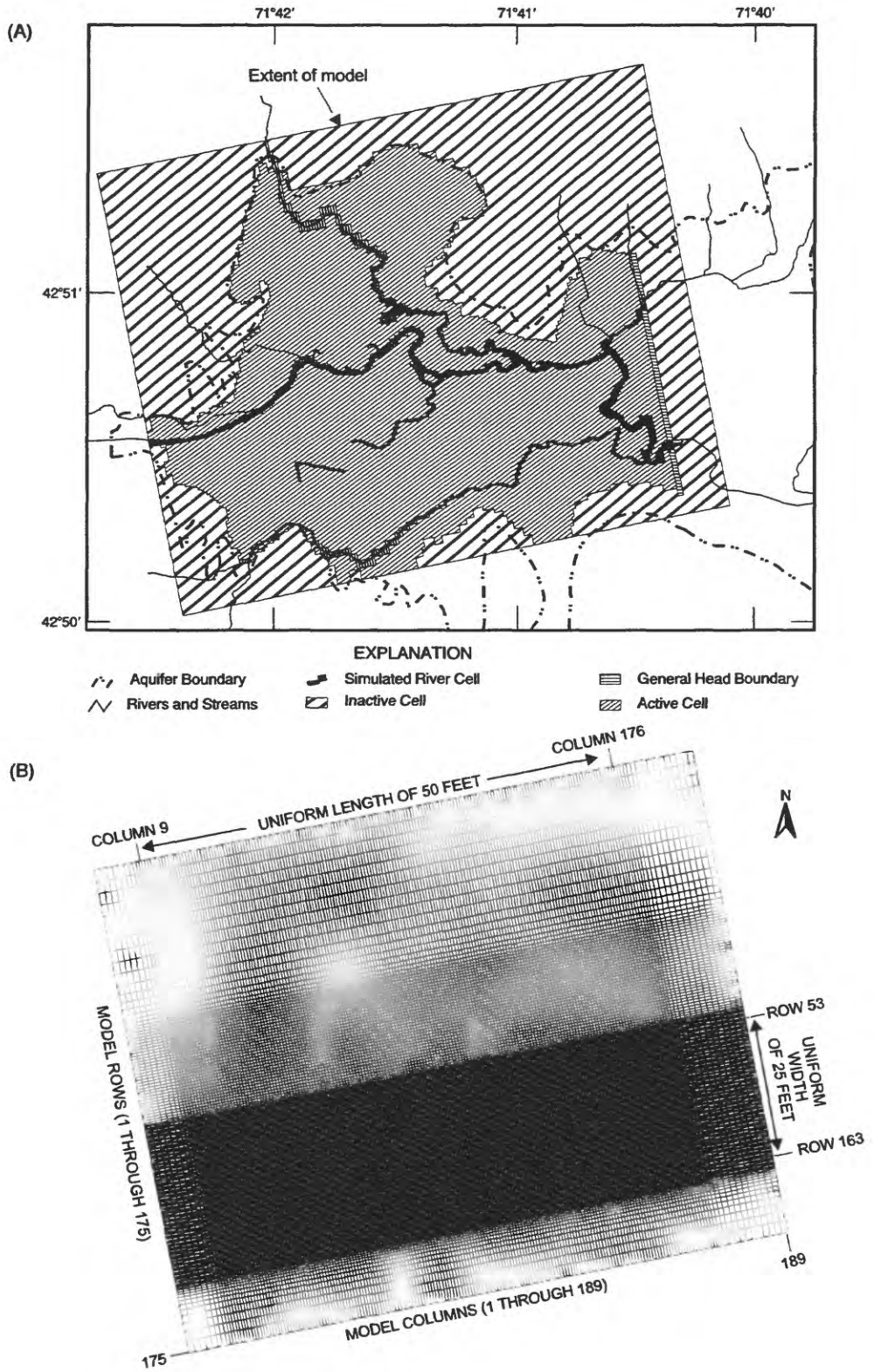

Figure 3. Areas of inactive and active grid cells, simulated river cells, and location of general-head boundary (A), and grid cells (B), for model of the Milford-Souhegan glacial-drift aquifer, Milford, New Hampshire.

assumed that the longitudinal axis of the contaminant plume approximates the orientation of the average ground-water flow direction over the life of the plume. Orienting the model with the longitudinal axis of the plume will help reduce inaccuracies associated with the finite-difference solution of the ground-water-flow equation caused by not aligning the grid with the principal axis of the hydraulic conductivity tensor. Otherwise, the finite-difference-flow equation would need to include cross product terms if anisotropy is specified in the model (Trescott and others, 1976).

Horizontal cell sizes range from 50 by 25 ft to 100 by 200 ft. Cell size in the x-direction across model columns (southwest to northeast) range from 50 to 100 ft. Cell size in the y-direction across model rows (northwest to southeast) range from 25 to 200 ft. Smallest cell sizes occur in the area of the contaminant plume, to allow for simulation of low pumping rate withdrawal wells without problems associated with weak sinks (Harte and Mack, 1996).

The model is vertically discretized into 5 layers, each 5 to 25 ft thick, following procedures similar to Harte and Mack (1992), with one important exception. Unlike, vertical discretization in previous models of the MSGD aquifer that used the land surface as the uppermost surface for the starting point of vertical discretization (Harte and Mack, 1992, fig. 14), a pre-stressed simulation of the water-table surface, which was computed from a model of the MSGD described by Olimpio and Harte (1994), was used as the starting surface in this study. The use of the water-table surface as the uppermost surface produces a smoother delineation of model layers than that produced with the land surface as a starting surface. As in the original model described by Harte and Mack (1992), the lowermost boundary is the bedrock surface.

There are 33,075 cells (175 rows and 189 columns) per model layer. The number of active cells decreases with depth from 24,641 cells in layer 1 to 2,027 cells in layer 5 because the lateral extent of the MSGD aquifer with depth below the water-table surface decreases. The percent of active cells per total number of cells per model layer (33,075) is 75 percent for layer 1, 68 percent for layer 2, 46 percent for layer 3, 20 percent for layer 4, 6 percent for layer 5.

The distribution of the active model cells can be used as a guide to the saturated thickness of the MSGD aquifer. For example, layer 5 active cells denote areas where the saturated thickness of the MSGD exceeds 80 ft, layer 4 active cells denote areas where the saturated thickness exceeds 60 ft, and so on.

Time Discretization

The division of time (called time discretization) is an important consideration in simulating steady-state and transient models. Steady-state-model simulations represent a single view of hydrologic conditions that are representative of average conditions over some predetermined period in time. During this period, storage changes are considered negligible and aquifer stresses and boundaries can be averaged into constant values of recharge, ground-water withdrawals, and river stage, respectively. Transient simulations represent multiple views of hydrologic conditions that represent various hydrologic conditions over some period in time. The number of views correspond to the frequency of time discretization. Transient simulations allow for changes in storage and specification of varying aquifer stresses and river stage between each discretized time. In this report, the steady-state simulation represents a single view of average annual hydrologic conditions during June 1994 to June 1995. The transient simulation presented in this report, referred to as the transient-seasonal simulation, represents a series of 26 views (or time steps) for the same period as the steady-state simulation and simulates changes of hydrologic conditions over that period in a discretized step-like process. In the transient-seasonal model, aquifer stresses and river stages were specified monthly. Therefore, stresses are constant for a month and are referred to as monthly stress periods. Two constant interval time steps (each 15-day in length) are used for each stress period, except during September 1994, which had two stress periods to simulate abrupt river stage changes.

Hydraulic Conductivity

Hydraulic conductivity is specified for all five model layers because the model is constructed to allow for dewatering of model cells, which requires data on both hydraulic conductivity and model-layer thicknesses (figs. 4-8). Horizontal hydraulic conductivity is differentiated into three to seven zones per model layer. Within each zone, horizontal hydraulic conductivity is considered to be homogeneous and isotropic. Vertically, the model is isotropic and heterogeneous between layers 1 and 2, and anisotropic and heterogeneous between layers 2 through 5. Therefore, no vertical anisotropy is specified between layers 1

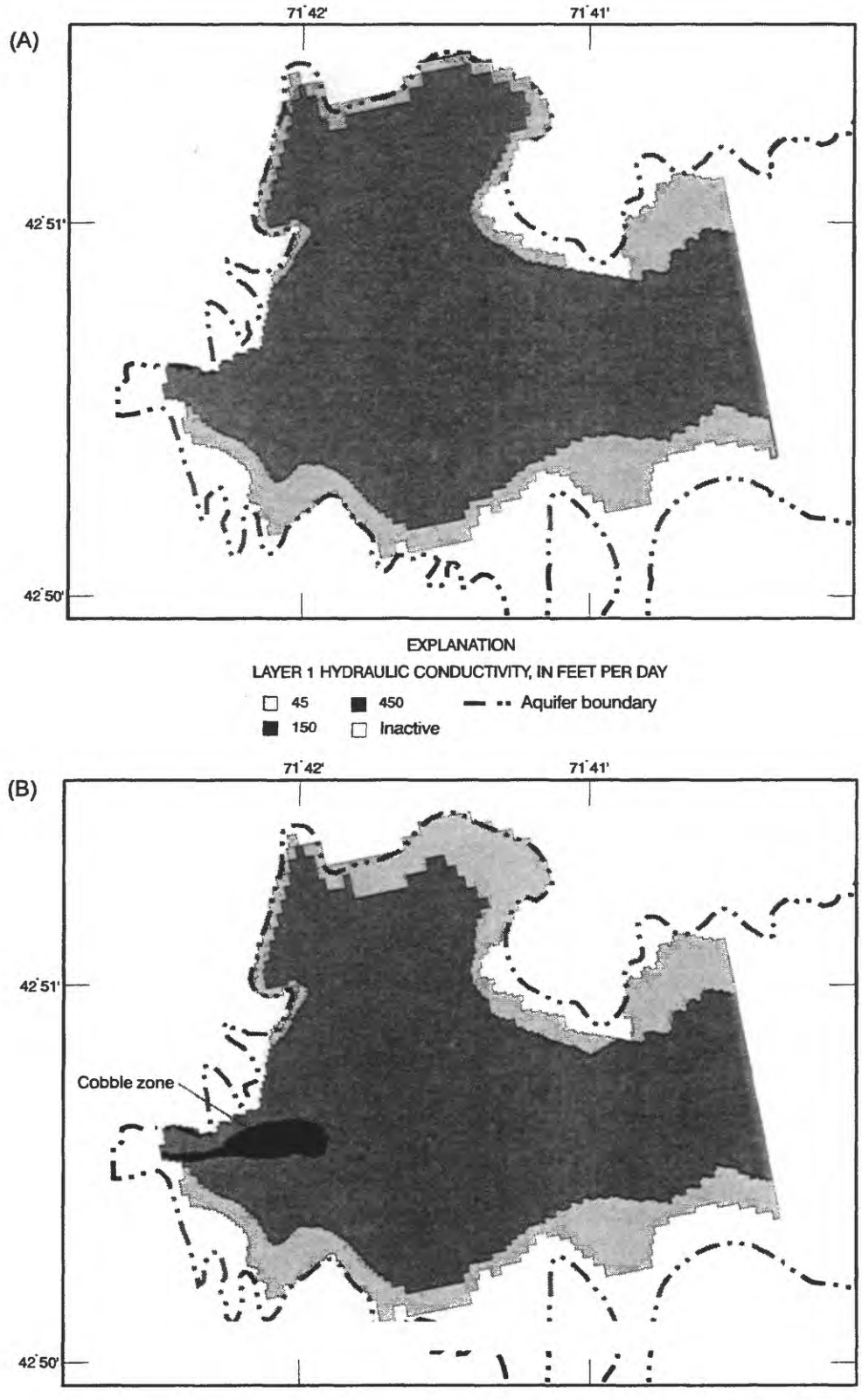

Figure 4. Initial input of active areas and horizontal hydraulic conductivity zones for model layer one (A), and final input for layer one (B), for Milford-Souhegan glacial-drift aquifer, Milford, New Hampshire.

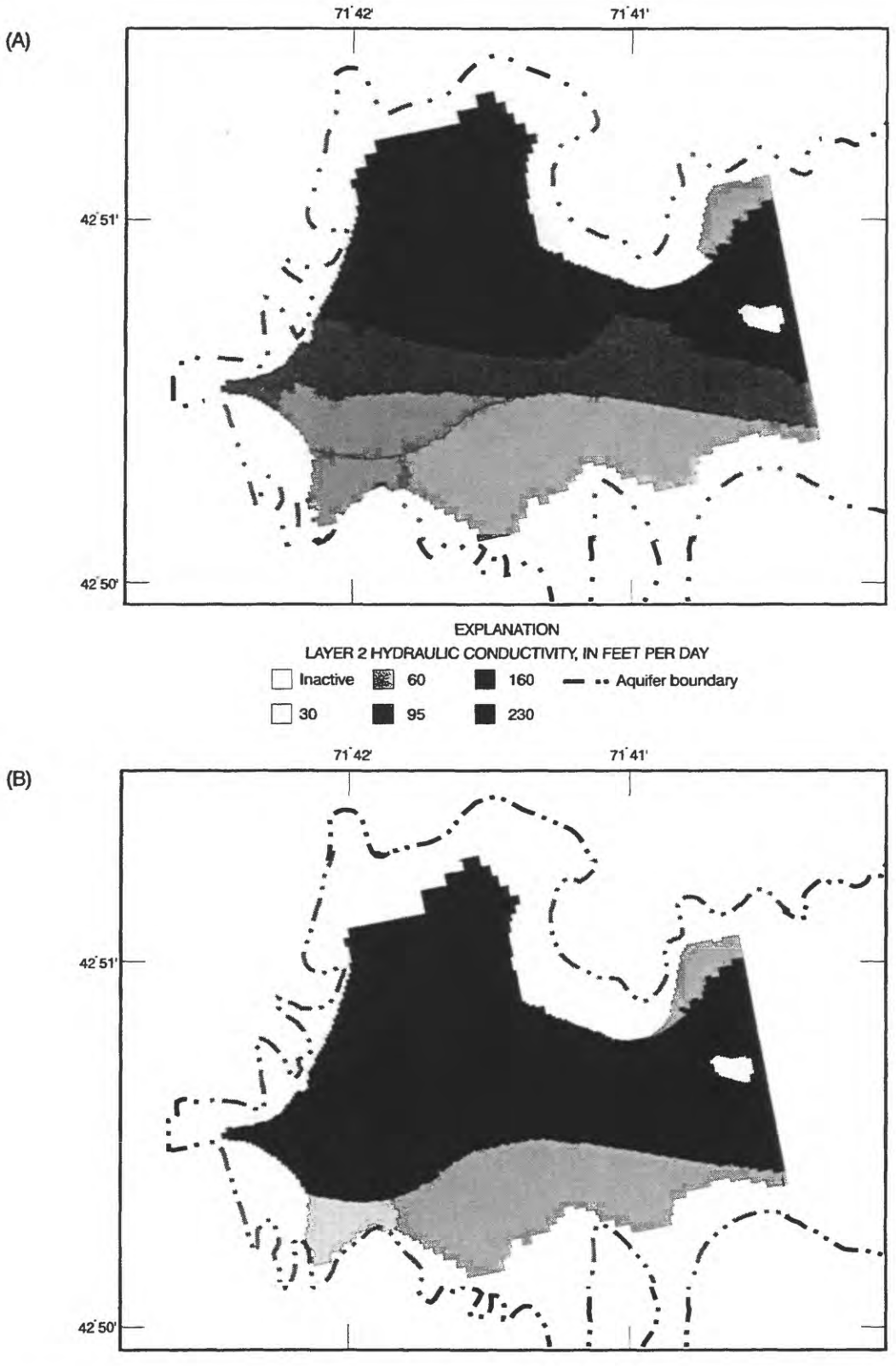

Figure 5. Initial input of active areas and horizontal hydraulic conductivity zones for model layer two (A), and final input for layer two (B), for Milford-Souhegan glacial-drift aquifer, Milford, New Hampshire.

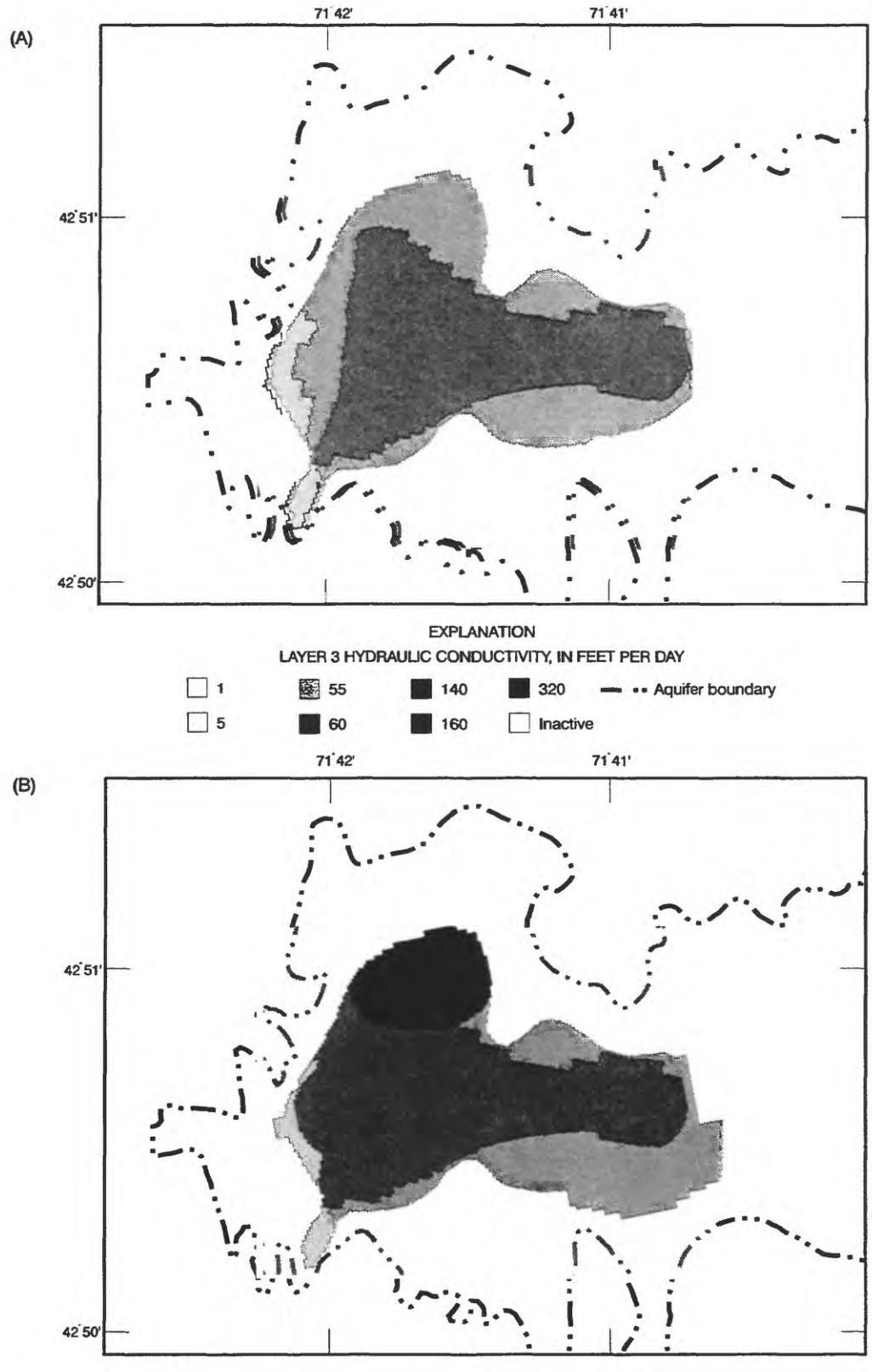

Figure 6. Initial input of active areas and horizontal hydraulic conductivity zones for model layer three (A), and final input for layer three (B), for Milford-Souhegan glacial-drift aquifer, Milford, New Hampshire.

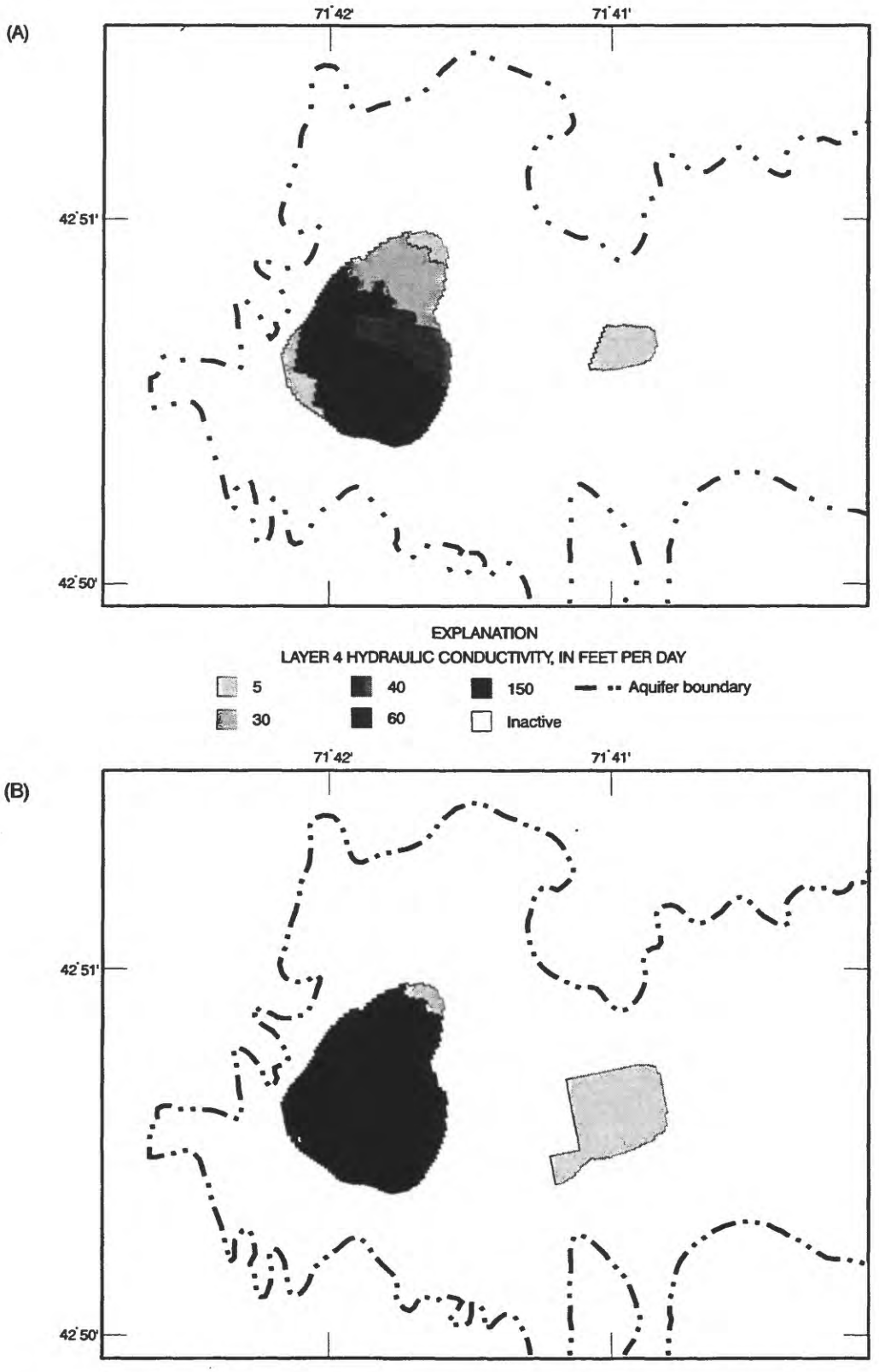

Figure 7. Initial input of active areas and horizontal hydraulic conductivity zones for model layer four (A), and final input for layer four (B), for Milford-Souhegan glacial-drift aquifer, Milford, New Hampshire.

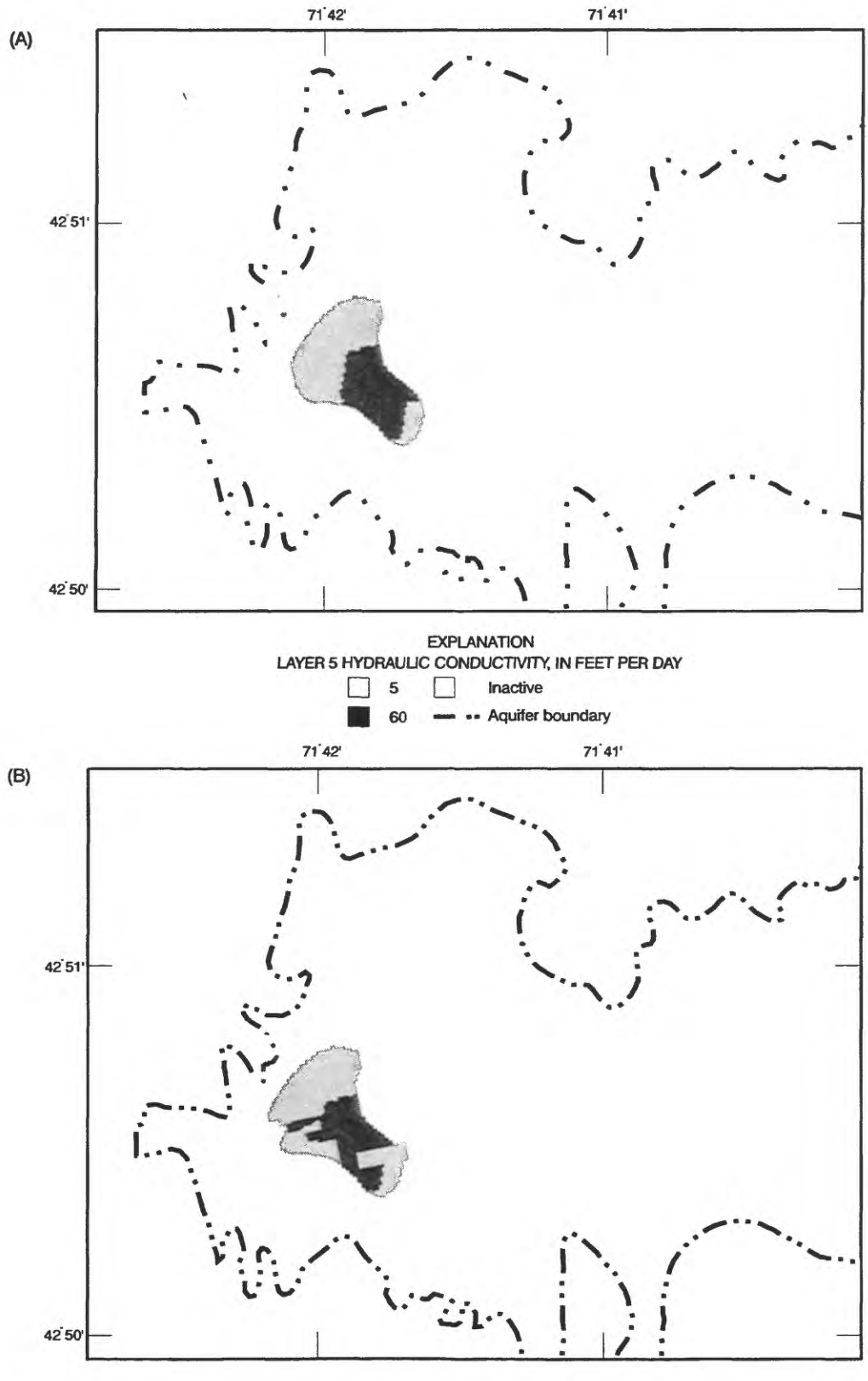

Figure 8. Initial input of active areas and horizontal hydraulic conductivity zones for model layer five (A), and final input for layer five (B), for Milford-Souhegan glacial-drift aquifer, Milford, New Hampshire.

and 2 and the ratio of horizontal to vertical hydraulic conductivity is 1:1. The upper two model layers consist of outwash plain deposits that probably vary equally in the horizontal and vertical directions. Vertical anisotropy is specified between layers 2 through 5. The ratio of horizontal to vertical hydraulic conductivity is 2:1 between layers 2 and 3 and is 4:1 between layers 3 through 5. Vertical heterogeneity is also incorporated into the model because a different pattern of horizontal spatial variability exists in each model layer.

The initial distribution of hydraulic conductivity assigned to each layer of the model (figs. 4A-8A) was based on results of previous models of the MSGD aquifer (Olimpio and Harte, 1994; and Harte and Mack, 1992). The assigned distribution of hydraulic conductivity during model simulations was changed (1) to incorporate information on geology and hydraulic characteristics from field data collected during the course of this study, including data collected to improve delineation of the plume (Camp, Dresser, and McKee, Federal Programs Corporation, 1995; Environmental Science and Engineering, Inc., 1995; and Camp, Dresser, and McKee, Inc., 1996); (2) to improve calibration targets such as hydraulic heads and river seepages; and (3) to evaluate sensitivity of the constructed ground-water-flow model to changes in hydraulic conductivity.

Two high hydraulic conductivity zones were specified during model performance testing and are shown on figures 4b and 6b as plots of final distribution of hydraulic conductivity. The zones included a high hydraulic conductivity zone originating from glacial fluvial deposits transported in the upland channel now occupied by Purgatory Brook (figs. 2 and 6b) and a shallow high hydraulic zone (fig. 4b) from a glacial outburst flood originating from the Stony Brook valley located several miles to the west of the study area (not shown on any map). Evidence of these glacial processes are reported by Koteff (1970) and Moore (1995), who describe the occurrence of high-energy meltwater channels in the valleys presently drained by Purgatory Brook and Stony Brook during the last glaciation.

Vertical hydraulic conductivity was calculated from horizontal hydraulic conductivity and model layer thickness data, using a method described by McDonald and Harbaugh (1988, p. 5-13). A vertical to horizontal hydraulic conductivity of 0.5 was applied between layers 2 and 3, and a ratio of 0.25 between layers 3 and 4, and 4 and 5.

Storage Properties

Storage properties of the aquifer are specified in transient simulations of ground-water flow and are not required in steady-state simulations. Implicit in steady-state simulations is the assumption that no change in aquifer storage occurs over the period of simulation.

Uniform values of storage properties were applied to each model layer based on position of the water-table surface. The uppermost model layer (one) (fig. 4), which largely contains the water table except near areas of ground-water withdrawals, was assigned a high storage value corresponding to values appropriate for specific yield[1] of the aquifer. The lowermost model layers, below the uppermost active layer (model layers 2 through 5, figs. 5-8), were assigned dual storage properties; a low storage value to simulate the storage coefficient[2] of the aquifer and a high value of storage to simulate specific yield for situations when the water table is lowered to those layers. This option of simulating dual storage properties is called a convertible model layer in the computer program MODFLOW (McDonald and Harbaugh, 1988).

Specific yield for the aquifer was estimated from fluctuations of water levels at the long-term (36 years) observation well MI-18 (plate 1, appendix 2) on the basis of methods described by Rasmussen and Andreason (1959). A specific yield of 0.23 was determined from this method and subsequently used in model simulations. The effects of using different values of specific yield, however, were evaluated in several transient-seasonal simulations. Specified specific yield input values ranged from 0.15 to 0.30.

Storage coefficients for the aquifer was assigned based on results of aquifer tests from Harte and Mack (1992, p. 12-13). A storage coefficient of 0.0003 was assigned to transient-seasonal simulations but ranges of 0.00003 to 0.003 were also tested.

---

[1]The specific yield term in the ground-water-flow equation represents the draining or wetting of pore spaces.

[2]The storage coefficient term in the ground-water flow equation represents the process of aquifer expansion and compression of water.

Boundary Conditions

Boundary conditions for the model are treated similarly to previous models of flow constructed by Harte and Mack (1992) and Olimpio and Harte (1994) with the exception of the eastern boundary of this model. The upper model boundary, the water table, is a specified-flux boundary and receives recharge from precipitation. The outermost active cells in the upper model boundary that correspond to adjacent till and bedrock areas also receive specified flow from these upland areas. The outermost active cells are visible in figure 3 as the contact between the active and inactive cells. The lower model boundary represents the bedrock surface, which is assumed to be a no-flow boundary[3]. Perennial streams such as the Souhegan River, Tucker Brook, and Purgatory Brook are simulated as head-dependent flux boundaries.

The eastern boundary of the model differs from previous models because the boundary cuts across the valley and therefore it was necessary to simulate the exchange of flow across this area. The eastern boundary is simulated as a head-dependent flux boundary and utilizes the general-head boundary option of MODFLOW (McDonald and Harbaugh, 1988, chap. 11). This boundary specification allows for the exchange of water between an external source, in this case the eastern part of the aquifer that is not explicitly simulated in the model, and the simulated model of the western part of the aquifer. Model-input parameters for the general-head boundary (GHB) include external hydraulic head and hydraulic conductance (hydraulic conductivity multiplied by cross-sectional area of flow divided by length of flow).

The location of the GHB was positioned to provide adequate representation of ground-water flow in the western part of the aquifer, to simulate the exchange of flow between ground water in the western and eastern parts of the aquifer, and to maximize the level of discretization in the area of the contaminant plume. The boundary corresponds to a relatively thin and narrow section of the aquifer where the saturated thickness is generally less than 30 ft and where ground-water flow is largely controlled by the Souhegan River. The boundary is located at model column 181 (fig. 3), eight columns west of the extreme edge of the model. Model cells in columns 182 to 189 are not simulated. The placement of the GHB at column 181 allows for repositioning of the boundary further eastward if future model testing shows the GHB to have adverse effects on flow. The positioning of the boundary at column 181 just east of the Souhegan River is also useful because the Souhegan River in the middle part of the aquifer is a strong discharge reach and captures much of the flow from the western part of the aquifer (Harte and Mack, 1992). One reason the Souhegan River acts as a strong sink in this part of the aquifer is that its depth of incisement relative to aquifer thickness is greater in this area of the aquifer than it is in other areas with the exception of the extreme eastern edge of the valley.

Hydraulic heads for the GHB were derived from computed heads of the same area from the 1988 steady-state model of average annual conditions (Olimpio and Harte, 1994). Ground-water withdrawals in the valley in 1994-95 (table 1) have little effect on heads in this area of the model, and heads from the 1988 model of the MSGD aquifer are a good approximation of heads in this area regardless of current or past changes in ground-water withdrawals.

Conductances for the boundary were computed from the hydraulic conductivity of the corresponding model layer (both layers 1 and 2 were simulated), and from the cross-sectional area along column 181. The cross-sectional area of each GHB cell corresponds to the width of the cell in the row direction multiplied by the saturated thickness of the cell. Conductances of GHB cells vary from 0.36 to 1.12 ft^2/s for layer 1 and 0.41 to 4.26 ft^2/s for layer 2.

Recharge

Recharge was applied to the uppermost active cells to simulate infiltration of direct precipitation onto the aquifer, lateral inflow of water from adjacent uplands, and infiltration of surface water from ephemeral streams (tributaries 1 and 2, fig. 2). Recharge from perennial streams was accounted for in simulations of river-aquifer interactions by use of the river package of MODFLOW (described in the section "River-Aquifer Interactions").

[3]Undoubtedly, there is some amount of flow between the glacial-drift deposits and underlying bedrock. Most likely the MSGD aquifer is a sink from a net flow perspective and receives recharge from the bedrock. The assumption that the boundary can be treated as a no-flow boundary means that the magnitude of flow between the bedrock and the MSGD aquifer is relatively small compared to the total flow in the MSGD aquifer.

Recharge from infiltration of precipitation was applied uniformly over the active model area. Lateral inflow of water from uplands was apportioned to the edge of the active model area based on upland area-weighted calculations discussed in Harte and Mack (1992). A lateral-inflow rate of 0.5 ft^3/s was used for the simulated area.

Rates of direct precipitation were derived from two independent techniques and then specified in steady-state and transient-seasonal models of flow. The appropriateness of calculated recharge rates was evaluated by comparing computed heads and river leakages with observed heads and river leakages. The independent techniques used include a quasi two-dimensional water-balance model, called HELP (U.S. Environmental Protection Agency, 1994a,b), and a water-level accretion method described by Rasmussen and Andreason (1959).

Recharge rates from the water-balance model were calculated by Environmental Science and Engineering, Inc. (1997b) for the period March 1994 to June 1995 and tested in model simulations. The water-balance model computes monthly recharge from daily inputs of temperature and precipitation, and from characteristics of soil properties. Two sets of values were calculated that differed on the basis of the amount of simulated overland runoff (table 2). The set of recharge values with no overland runoff are proportionally greater than the set with overland runoff.

Recharge rates using the water-level-accretion technique were calculated for a similar period of time as the water-balance model. The technique involves computation of recharge based on the assumption that the water-level rise projected above a previous ground-water recession is equal to the rate of ground-water recharge divided by the specific yield of the aquifer

Table 2. Estimates of ground-water recharge from a water-balance model of the Milford-Souhegan glacial-drift aquifer and water-level-accretion technique for long-term observation well MI-18 (MOW-36, well number 29), Milford, New Hampshire

[Location of MI-18 is shown on plate 1. Abbreviations: in/m, inch/month; ft^3/s, cubic foot per second; Bold numbers represent maximum estimate for that month.]

Date	Precipitation (in/m)	Precipitation (ft^3/s)	Water-balance model with runoff[1] (low recharge) (in/m)	Water-balance model with runoff[1] (low recharge) (ft^3/s)	Water balance model with no runoff[2] (medium recharge) (in/m)	Water balance model with no runoff[2] (medium recharge) (ft^3/s)	Water-level accretion (high recharge) (in/m)	Water-level accretion (high recharge) (ft^3/s)
March 1994	5.99	8.57	0.31	0.44	**7.20**	**10.30**	3.57	5.11
April 1994	2.50	3.70	1.25	1.85	**2.38**	**3.52**	1.80	2.66
May 1994	5.07	7.26	0.61	0.87	0.63	0.90	**1.89**	**2.71**
June 1994	1.77	2.62	0.46	0.68	0.47	0.70	**1.00**	**1.48**
July 1994	4.33	6.20	0.36	0.51	0.36	0.52	**0.98**	**1.40**
August 1994	4.89	7.00	0.25	0.36	0.27	0.39	**2.55**	**3.65**
September 1994	5.83	8.62	1.69	2.5	1.69	2.51	**3.72**	**5.50**
October 1994	0.63	0.90	2.12	3.03	**2.19**	**3.13**	1.21	1.73
November 1994	3.88	5.74	0.89	1.32	0.89	1.32	**3.60**	**5.32**
December 1994	6.12	8.76	4.28	6.13	4.44	6.35	**5.95**	**8.52**
January 1995	3.82	5.47	2.17	3.11	2.11	3.02	**3.47**	**4.97**
February 1995	2.99	4.74	0.54	0.86	0.56	0.89	**1.85**	**2.93**
March 1995	1.97	2.82	0.32	0.46	**3.23**	**4.62**	2.83	4.05
April 1995	2.03	3.00	0.85	1.26	1.65	2.44	**1.82**	**2.70**
May 1995	3.23	4.62	0.61	0.87	0.80	1.15	**2.35**	**3.36**
June 1995	1.78	2.63	0.39	0.58	0.38	0.59	**1.12**	**1.66**
Total	56.83	82.65	17.10	24.83	29.24	42.35	39.80	57.75
Monthly mean	3.55	5.17	1.07	1.55	1.83	2.65	2.49	3.61
Standard deviation	1.65	2.37	1.03	1.47	1.80	2.56	1.29	1.85
Percentage of precipitation	100	100	30	30	52	51	70	70

[1]Environmental Science and Engineering, Inc. (1997b).
[2]Environmental Science and Engineering, Inc. (1997b).

(assumed to be 0.23). Therefore, recharge over a given time period equals the summation of recharge from individual water-level rises. The water-level-accretion technique produced higher rates of recharge than the water-balance method.

Based on these recharge analyses, a relation between precipitation and direct recharge was established and used to assign recharge rates for the simulated stress periods. Recharge values of 30, 52, and 70 percent of direct precipitation were assigned to the model to test the appropriateness of these rates.

Total amounts of recharge that were applied to steady-state and transient-seasonal models varied based on the stress period. Steady-state recharge ranged from 2.06 ft^3/s (30 percent of precipitation) to 3.89 ft^3/s (70 percent of precipitation). A final value of 3.26 ft^3/s (60 percent of precipitation) was chosen as most representative of average annual conditions. Transient recharge varied from a monthly low of 0.39 ft^3/s in August 1994 to a monthly high of 10.3 ft^3/s in March 1994.

River-aquifer Interactions

River-aquifer interactions of perennial streams including the Souhegan River, Purgatory Brook, Tucker Brook, Hartshorn Brook, and the discharge ditch were simulated with the river package of MODFLOW, in which flow between the perennial streams and the aquifer is a function of head gradient and riverbed conductance. Therefore, river-aquifer interactions act as a head-dependent flow boundary. Perennial streams are represented by over 1,800 model cells.

Model-input specifications for each cell containing a perennial stream include altitude of the river stage and riverbed and riverbed conductance [which is a product of the riverbed hydraulic conductivity (K), width, and length of riverbed within the cell, divided by the thickness of the riverbed (M)]. All parameters except riverbed thickness and hydraulic conductivity are readily measurable.

River stages were based on measurements of altitude of river stage and riverbed from eight river gaging stations on the Souhegan River, four stations on the discharge ditch, and several miscellaneous stations on the remaining perennial streams (Harte and others, 1997). Values of river stage were assigned to all river cells from linear interpolation of the measured river stage at each of the gaging stations.

River stage assigned to the steady-state models of flow were based on the arithmetic mean stage of the river-gaging stations during 1994 and 1995. River stage assigned to the transient-seasonal models of flow were based on the mean monthly stage of the stations. As an example, river stage assigned to model cell row 81 and column 13 for the transient-seasonal model is shown in figure 9. Riverbed altitudes were constant for the steady-state and transient-seasonal models because this parameter is assumed to remain unchanged during this period. Riverbed altitudes were calculated from the height of the water column above the riverbed at gaging stations and were linearly interpolated between river-gaging stations.

Riverbed widths were computed from stream-flow measurements made at over 40 sites on perennial streams and values for all cells linearly interpolated from these sites. These data also were used to assure that correct distances were used between the altitudes of river stage and riverbed.

The remaining parameters for the river-package input, riverbed thickness and hydraulic conductivity, were lumped into one parameter, called riverbed leakance, (K/M), and assigned rates comparable to those assigned in earlier steady-state models of flow in the aquifer (Harte and Mack, 1992). The distribution of riverbed leakance are provided in table 3.

Ground-water Withdrawals

Specifying appropriate rates of ground-water withdrawals is important because of the effect withdrawals have on ground-water flow. Rates of specified withdrawals in the models for the major public-water supply, commercial, and industrial water suppliers are provided in table 4 for various simulated stress periods.

Estimates of withdrawals are based on well records and written and oral communications with personnel from the State of New Hampshire Fish Hatchery and other facilities in Milford. Because of imprecision in the measurements of withdrawals at the State Fish Hatchery, probable ranges of withdrawals are listed in table 4. Managers evaluating remedial schemes should test the effect of these ranges of withdrawals on contaminant clean-up. For example, State Fish Hatchery well FH-4 (well number 87) (fig. 2) withdrawals may vary between 950 and 1,350 gal/min and State Fish Hatchery well FH-5 (well number 208) (fig. 2) may vary between 600 and 800 gal/min.

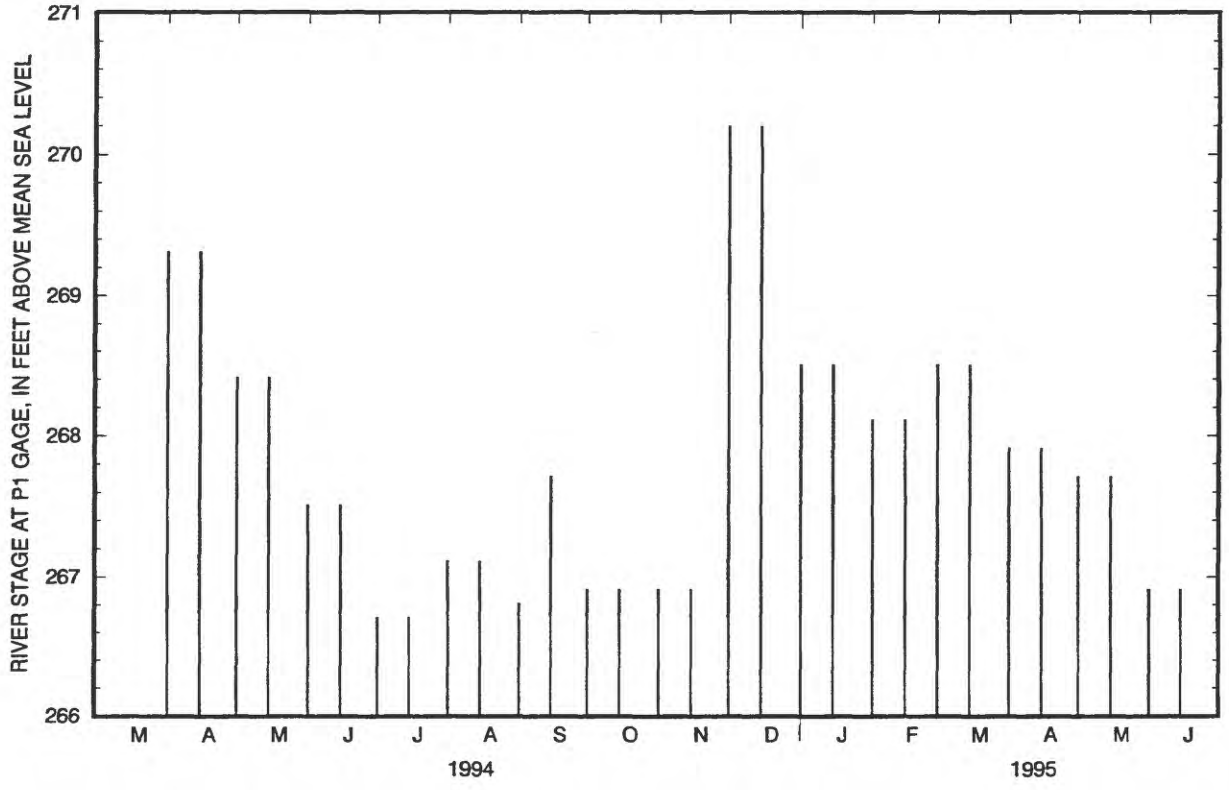

Figure 9. River stage specified in model cell row 81 and column 13 for the transient-seasonal model of the Milford-Souhegan glacial-drift aquifer, Milford, New Hampshire. (P1 gage is shown on plate 1.)

Table 3. Assigned values of riverbed leakance (hydraulic conductivity divided by riverbed thickness) to models of flow of the Milford-Souhegan glacial-drift aquifer, Milford, New Hampshire

[Units of riverbed leakance is measured in 1/day. Locations of streams are shown in plate 2]

Stream	Reach description	Riverbed leakance
Souhegan River	Upstream of column 135	2
Souhegan River	Downstream of column 135	0.75
Purgatory Brook	All	2
Tucker Brook	All	1.33
Discharge ditch	All	0.66

Table 4. Simulated ground-water withdrawals for stress periods in simulations of the Milford-Souhegan glacial-drift aquifer, Milford, New Hampshire

[Note: Not all results of simulations listed here are presented in this report. Results of transient historical simulations presented in Harte and Wilky (1997). ft^3/s, cubic foot per second (to convert withdrawals in ft^3/s to gallons per minute, multiply by 448.8)]

Well name and number shown on plate 1	Model		Model layer	Simulated	
	Row (plate 2)	Column (plate 2)		Ranges of rates of withdrawal tested, in ft^3/s	Final rate of withdrawal, in ft^3/s
				Steady-state simulation, 1994-95	
FH-5(208)	28	59	3	1.44-1.63	1.63
FH-4(87)	40	55	2, 3	1.56-2.05; layer 2 0.39-0.51; layer 3	1.56; layer 2 0.39; layer 3
MI-88(395)	128	39	2	0.38	0.38
PFH(354)	70	159	2	0.22	0.22
				Transient-seasonal simulation, 1994-95	
FH-5(208)	28	59	3	1.59-1.78 from Jan. to May of 1994 and Jan. to May 1995, and Oct. to Dec. 1994. 0 in June 1994. 1.50-1.78 from July to Sept. 1994. 1.50-1.78 in June 1995.	1.78 from Jan. 1994 to Mar. 1995 except for June 1994 which was 0. April 1995 to June 1995 was 1.67.
FH-4(87)	40	55	2, 3	1.60-2.1 in layer 2 and 0.40-0.53 in layer 3 in 1994. 1.42 in layer 2 and 0.36 in layer 3 from Jan. 1995 to June 1995.	1.60 in layer 2 and 0.40 in layer 3 in 1994. 1.42 in layer 2 and 0.36 in layer 3 from Jan. 1995 to June 1995.
MI-88(395)	128	39	2	0.38	0.38
PFH(354)	70	159	2	0.38 from Jan.-Oct. 1994. 0.22 from Nov. 1994-June 1995.	0.38 from Jan.-Oct. 1994. 0.22 from Nov. 1994-June 1995.
				Transient historical simulation, 1965-96	
Savage (128)	118	99	2,3	0.162 in layer 2 0.162 in layer 3	0.162 in layer 2 0.162 in layer 3
				Transient historical simulation, 1965-71	
MI-33(47)	128	40	3	0.56	0.56
Savage (128)	118	99	2,3	0.162 in layer 2 0.162 in layer 3	0.162 in layer 2 0.162 in layer 3
				Transient historical simulation, 1971-74	
FH-1(84)	28	60	3	1.33	1.33
MI-33(47)	128	40	3	0.56	0.56
Savage (128)	118	99	2,3	0.162 in layer 2 0.162 in layer 3	0.162 in layer 2 0.162 in layer 3
				Transient historical simulation, 1974-Sept. 1976	
FH-1(84)	28	60	3	1.33	1.33
MI-33(47)	128	40	3	0.56	0.56
Savage (128)	118	99	2,3	0.162 in layer 2 0.162 in layer 3	0.162 in layer 2 0.162 in layer 3
MI-35(49)	130	59	3	0.26	0.26
				Transient historical simulation, Sept. 1976-Feb. 1983	
FH-1(84)	28	60	3	1.07	1.07
FH-3(86)	40	51	3	0.61	0.61
MI-33(47)	128	40	3	0.56	0.56
Savage (128)	118	99	2,3	0.162 in layer 2 0.162 in layer 3	0.162 in layer 2 0.162 in layer 3
MI-35(49)	130	59	3	0.26	0.26

Table 4. Simulated ground-water withdrawals for stress periods in simulations of the Milford-Souhegan glacial-drift aquifer, Milford, New Hampshire—Continued

Well name and number shown on plate 1	Model		Model layer	Simulated	
	Row (plate 2)	Column (plate 2)		Ranges of rates of withdrawal tested, in ft^3/s	Final rate of withdrawal, in ft^3/s
				Transient historical simulation, Feb. 1983-Oct. 1986	
FH-1(84)	28	60	3	0.73	0.73
FH-3(86)	40	51	3	0.61	0.61
MI-33(47)	128	40	3	0.56	0.56
MI-35(49)	130	59	3	0.26	0.26
				Transient historical simulation, Oct. 1986-Jan. 1988	
FH-1(84)	28	60	3	0.56	0.56
FH-4(87)	40	55	2,3	1.42-2.05 in layer 2 0.36-0.51 in layer 3	1.42-2.05 in layer 2 0.36-0.51 in layer 3
MI-33(47)	128	40	3	0.56	0.56
MI-35(49)	130	59	3	0.26	0.26
				Transient historical simulation, Jan. 1988-Jan. 1989	
FH-5(208)	28	59	3	1.78	1.78
FH-4(87)	40	55	2,3	1.42-2.05 in layer 2 0.36-0.51 in layer 3	1.42-2.05 in layer 2 0.36-0.51 in layer 3
MI-33(47)	128	40	3	0.56	0.56
MI-35(49)	130	59	3	0.26	0.26
				Transient historical simulation, Jan. 1989-April 1990	
FH-5(208)	28	59	3	1.78	1.78
FH-4(87)	40	55	2,3	1.42-2.05 in layer 2 0.36-0.51 in layer 3	1.42-2.05 in layer 2 0.36-0.51 in layer 3
MI-88(395)	128	39	3	0.56	0.56
MI-35(49)	130	59	3	0.001	0.001
				Transient historical simulation, April 1990-Aug. 1992	
FH-5(208)	28	59	3	1.63	1.63
FH-4(87)	40	55	2,3	1.42-2.05 in layer 2 0.36-0.51 in layer 3	1.42-2.05 in layer 2 0.36-0.51 in layer 3
MI-33(47)	128	39	3	0.40	0.40
MI-35(49)	130	59	3	0.001	0.001
PFH(354)	70	159	2	0.334	0.334
				Transient historical simulation, Aug. 1992-Oct. 1994	
FH-5(208)	28	59	3	1.44-1.63	1.44-1.63
FH-4(87)	40	55	2,3	1.42-2.05 in layer 2 0.36-0.51 in layer 3	1.42-2.05 in layer 2 0.36-0.51 in layer 3
MI-33(47)	128	39	3	0.38	0.38
PFH(354)	70	159	2	0.334	0.334
				Transient historical simulation, Nov. 1994-Dec. 1995	
FH-5(208)	28	59	3	1.44-1.63	1.44-1.63
FH-4(87)	40	55	2,3	1.42-2.05 in layer 2 0.36-0.51 in layer 3	1.42-2.05 in layer 2 0.36-0.51 in layer 3
MI-33(47)	128	39	3	0.38	0.38
PFH(354)	70	159	2	0.22	0.22

CALIBRATION OF AND PERFORMANCE CRITERIA FOR NUMERICAL MODELS

Computed heads and fluxes from steady-state and transient-seasonal models of flow were calibrated to observed heads and river leakages. Observed river stages are explicitly specified in the model and, therefore, are not used in calibration. A listing of observation wells, where heads were measured is given in appendix 3; well construction information is given in appendixes 2 and 4. River-gaging stations, where river leakage were calculated, are shown on plate 1.

The observed data used to calibrate the model differ for the steady-state and transient models of flow based on the time dependency of the simulation and relevancy of field observations to the simulated stress period. For example, in steady-state simulations, average values or values that approximate average conditions are used to judge model performance, whereas in transient simulations, actual discrete values that change with time are used.

Computed heads were compared to more than 70 values of observed head (appendix 3). The steady-state model was calibrated to heads calculated from the arithmetic mean head of biweekly measured water levels from wells measured June 1994-95. The transient-seasonal model was calibrated to observed of heads from the same wells using discrete measurements of heads from the same period. Additional head data were also used to check model performance and include 3 synoptic rounds of head measurements made from more than 100 wells in 1988, 1990, and 1994.

Computed river seepages[4] of simulated rivers were compared to observed river leakages[5] from a comprehensive 1988 round of streamflow measurements (Harte and Mack, 1992) for selected drainage subbasins (plate 1), and to the calculated mean of river leakages from streamflow measurements made in 1994-95 at two river reaches. The two river reaches include an upstream reach between stations WLR1 and P2 (plate 1) and a downstream reach between WLR5 and bedrock outcrop (plate 1). Observed river leakages were calculated from streamflow measurements of coupled upstream and downstream river-gaging stations based on techniques described by Harte and others (1997). The 1988 calculated leakages were measured during low to moderate flow conditions (77 percent flow duration at continuous gaging stations in the region). The 1994-95 leakages include 13 coupled measurements at the upstream reach and 10 at the downstream reach that were measured in low to high flow (30 to 90 percent flow duration at continuous gaging stations in the region).

An exact calibration between model-computed river seepage and observed river leakage is not possible because of a number of factors; first, there are inaccuracies in the observed river leakages that are intrinsic to techniques of measuring streamflow and, second, there is a difference between a seepage value and a leakage value. Seepage is entirely comprised of baseflow, whereas leakage may include other components of streamflow besides baseflow. In general, computed river seepages were considered acceptable if they were within 50 percent of observed river leakages during streamflows with less than a 50 percent flow duration, and greater than 50 percent when observed river leakages were made during streamflows with greater than a 50 percent flow duration.

Summary statistical functions used for calibrating ground-water head include two statistical means, the standard mean and absolute mean, root mean square error, and standard deviation. The standard mean is calculated as

$$= \frac{1}{n}\sum(h_m - h_o) \qquad (1)$$

the absolute mean is calculated as

$$= \frac{1}{n}\sum|(h_m - h_o)| \qquad (2)$$

where

h_m = model computed head,

h_o = observed head, and

n = number of observations.

[4]The term seepage is used to describe ground-water recharge and discharge interactions with streams.

[5]The term leakage is used to describe all processes contributing to gains and losses in streams.

Summary statistics were used to measure model performance and adequacy in order to minimize mean differences between computed and observed heads without producing spatial bias.

Results of simulations were also checked by comparing advective transport of contaminated ground waters in the plume, by use of a semi-quantitative particle-tracking scheme called MODPATH (Pollock, 1994), to the observed distribution of contaminants (fig. 2a). The observed distribution of contaminant was determined from water-quality data from previous studies (New Hampshire Department of Environmental Services, 1985; HMM Associates Inc., 1989, 1991; Environmental Science and Engineering, Inc., 1997; Camp, Dresser, and McKee-Federal, Inc. 1995; Camp, Dresser, and McKee Inc., 1996). Model performance based on particle tracking was done by comparing a steady-state simulation of particle distributions that was forward tracked for 5 years from a reported plume distribution in 1989, with the reported plume distribution in 1994 (fig. 10).

The comparison of plume distributions at different points in time using advective-transport simulations implicitly assumes that advective transport is the most important component of solute transport and that dispersion, diffusion, adsorption/desorption, decay, and additional sources and sinks of contaminants are relatively small factors in the solute transport of contaminants. Because for this study there was no attempt to independently differentiate the effects of advective transport from the other components of solute transport on the formation of the contaminant plume, direct comparisons of the observed plume and simulated advective transport are only qualitative.

Steady State

Results of steady-state simulations of flow of 1994-95 were compared to mean-observed heads and mean-observed-river leakages for the period of simulation. The principal mechanisms of comparison were:

1. Mean differences between computed and observed heads from the arithmetic average of biweekly measurements of water levels from more than 70 wells (Harte and others, 1997) (appendix 3),
2. Spatial analysis of residuals between computed and observed heads from wells,
3. Vertical-head gradients at clustered wells,
4. River leakage estimates made during baseflow conditions, and
5. Arithmetic mean of river leakage from two reaches on the Souhegan River where multiple coupled measurements of streamflow were made (Harte and others, 1997).

During calibration, head residuals were reduced to avoid spatial bias and to help assure a random error distribution. Maps of head residuals and gradients along transects of the aquifer were produced. Calibration was considered complete when head residuals were calibrated to less than the observed fluctuation of ground-water levels at the observed well location, which was generally 3 ft at locations remote from ground-water withdrawals, and 6 feet at pumping locations. Computed vertical gradients were compared observed gradients at well clusters.

Transient Seasonal

Results of transient-seasonal model of flow during 1994-95 were compared to biweekly observations of heads and monthly measurements of river leakage. The principal mechanisms of comparison were:

1. Seasonal mean differences between simulated and observed heads from wells,
2. Spatial analysis of water-level fluctuations,
3. Analysis of variations between the computed and observed principal directions and magnitude of maximum slope in heads at selected triangular grouped wells, and
4. River leakages from two reaches on the Souhegan River where multiple coupled measurements of streamflow were made (Harte and others, 1997).

Variations in principal direction and magnitude of maximum slope of head were analyzed by use of procedures described by Johnston and Harte (1998), in which a three-point planar solution was applied to a triangular grouping of observations of ground-water levels. In the analysis presented in this report, triangular groupings of computed heads during June 1994-1995 were compared to observed observations reported in Harte and others (1997, table 8).

Criteria used to judge the performance of the transient model include comparisons discussed in the steady-state model but also include analysis of temporal trends in computed and observed heads and computed river seepages and observed river leakages. Analysis of temporal trends include plotting of hydrographs, summary statistics grouped per season, time-series plots of river leakage, and analysis of standard deviation of biweekly head gradients.

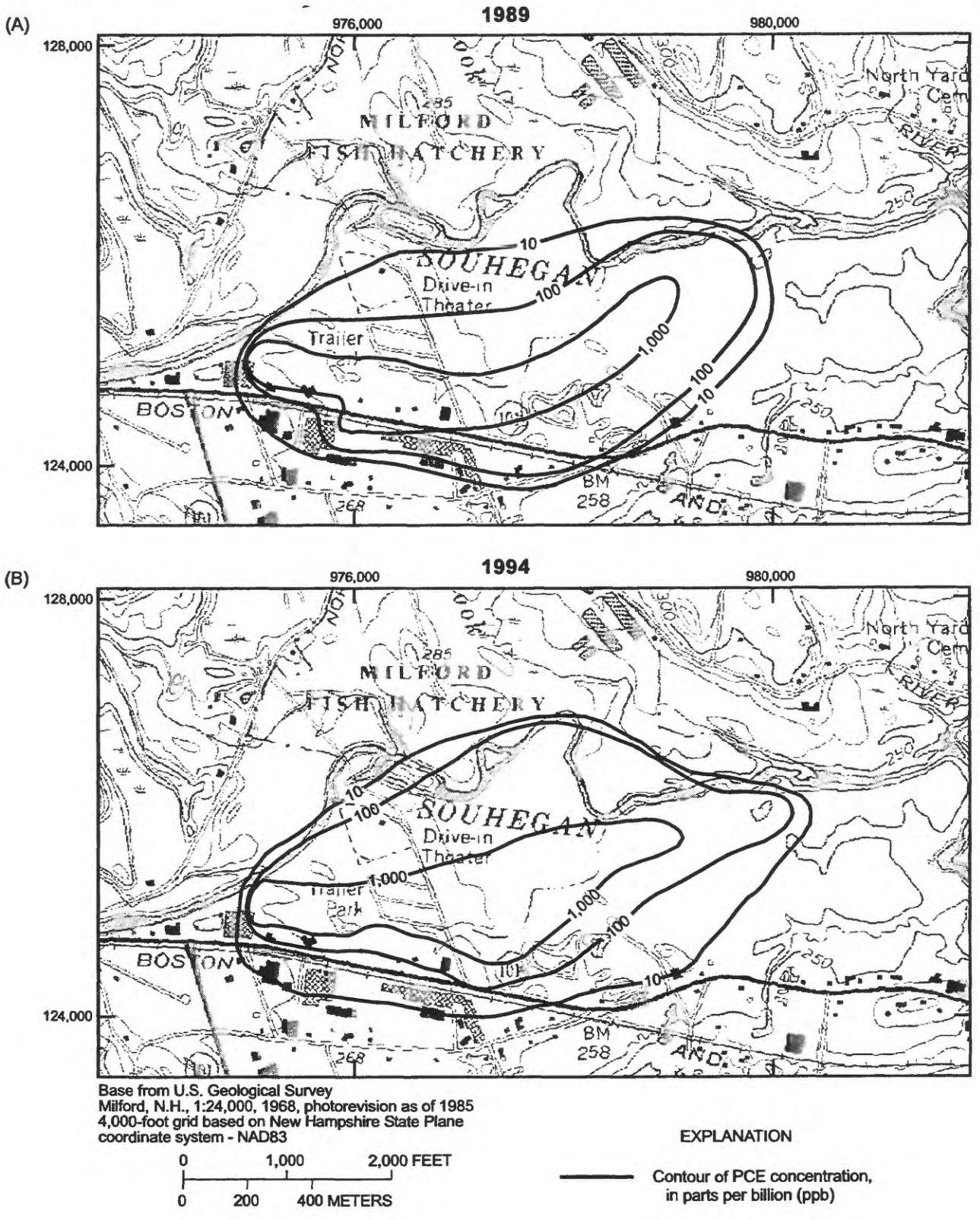

Figure 10. Concentration of tetrachloroethylene (PCE) in 1989 (A), and 1994 (B), in the Milford-Souhegan glacial-drift aquifer, Milford, New Hampshire.

Calibration reduced the temporal and spatial bias in head residuals. Calibration of computed river seepages based on ranges of observed river leakages, where multiple coupled streamflow measurements were made was not possible because the model simulates only ground-water flow, whereas observed river leakages incorporate other hydrologic processes. Thus the range in observed river leakages greatly exceed the range in computed river seepages.

EVALUATION OF SELECTED MODEL PARAMETERS

During testing of the flow models, important model parameters and conditions were evaluated to ascertain their effect on model results. Model parameters evaluated included boundary conditions, ground-water recharge, hydraulic conductivity, river-aquifer interactions, and storage parameters.

Previous model studies of the MSGD aquifer helped focus model testing during this study. Computed model results of sensitivity analysis of the post-calibrated model performed by Harte and Mack (1992) provided insight into what additional simulations should be performed. As a result, selected model parameters were tested concurrently with model calibration. This section outlines important simulated results from a trial-and-error calibration process. This trial-and-error calibration process also can be used as a pre-calibrated sensitivity analysis of the aquifer.

Boundary Conditions

The eastern boundary of the model, which contains the general-head boundary along column 181(fig. 3), underwent rigorous testing to insure that it adequately approximated ground-water-flow conditions in the western half of the MSGD. In particular, it was important to demonstrate that the general-head boundary did not affect the final discharge locations and flow of ground water associated with the contaminant plume.

The effect of the general-head boundary on steady-state ground-water withdrawals in the western-half of the MSGD was tested by examining the extent of drawdowns from withdrawals at the private fish hatchery, which is the closest withdrawal well to the boundary. No-flow and constant-head boundary conditions were tested along the same location of the aquifer and model-computed heads were compared at the withdrawal well near the private fish hatchery. These boundary conditions were initially compared with a 1988 model of the MSGD aquifer (Olimpio and Harte, 1994) because that model simulates the entire MSGD aquifer. No changes in drawdowns resulted at the private fish hatchery from incorporation of no-flow or constant-head boundaries along the area marked by column 181 of the 1994 model described in this report.

Steady-state flows from the general-head boundary of the 1994 model were checked against flows across this area of the aquifer with the 1988 model of the MSGD aquifer (Olimpio and Harte, 1994) to insure that rates of ground-water flow in both models were comparable. Both the 1988 model and the 1994 model simulated the same average annual steady-state flow conditions. The net flow across this area of the aquifer was computed with the 1988 model at a net rate of 0.23 ft^3/s into the western part of the aquifer. Most of this flow occurred as inflow in the area occupying the northeastern part of the 1994 model, approximately between rows 31 to 80 along column 181 of the 1994 model (plate 2). Simulations with the 1994 model using nearly identical model parameters as that of the 1988 model resulted in an initial net rate of 0.33 ft^3/s into the 1994 modeled area from the GHB. Model adjustments during the calibration process resulted in increased rates of flow into the model from the general-head boundary. Specifically, increases in hydraulic conductivity and adjustments of river stage caused inflows of 0.57 ft^3/s to occur from the general-head boundary. A rate of 0.57 ft^3/s represents about 7 percent of total flow through the simulated western half of the aquifer. Because little data exist in the northeastern part of the study, rates of inflow ranging from 0.57 to 0.23 ft^3/s are considered acceptable.

The use of general-head boundary also results in an adequate approximation of the patterns of advective transport of ground water near the leading edge of the contaminant plume. Steady-state advective transport of ground water near the leading edge of the contaminant plume were forward tracked to test the effect of the general-head boundary on discharge of contaminated ground water. Simulations using the 1994 model of the western half of the MSGD aquifer were compared with the 1988 model of the MSGD (Olimpio and Harte, 1994) to assess differences caused by the contrast in the areal extent of the

models. Again, identical flow conditions were simulated. Particles were tracked from the same starting locations, column 110 of the current model and column 58 of the previous model. All particles from the two models discharged to similar reaches of the Souhegan River (fig. 11) and showed a consistency in the locations of final discharge between the two models.

Specification of the GHB near the eastern boundary of the model does not affect the final discharge locations of contaminated ground waters for simulations testing alternative distributions (or realizations) of hydraulic conductivity in the aquifer. This is an important result because there is always uncertainty in model parameterization of aquifer properties and the testing of alternate possibilities of hydraulic conductivities near the GHB provides additional confidence in simulated results. Specifically, it is important to demonstrate that advective transport of ground water near the leading edge of the contaminant plume is unaffected (if alternate possibilities of hydraulic conductivity exist in the aquifer near the GHB) by the GHB. The distributions of alternate hydraulic conductivity included a simulation that tested for a highly conductive (hydraulic conductivity of approximately 600 ft/d deep) buried-esker deposit underlying the Souhegan River. Further information on buried-esker deposits in the aquifer is described in Mack and Harte (1996). A hydraulic conductivity value of 600 ft/d represents the likely uppermost range of hydraulic conductivity in the aquifer. A continuous deeply buried esker deposit underlying the area of the aquifer by the GHB potentially could facilitate the eastward flow of contaminants. Forward tracking of particles showed that discharge to the Souhegan River did not flow past the area marked by the GHB in the 1988 model and, therefore, supports the placement of the boundary at this location.

Evaluation of the effect of the GHB on model simulations of seasonal variations in recharge and discharge for 1994-95 indicates that because stable heads are specified at the boundary, computed heads at model cells along columns 179 to 181 are dampened. For model columns less than 179 (west of column 179), however, simulated-head fluctuations appear unaffected and fluctuate similarly to heads elsewhere in the model. The fluctuations of computed heads near column 181 are dampened because of the assignment of average heads, which are static over time, at the GHB. This dampening effect is restricted to several hundred feet of the boundary, in an area of the aquifer in which little data are available, and removed from areas of the aquifer that affect advective transport of the contaminant plume.

Recharge

High (70 percent of precipitation), medium (52 percent of precipitation) and low (30 percent of precipitation) rates of ground-water recharge were simulated for the steady-state and transient-seasonal models. These recharge rates are based on calculations of flow based on computations of recharge previously described under "Construction of Numerical Models and Recharge."

Steady-state simulations showed small differences in computed heads between the high and low recharge rates. The average head difference (standard mean error) from observation wells (appendix 3) differed by only 0.4 ft between the high and low recharge simulations. The standard mean error represents the average head difference, from observation wells, between the model-computed heads produced from the steady-state simulation of 1994-95 average annual conditions and the arithmetic mean of biweekly measurements of water levels. The standard mean error from the high recharge rate was the lowest (-0.16 ft) and provided the best overall match with observed data.

The simulated high-recharge rate also produced the best match between calculated river leakages and measured river leakages across the western aquifer. For the simulated low and medium recharge rates, computed river losses to the aquifer exceeds river gains from the aquifer by 1.31 ft^3/s for the low recharge rate and 0.87 ft^3/s for the medium recharge rate. For the simulated high recharge rate, river gains exceeds river losses by 0.4 ft^3/s. Nine coupled upstream and downstream measurements of streamflow across the study area showed a tendency of small gains between 1 to 2 ft^3/s (in six out of nine measurements) between 1994-95.

Results of transient-seasonal simulations to assess the appropriateness of low, medium, and high monthly recharge rates (table 2) showed that computed heads using medium to high recharge rates best approximated observed water levels. A representative example of the variations in computed heads produced from specifying three different rates of recharge is

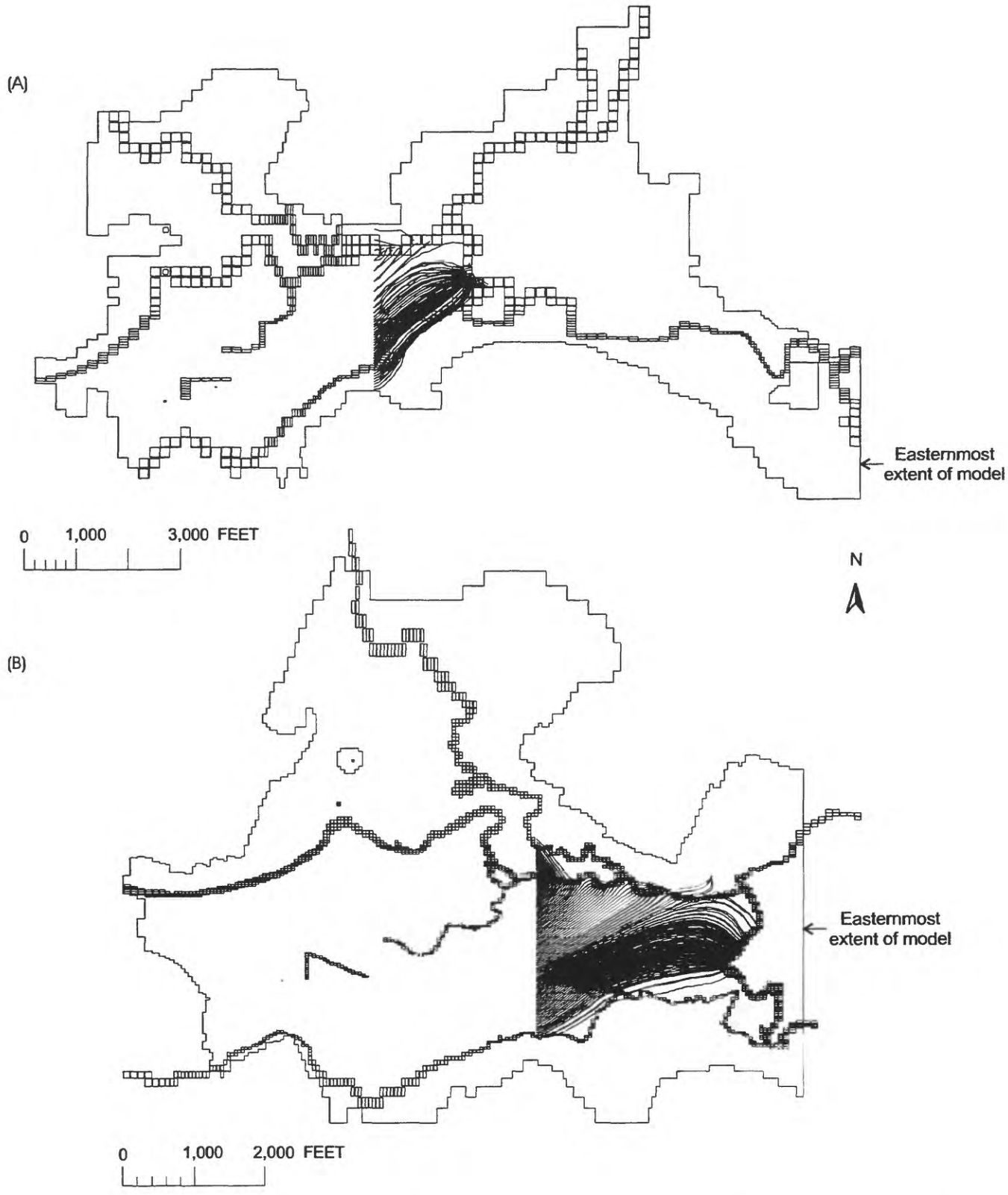

Figure 11. Advective transport of ground water from areas corresponding to the leading edge of the contaminant plume for the 1988 model of the entire Milford-Souhegan glacial-drift aquifer (A), and 1994 model of the western half of the same aquifer (B), Milford, New Hampshire.

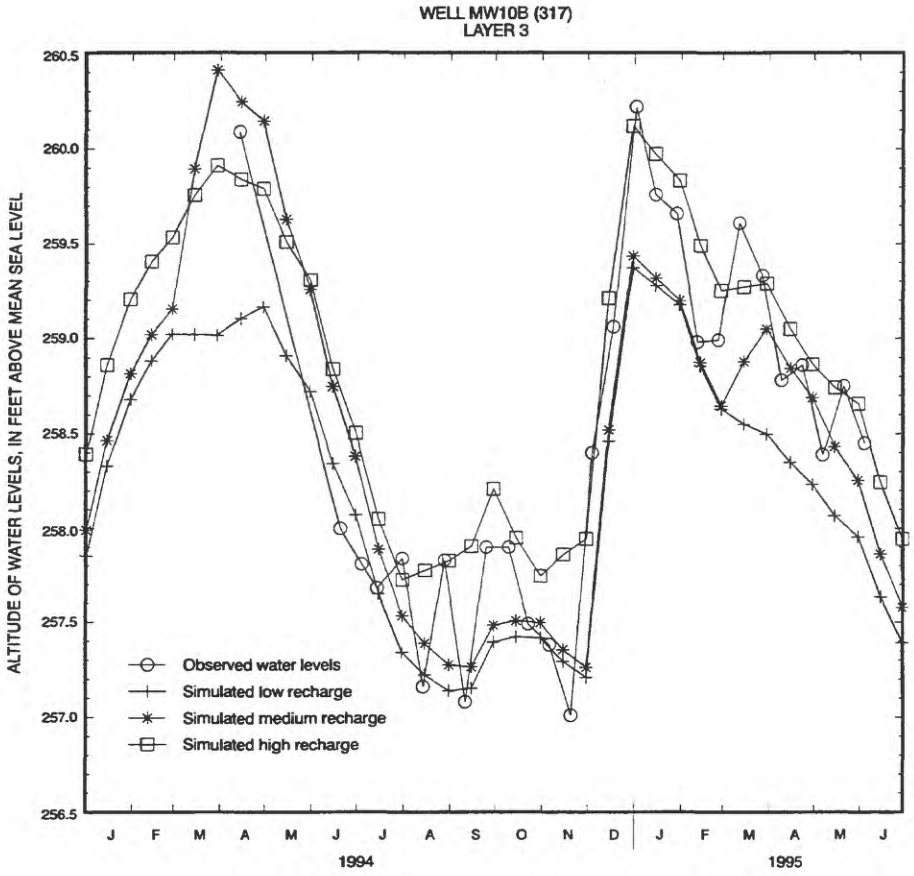

Figure 12. Model-computed heads for low, medium, and high monthly recharge rates from the transient-seasonal simulation with the observed water levels at well MW-10B (well number 317, plate 1), Milford, New Hampshire.

shown in figure 12. The hydrograph is from well MW-10B (well number 317 m, plate 1), located in the middle of the aquifer. The computed heads are closest to observed heads for simulations specifying high to medium recharge. The observed head fluctuation is 3.7 ft and is caused primarily by the variability in recharge rates throughout the year. Low rates of recharge occur during the summer and early fall and high rates of recharge occur in the late fall, winter and early spring. Specifically, the analysis showed

1. For wet periods of the year, which experience the highest amounts of recharge, such as the early spring, the high monthly recharge rates produce computed heads that best match observed water levels. Simulated fluctuations with lower assigned rates of recharge poorly approximated observed water-level fluctuations. Simulated results support the general field observations that surface runoff is minimal in the valley because the low assigned recharge rates assumes that recharge is reduced by the diversion of precipitation to surface runoff in the valley.
2. For dry periods of the year, the low to medium monthly recharge rates produce computed heads that best match observed heads.

To quantitatively assess differences in model fit per season, model-computed heads were grouped by season and compared to observed seasonal averages. The results of this analysis is provided in table 5. The reported mean difference (standard error) represents the average difference between all computed and observed heads.

Results shown in table 5 indicate that the low-recharge simulation underestimates heads during the winter and fall and that the high-recharge simulation best matches heads during this period. For the summer and fall, the medium-recharge simulation best approximates heads although there is little difference

between the medium and low recharge for this period. In summary, the best match is produced from a combination of the medium recharge during the summer and fall and the high recharge during the winter and spring.

Although there is a seasonal variability in recharge rates, seasonal variability in precipitation is small (table 6). The variability in seasonal rates of recharge results primarily from seasonal variation in the ability of precipitation to recharge the aquifer. Many factors contribute to this temporal "recharge efficiency," the primary factor is most likely evapotranspiration. Seasonal evapotranspiration contributes to seasonal depletion of soil moisture and that controls recharge efficiency. The term "recharge efficiency" is a measure of the ability of precipitation falling onto the land overlying the aquifer to recharge the aquifer. For the summer and fall, ground-water recharge is about 27 percent of precipitation (low efficiency) and for the winter and spring, ground-water recharge is about 91 percent of precipitation (high efficiency). The annual ground-water recharge estimate is 24.2 in/yr or 58 percent of precipitation (total recharge is, therefore, 26.2 in/yr when incorporating estimates of lateral recharge), 75 percent of recharge specifically occurs in the late fall through early spring.

The overall sensitivity of the model to variable rates of recharge is spatially dependent. Near perennial streams, variations in recharge have a small effect on computed heads and vary by as little as 0.2 ft due to specification of high or low recharge. Away from perennial streams, variations in recharge affect heads by as much as 2.0 ft.

Table 5. Differences between computed steady-state heads and observed mean heads from biweekly measurements (June 1994 to June 1995) in the Milford-Souhegan glacial-drift aquifer, Milford, New Hampshire

[All units are in feet. Negative numbers mean computed heads are less than observed heads.]

Season	Standard-mean error		
	Low recharge	Medium recharge	High recharge
Summer	-0.23	-0.04	0.24
Fall	-0.08	-0.02	0.48
Winter	-0.60	-0.53	-0.08
Spring	-0.56	-0.27	-0.03
Annual	**-0.37**	**-0.22**	**0.16**

Table 6. Seasonal precipitation, amount of recharge from precipitation, and percent of precipitation recharged to the Milford-Souhegan glacial-drift aquifer, Milford, New Hampshire

[Precipitation is measured in inches; percent is in parentheses]

Season	Precipitation	Low recharge	Medium recharge	High recharge
Summer and fall	21.33 (100)	5.77 (27)	5.88 (28)	13.06 (61)
Winter and spring	20.16 (100)	8.77 (44)	12.79 (63)	20.16 (100)

The high and low monthly recharge rates produce similar temporal patterns of river seepage, except that the magnitude of river seepage varies depending on the recharge rates used (fig. 13). For example, high and low recharge show the same months of ground-water discharge to the aquifer. River gains (ground-water discharge from the aquifer) for subbasin 4 (plate 1) are shown in figure 13 by positive values of river seepage (0 to 2.0 ft^3/s), and conversely, river losses (ground-water recharge from rivers to the aquifer) are shown by negative values of river seepage(0 to -0.8 ft^3/s). Subbasin 4 is a strong ground-water discharge area. The western most extent of subbasin 4 is marked by the confluence of the Souhegan River with Purgatory Brook and its eastern-most extent by the intersection of the Souhegan River with the eastern boundary of the model (plate 1; see also Harte and Mack, 1992, fig. 25). Computed river seepage for subbasin 4 of the aquifer is about 50 percent higher for the high monthly recharge than for the low monthly recharge simulations.

The simulated results show that monthly recharge affects river leakage, however, river stage also affects river seepage. A sharp rise in river stage of several feet from snowmelt in December of 1994 (fig. 9) results in river seepage to the aquifer (shown by negative river seepage values on fig. 13). The sharp rise in river stage causes a gradient reversal between the river and ground water.

Hydraulic Conductivity

Evaluation of hydraulic conductivity of the aquifer and sensitivity of the model to this parameter focused on refining the distribution of hydraulic conductivity that was based on additional data from test borings and wells constructed between 1992 and

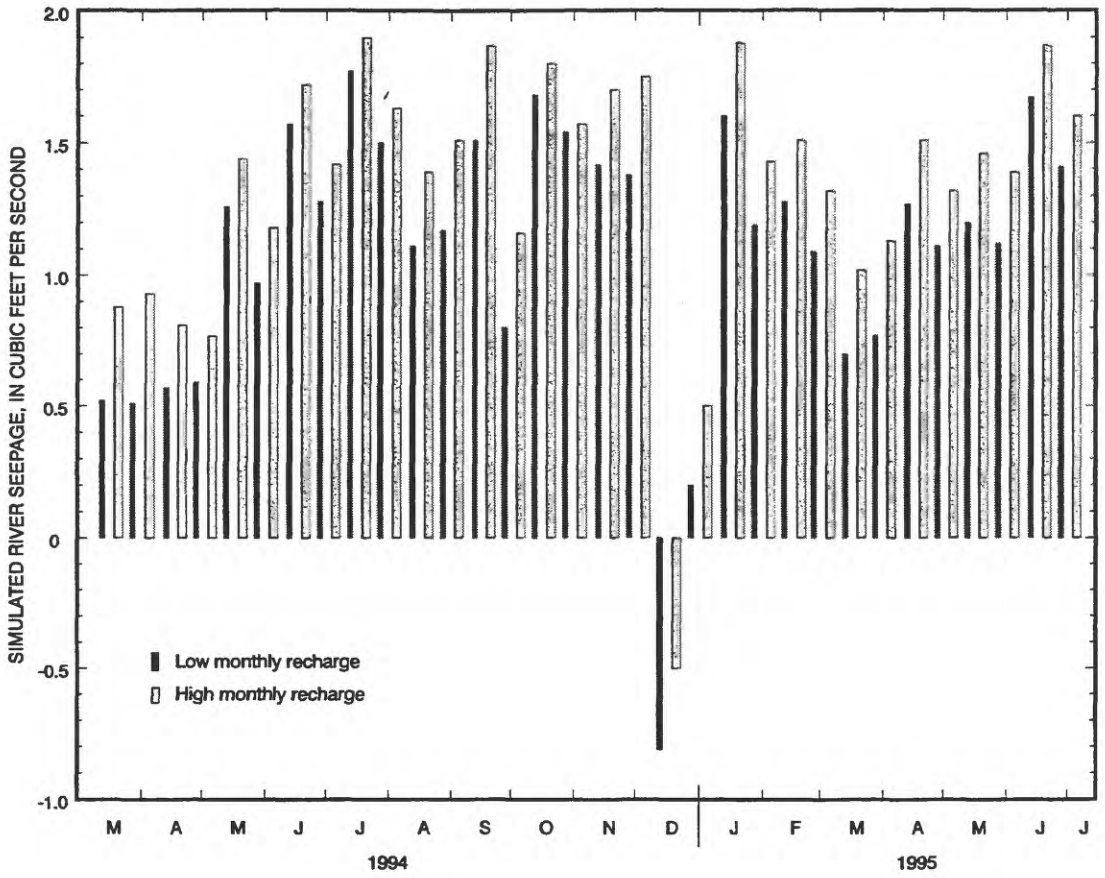

Figure 13. Computed river seepage from the transient-seasonal simulation for subbasin 4 of the Milford-Souhegan glacial-drift aquifer, Milford, New Hampshire. (Location of subbasin 4 is shown on plate 1.)

1997. These new data suggest that bulk hydraulic conductivity of the aquifer could be higher than original estimates from previous work (Harte and Mack, 1992). From this new information, several areas were identified where higher hydraulic conductivity than previously assigned were justified, including the lower layers of the aquifer near the contaminant source area, a high hydraulic conductivity zone in the upper layer of the aquifer by the contaminant-source area (cobble zone), and a high hydraulic conductivity zone by the State Fish Hatchery wells.

The observation that some increases in hydraulic conductivity was justified is also supported by earlier sensitivity analyses done by Harte and Mack (1992). Their work showed that a spatially-dependent, improved match between computed and observed heads occurred when hydraulic conductivity was universally increased from that used for the calibrated model. Specifically, 11 out of the 17 zones of uniform hydraulic conductivity in the aquifer showed an improvement (Harte and Mack, 1992, table 14). In contrast, an almost globally poor approximation of computed heads with observed heads occurred when hydraulic conductivity was universally decreased from the calibrated model. Differences between simulated and observed heads increased in 14 out of 17 hydraulic conductivity zones with a universal decrease in hydraulic conductivity.

Improved knowledge of hydraulic properties of the aquifer by the contaminant source area result from detailed geologic mapping of subsurface deposits by NHDES (Camp Dresser and McKee Inc., 1995). Information from more recent lithologic logs showed two features that differed from previous logs. First, lower layers of the aquifer were shown to consist of more permeable sands than were shown in previous logs of the area, which showed thick till deposits. Second, a permeable cobble zone was delineated in the upper layer of the aquifer (fig. 4B).

Increases in hydraulic conductivity of lower layers of the aquifer near the contaminant source area from 5 to 50 ft/d had a negligible effect on computed heads. The increases, however, affect travel times of average interstitial waters (advective transport of ground water) from the contaminant source area to final discharge locations. Steady-state tracking of ground-water particles was done for three zones of highly contaminated ground water (fig. 14) to evaluate the effects of increases in hydraulic conductivity on advective transport of contaminated ground water. Maximum travel times decreased five-fold from 63 to 12 years as a result of specifying high values of hydraulic conductivity in layers 4 and 5 of the aquifer for simulated 1994-95 average annual conditions. These differences in travel times are due to increases in computed ground-water velocity in the lower layers of the aquifer resulting from the use of high hydraulic conductivities for the lower layers.

A three-fold increase in hydraulic conductivity of the uppermost layer of the aquifer by the contaminant source area (cobble zone) from 150 to 450 ft/d has a small effect on computed heads and river seepage. Nevertheless, small improvements in the model result. The standard mean error of the steady-state model decreased from -1.68 to -1.47 ft at well MW-28 (well number 234, plate 1) when simulating the cobble zone. Well MW-28 has the largest difference between simulated and observed heads near the source area. Steady-state river seepages and recharge to the aquifer between gages P1 and P2 (plate 1) increased by 10 percent (from approximately 0.62 to 0.68 ft^3/s) when simulating the cobble zone. These results are more consistent with observed measurements of river leakage that show higher rates of observed river leakage (Harte and others, 1997) than computed river seepage.

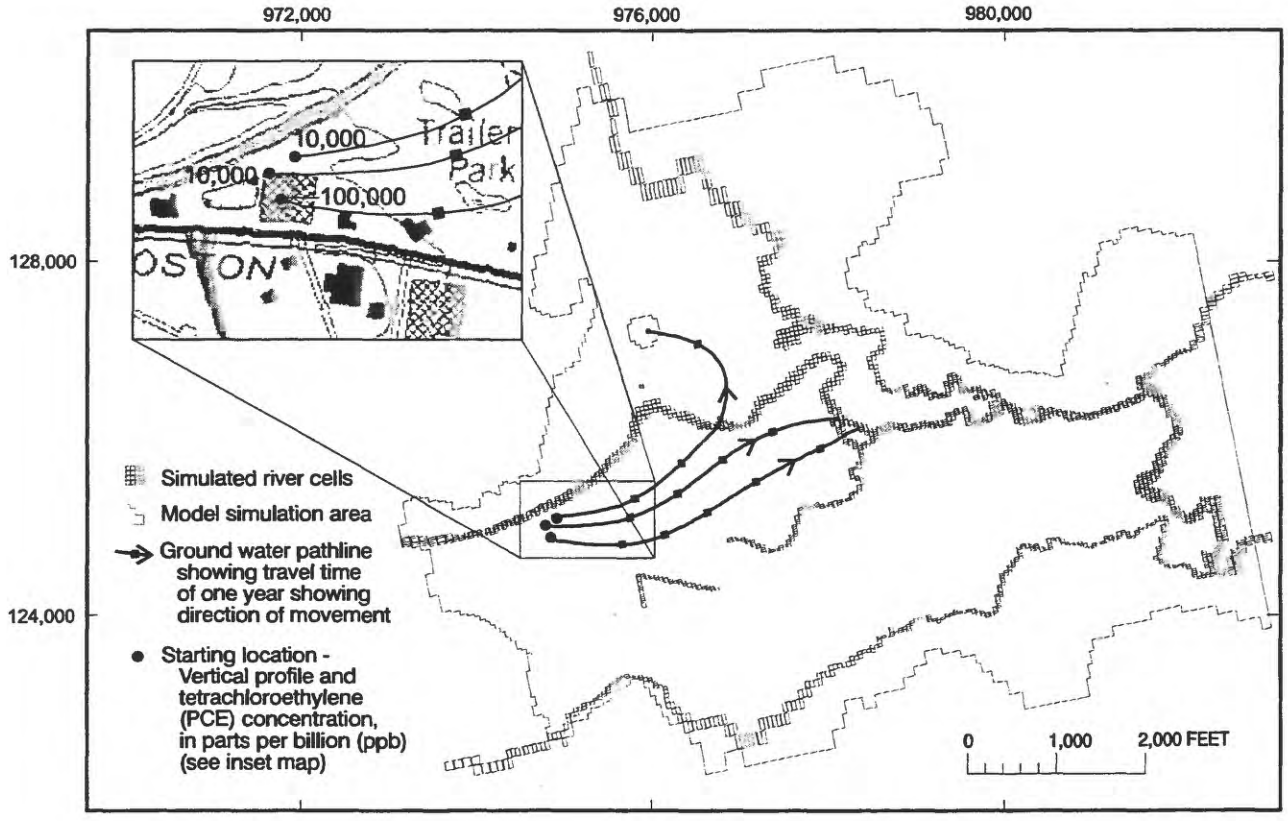

Figure 14. Steady-state simulation of advective transport of ground-water particles showing pathlines from high zones of contamination to final discharge locations, Milford-Souhegan glacial-drift aquifer, Milford, New Hampshire.

River-aquifer Interactions

River-aquifer interactions exert a major influence on ground-water flow in the aquifer. Perennial and ephemeral streams are sources of ground-water recharge in some areas of the aquifer, and in other areas they are sinks that receive ground-water discharge. Perennial streams in the model have the capability of exchanging large amounts of water to the aquifer because they are head-dependent boundaries. For this reason, accurate estimates of riverbed hydraulic parameters are needed to ensure accurate calculations of river seepage.

A previous analysis of steady-state river seepage in the aquifer showed that net river seepage was generally insensitive to increases in riverbed conductance (leakance multiplied by river area) but was adversely affected by decreases in riverbed conductance (Harte and Mack, 1992, p. 58). Therefore, additional model testing with the current model focused on evaluating simulations where increases in riverbed conductance were specified. Testing with the 1994 model showed that the net rate of river seepage generally was similar among model simulations with an increase in riverbed conductance greater than the final river conductance used for the model. Although the net rate of river seepage throughout the simulated aquifer and within subbasins in the aquifer showed little change with uniform increases in riverbed conductance, the amount of river seepage per individual model cell changed significantly.

Two steady-state simulations were made to evaluate the effect that increases in riverbed conductance had on model results. Riverbed conductances were increased by a factor of 2 and 10 from the base value. A comparison of head differences showed that the standard mean-head error and absolute mean-head error are similar between the base simulation and the simulation with conductance doubled. Head errors increased between the base conductance and the simulation with a 10-fold increase in conductance. Differences in net river leakage across the aquifer and within subbasins of the aquifer were negligible; however, the magnitude of river leakage into and out of the aquifer changed by 40 percent (table 7).

Computed aquifer recharge (streamflow loss) and discharge (streamflow gains) patterns along the Souhegan River are similar for the riverbed conductances evaluated. The distribution of computed river seepages of the Souhegan River shows that up to a

Table 7. Rates of river leakage for increases in riverbed conductance in the Milford-Souhegan glacial-drift aquifer, Milford, New Hampshire

[All units in ft^3/s; negative values indicate streamflow loss]

Steady-state simulation	River leakage		Net change in river leakage
	Into the aquifer (aquifer recharge)	Out of the aquifer (aquifer discharge)	
Base case	3.98	3.63	-0.35
Ten times riverbed conductance of base case	5.72	6.07	-0.35
Two times riverbed conductance of base case	4.19	3.92	-0.27

State Plane coordinate easting location of 977,800 ft on the Souhegan River (fig. 15, reach number 360, plate 1), river seepage into the aquifer occurs and the river recharges the aquifer. East of easting location 977,800 ft and reach number 360, aquifer discharge occurs for the base conductance (15A) and the simulation with a ten-fold increase in conductance. The largest rates of aquifer recharge from the river in both simulations occur by the State Fish Hatchery wells (FH-4, FH-5, plate 1) from withdrawals at these wells.

The general pattern of river seepage is similar for the riverbed conductances evaluated, but the magnitudes of river seepage differ for the two simulations. For the base simulation, withdrawals at the State Fish Hatchery (FH-4, FH-5, plate 1) cause smaller rates of aquifer recharge immediately adjacent to the well but induce greater rates of river leakage and aquifer recharge upstream of the State Fish Hatchery wells (between reach numbers 100 and 200, fig. 15A) than the simulation with increased riverbed conductance. Furthermore, downstream of the State Fish Hatcheries, aquifer discharges are much greater for the simulation with riverbed conductances at 10 times the base conductance than the simulation with the base conductance.

Although not shown in figure 15, differences in the rates of computed river seepage on the Souhegan River between the base simulation and the simulation with a two-fold increase in conductance are much smaller than those illustrated in figure 15. To help identify changes in model results caused by doubling the conductance, a spatial analysis of head differences

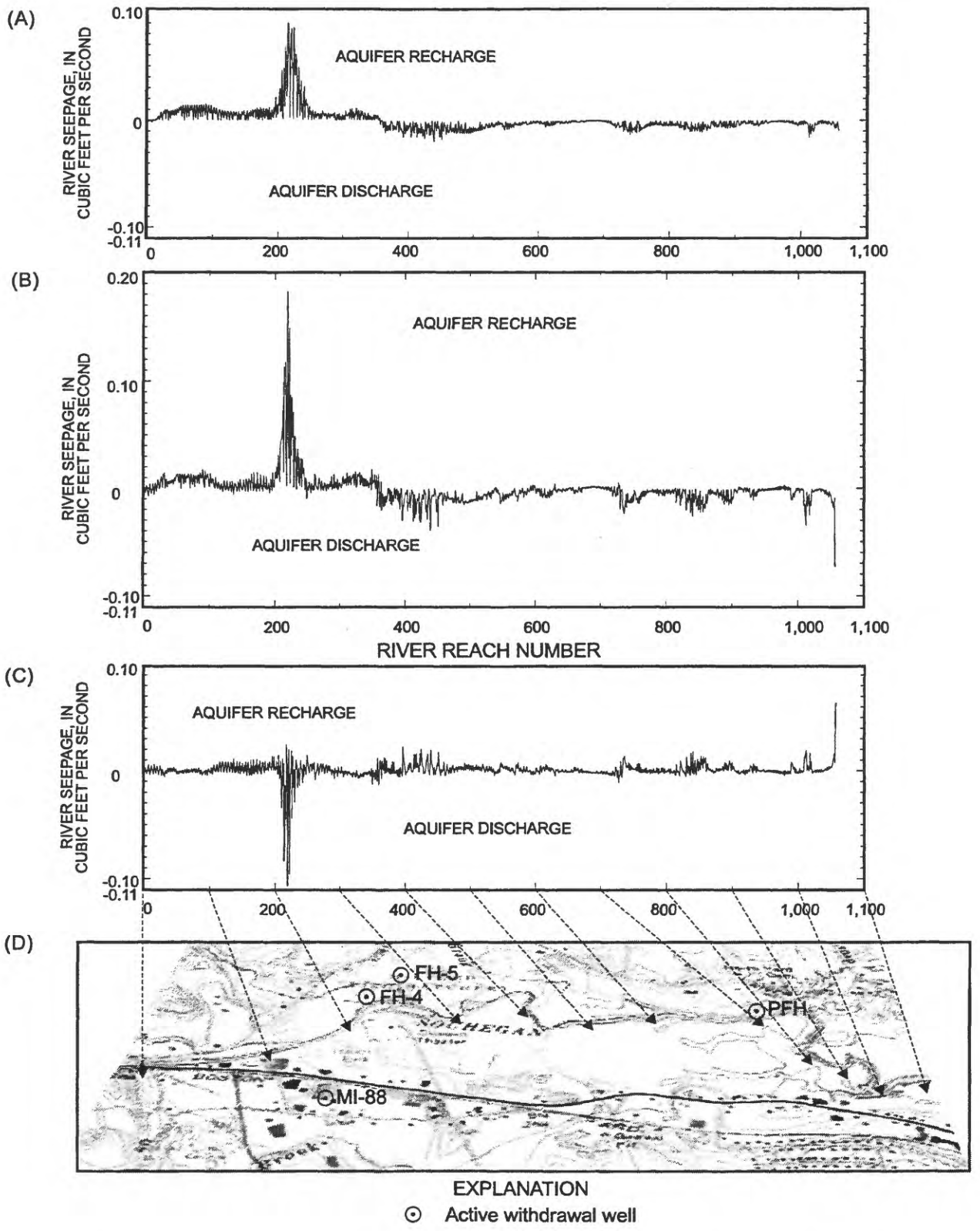

Figure 15. Model-computed river seepage for base riverbed conductance (A), ten-fold increase in riverbed conductance (B), difference in base value and ten-fold increase (C), and location map of simulated reach (D), Milford-Souhegan glacial-drift aquifer, Milford, New Hampshire.

was done between the base riverbed conductance and the simulation with a two-fold increase in riverbed conductance. Head differences between the two simulations are small and generally less than 1 ft (fig. 16). In general over most of the aquifer, computed heads from the simulation with a uniform two-fold increase in riverbed conductance do not match observed heads better than computed heads match observed heads from the simulation with base conductance. There are selected areas in the aquifer where some improvements in match did occur, namely by State Fish Hatchery wells, by well number 309, 307, and 209 (well cluster MW-1, appendices 2 and 4), and by some of the wells near the source area. Results imply spatial heterogeneity of riverbed conductance, such that an increase in riverbed conductance in upstream reaches of the Souhegan River and Tucker Brook, could improve model results.

Unlike the results from changing riverbed conductances, which generally had a small effect on computed heads, variations in river stage have a large effect on heads. Uniform increases in river stage caused an equivalent uniform increase in computed head. For example, a uniform river stage increase of 2 ft also caused an average rise in head of 2 ft. Furthermore, patterns and rates of river seepage were relatively unchanged with uniform increases in river stage, unlike variations in riverbed conductance that had a large effect on rates of river seepage.

Seasonal fluctuations in river stage also affect computed heads in the seasonal-transient simulations. The effect of river-stage fluctuations on computed heads is greatest near perennial streams, but river-stage fluctuations also affect computed heads further away from perennial streams. Two transient simulations were run to evaluate the effect that river-stage fluctuations have on computed heads. All model parameters in the two simulations were kept the same except for river-stage fluctuations, which were varied monthly based on observed river stages in one simulation and kept constant at the observed mean stage in the other. The results of the simulations are shown in figure 17 for well MI-18 (well number 29, plate 1). Fluctuations in river stage enhance fluctuations in computed heads and cause increases in computed heads by approximately 25 percent over computed heads for the constant river stage simulation during the spring of 1994 and 1995.

Storage Properties

Specific yield and storage coefficient were varied in the transient-seasonal model in a series of simulations to evaluate the effect of storage properties on model results. Values of storage that were tested represent the most probable ranges of storage given the types of sediments in the aquifer and degree of uncertainty of variations in aquifer properties. Specific yield was varied from 0.15 to 0.30 with an aquifer-wide base value of 0.23. Storage coefficient was varied from 0.00005 to 0.003, with a base value of 0.0003. The results of computed heads are shown in figure 18 for well MI-18 (well number 29, plate 1).

Fluctuations in computed heads using low to high values in storage are generally small and differ by less than 0.7 ft (fig. 18). From June 1994 to June 1995, when observed data are available for comparison, computed-head fluctuations (the difference between the minimum and maximum heads) ranged from 1.73 ft for high storage values, 2.05 ft for base storage values, and 2.42 ft for low storage values. The aquifer at well MI-18 (fig. 18) is more sensitive to variations in storage properties than areas that are closer to perennial streams. Near perennial streams, head fluctuations from variations in storage properties are smaller than fluctuations at locations further away from streams.

The analysis of the effects of storage properties of the aquifer on model results indicates that the transient-seasonal model of flow is less sensitive to uncertainties in this parameter than in the recharge parameter, and, therefore, the model is a useful tool in providing estimates of seasonal recharge. At well MI-18, and in other areas of the aquifer distant from perennial streams, variations in estimates of recharge caused a larger difference in computed heads than did variations in storage properties. For example, at well MI-18, the maximum difference in head between simulations of low and high recharge was 1.2 ft, whereas the difference in head from storage variations in storage properties was 0.7 ft.

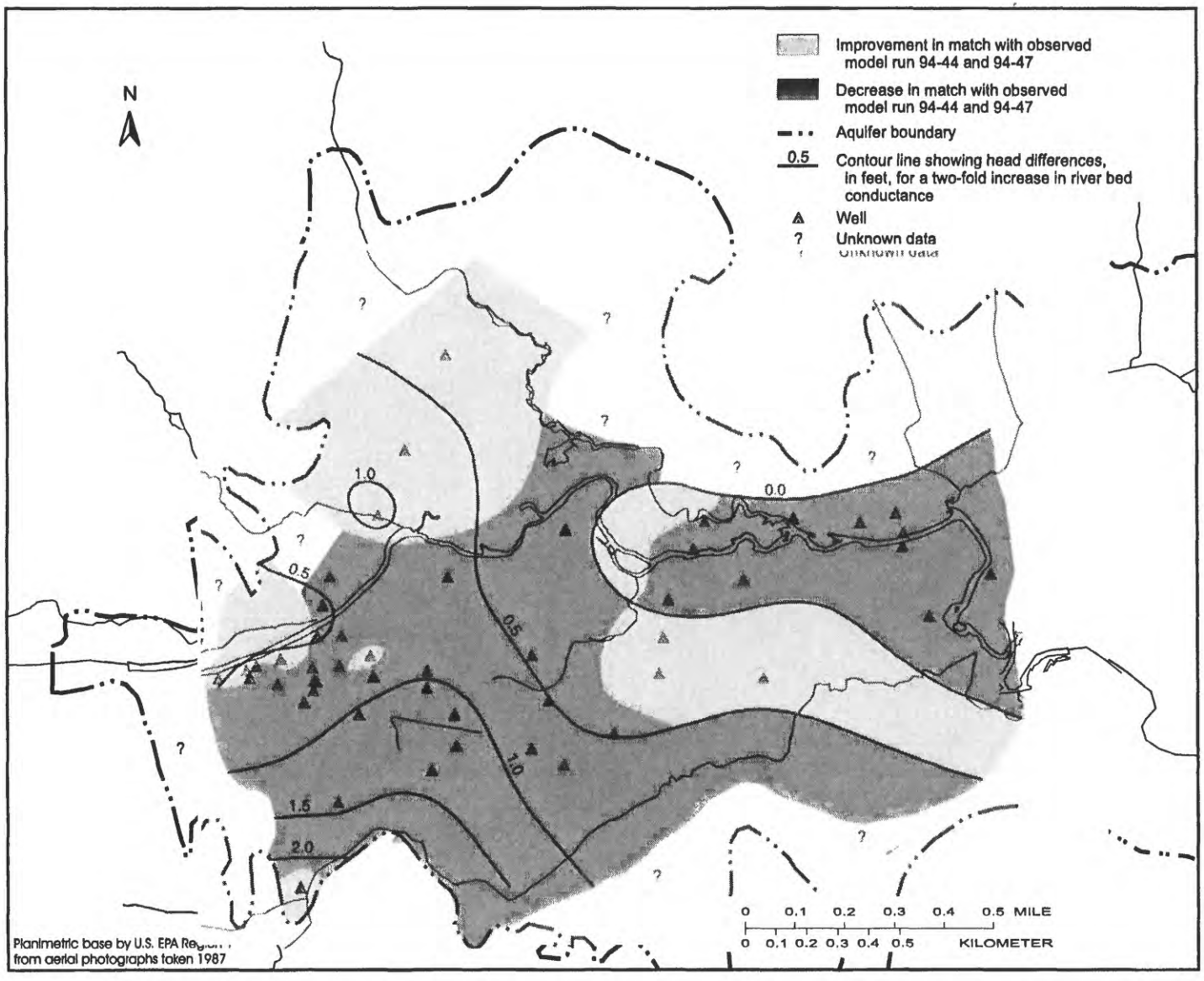

Figure 16. Differences in simulated head for a two-fold increase in riverbed conductance, Milford-Souhegan glacial-drift aquifer, Milford, New Hampshire. (Locations of wells are shown on plate 1.)

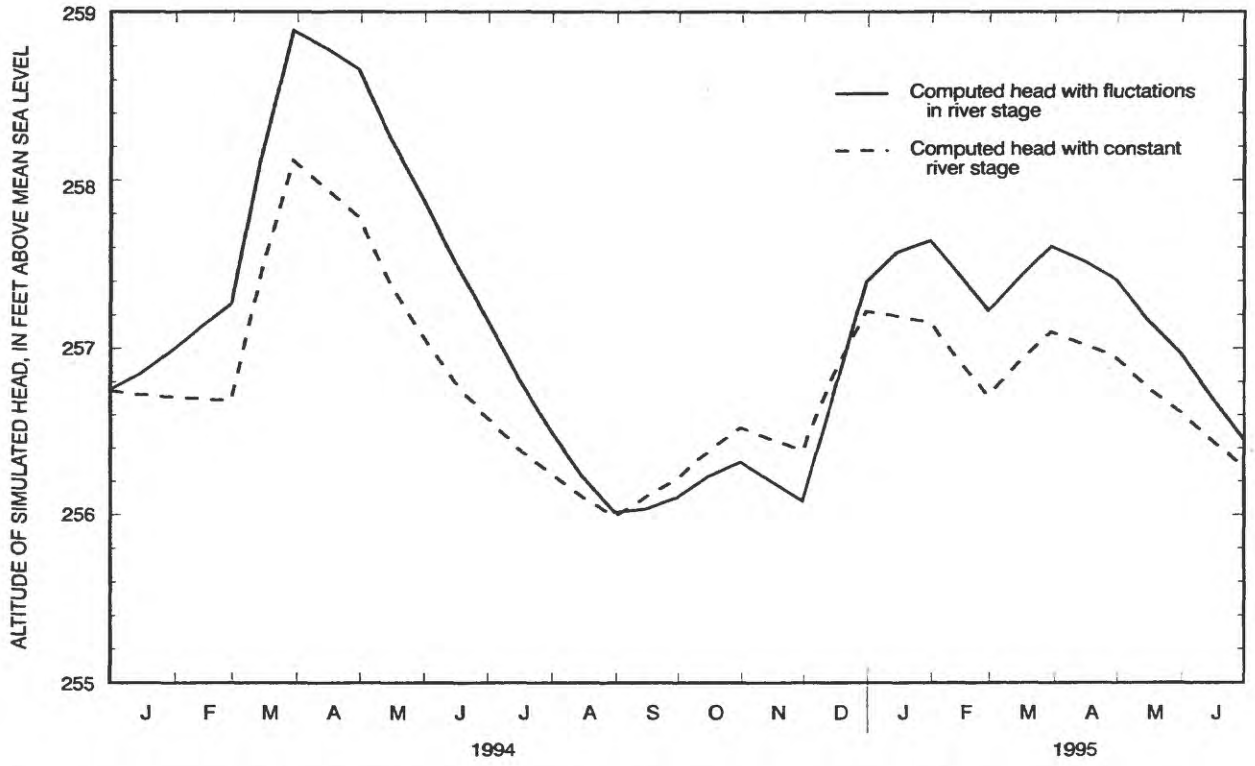

Figure 17. Transient model-computed heads at well MI-18 from simulated seasonal fluctuations in river stage, Milford-Souhegan glacial-drift aquifer, Milford, New Hampshire. (Location of well is shown on plate 1.)

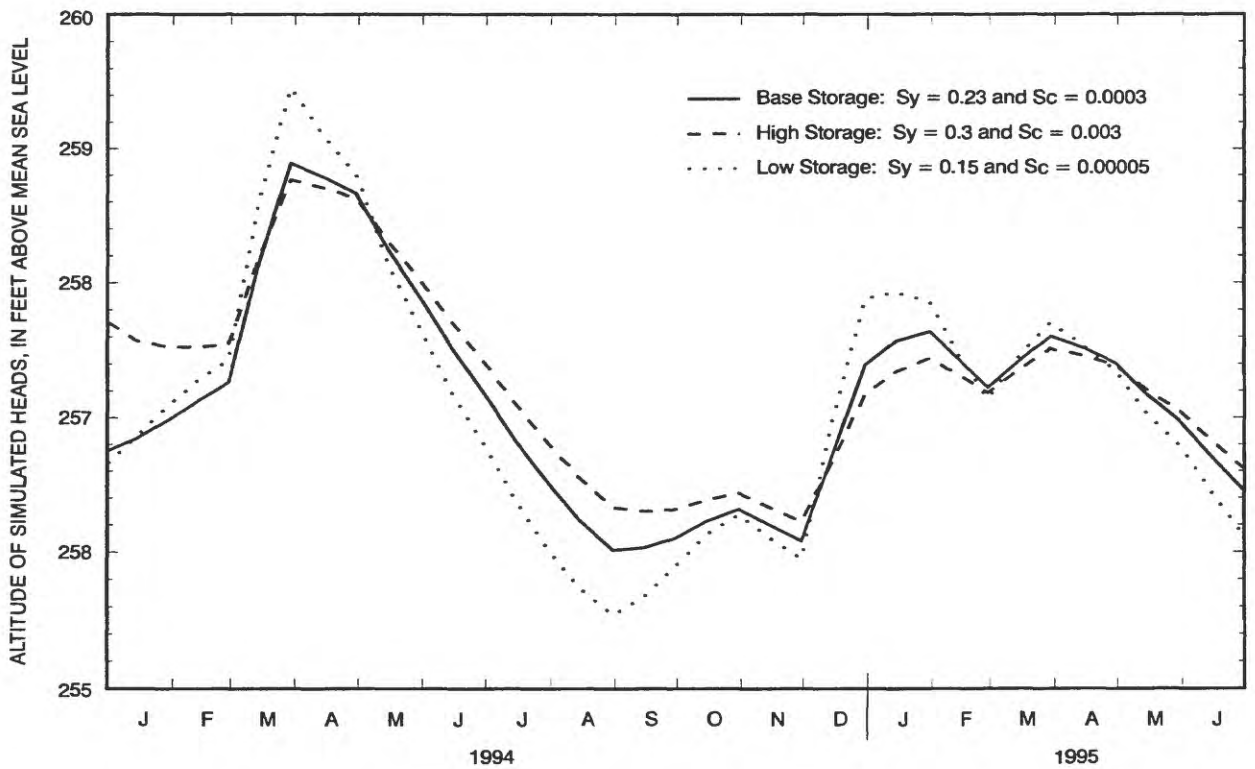

Figure 18. Transient-seasonal model-computed heads at well MI-18 from simulations of aquifer storage, Milford-Souhegan glacial-drift aquifer, Milford, New Hampshire. (Sy = specific yield, Sc = storage coefficient, Location of well is shown on plate 1.)

RESULTS OF SIMULATIONS WITH FINAL CALIBRATED MODEL

The final calibrated steady-state and transient-seasonal models use the same data-input values for model parameters of hydraulic conductivity, riverbed conductance, and altitude of riverbed, but use different values for model parameters that change with time, such as river stage, rates of ground-water recharge, and ground-water withdrawals. It is important to consider these differences when judging the adequacy of steady-state and transient-seasonal model performance.

Steady State

The final volumetric budget for the steady-state model is given in table 8. Large amounts of ground-water withdrawals from wells in the aquifer (4.18 ft^3/s) result in a net influx of 0.35 ft^3/s (computed from the difference between the input river seepage (3.98 ft^3/s) and the output river seepage (3.63 ft^3/s)) of river seepage into the aquifer (river loss).

Computed heads from the steady-state model closely approximate the arithmetic mean of the biweekly measured heads from the observed wells measured between June 1994 and June 1995 (appendix 3). The standard mean error is -0.12 ft, the absolute mean error is 0.59 ft and the root-mean-square residual (RMSE) is 0.89 ft. Head loss across the western aquifer is approximately 30 ft, therefore, an error of less than 1 ft represents a relative error of 3 percent. The 1994 model's approximation of observed heads is a significant improvement over the 1988 model's (Harte and Mack, 1992), which had a standard error of 0.78 ft and an absolute error of 1.81 ft when compared to observations of heads made in October of 1988 at 44 wells.

A spatial plot of head residuals shows that most computed heads (approximately 90 percent) are within 1.0 ft of observed heads (fig. 19). The largest difference in head is -4 ft (computed head less than observed head) and occurs at observation well FH5-obs (well number 240, plate 1), which is located within 5 ft of the State Fish Hatchery withdrawal well FH-5 (well number 208, plate 1). Large head differences are expected near withdrawal wells and the relatively poor match may be the result of several factors unrelated to model performance. These factors may include discrepancies between the location of the computed head, which in a finite-difference solution occurs at the cell's node, and the observed head, and the difference between a diffuse sink that is simulated in numerical models and a point sink that occurs in the field.

Computed vertical-head gradients are small and head differences are generally less than 0.01 ft between model layers. Observed vertical-head gradients from clustered wells in the aquifer generally show gradients between 0 to several tenths of a foot. The discrepancy between computed and observed vertical- head gradients is likely related to vertical heterogeneity in the aquifer that is not adequately represented by the model. Although model-computed head differences are small, the simulated model appear to approximate patterns of vertical flow in the aquifer (fig. 20) and show downward flow in recharge areas adjacent to areas of river seepage to the aquifer (such as near MW-11 cluster, well numbers 318 and 319, plate 1, appendix 2) and upward flow in discharge areas to the river (such as near MW-24 cluster, well numbers 255 and 333, plate 1, appendix 2).

Computed river seepages compare favorably with observed river leakages. Results of computed river seepage from two steady-state simulations using the 1994 model are given in table 9 and demonstrate the match between computed patterns and rates of river seepage and observed patterns and rates of river leakage. Observed river leakages are derived from

Table 8. Volumetric budget for the steady-state simulation (1994-95) of the Milford-Souhegan glacial-drift aquifer, Milford, New Hampshire

[Model area is 46, 011, 180 ft^2; ft^3/s, cubic foot per second; in/yr, inch per year (For conversion from ft^3/s to in/yr multiply by 8.2304)]

Inflow/ outflow	Source	Budget in ft^3/s	Budget in in/yr
Inflow	Eastern general-head boundary	0.67	5.5
	Wells	0	0
	Recharge	3.26	26.8
	River seepage	3.98	32.8
Outflow	Eastern general-head boundary	.10	.8
	Wells	4.18	34.4
	River seepage	3.63	29.9
Mass balance error		0	0

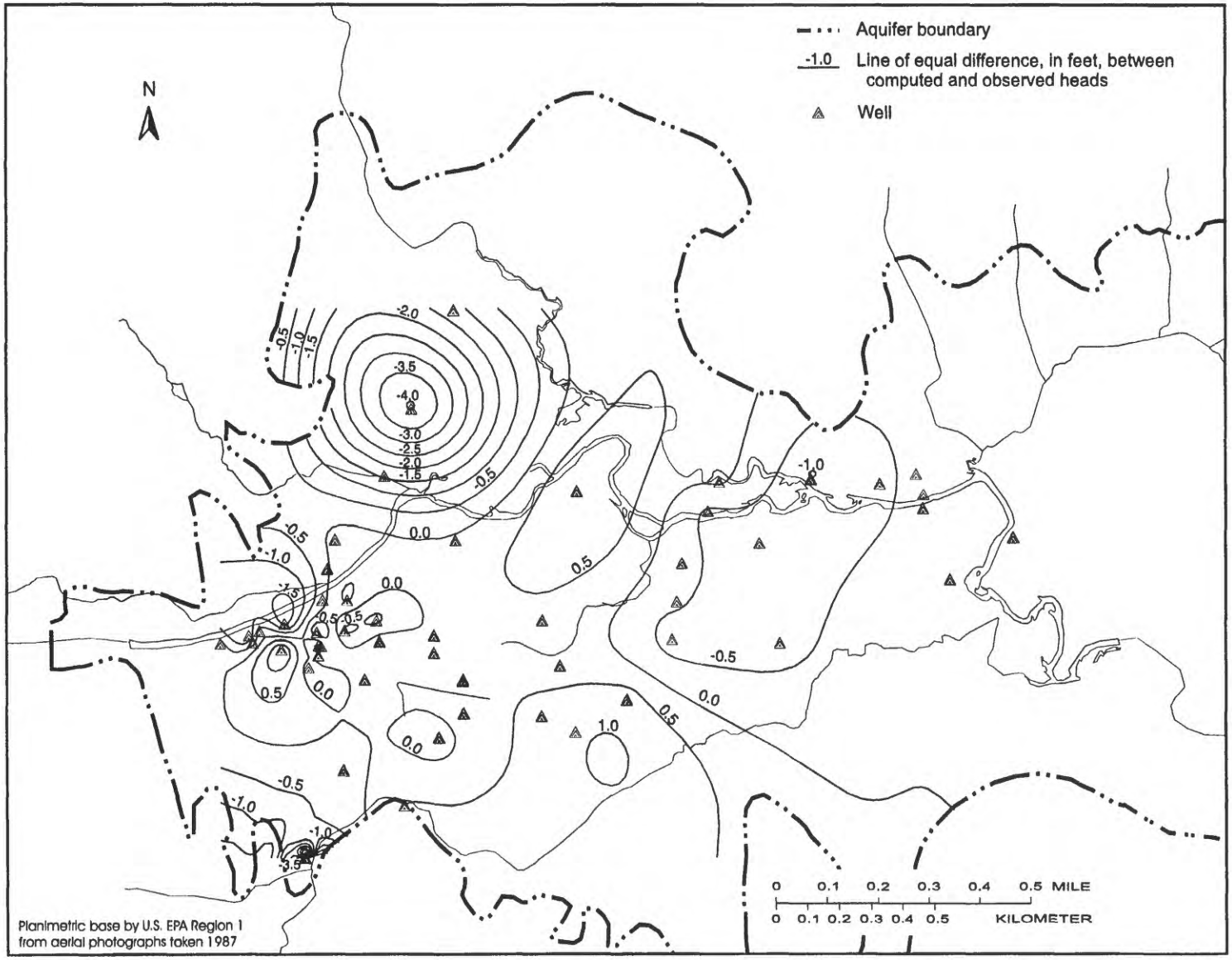

Figure 19. Head residuals (differences) between steady-state computed heads and observed heads calculated from the arithmetic mean of the biweekly measured water levels, Milford-Souhegan glacial-drift aquifer, Milford, New Hampshire. (Locations of wells are shown on plate 1.)

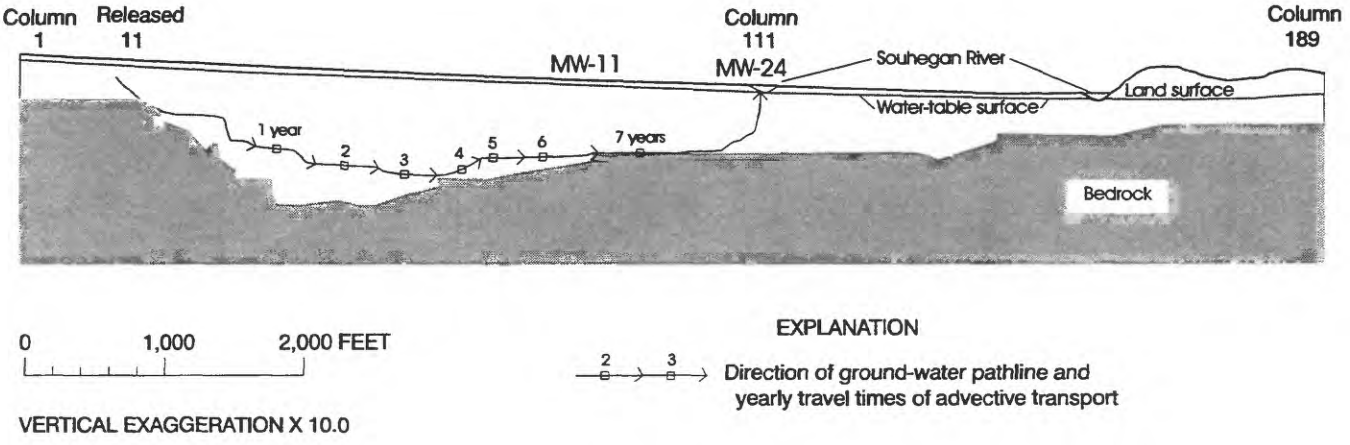

Figure 20. Cross section of steady-state advective transport of ground-water particle showing pathline projected along row 80, Milford-Souhegan glacial-drift aquifer, Milford, New Hampshire. (Row 80 location is shown on plate 2.)

Table 9. Summary of river seepages from steady-state simulations and measured river leakages in subbasins of the Milford-Souhegan glacial drift aquifer, Milford, New Hampshire

[All units are in cubic foot per second; negative value in column of measured net river leakage means streamflow loss; negative value in columns of computed river leakage mean aquifer recharge; computed river seepages from 1994 model]

Subbasin (plate 1)	Measured net river seepage 1988	Computed river seepage from simulation of 1988	Computed river seepage from simulation of 1994-95
2	-0.18	0.24	0.28
3	0.05	0.29	0.25
4	1.58	1.56	1.44
5	-0.27	-0.77	-0.67
6	-0.73	-1.41	-1.22
8	-0.31	0.10	-0.05
9	-0.47	-0.38	-0.33

streamflow measurements made in October of 1988. The values of river leakage represent net river leakage within subbasins of the aquifer (the location of subbasins are shown in plate 1). The results presented in table 9 are from two steady-state simulations, 1994-95 conditions, discussed in this report, and October 1988 conditions, discussed in Harte and Mack (1992). The two simulations differ in simulated ground-water withdrawals. The simulation results of October 1988 allow for a direct comparison between computed river seepage and observed river leakage because aquifer withdrawals changed between 1988 and 1994-95, and consequently, these changes affected patterns and rates of river seepage. Specifically, withdrawals decreased in industrial wells MI-88 and MI-33 (well numbers 395 and 47, fig. 2 and plate 1), and increased in private fish hatchery well PFH and State Fish Hatchery well FH-4 (well number 354 and 87, fig. 2 and plate 1). The average rate of withdrawal in 1988 was 4.38 ft^3/s and in 1994 it was 4.18 ft^3/s. Computed river seepages from the simulation of 1988 show greater recharge from rivers, river seepage from rivers into the aquifer (streamflow loss), than the amount of river recharge from 1994-95.

Computed-river seepages also were compared to the arithmetic mean of observed river leakages from multiple streamflow measurements made in 1994-95 between river-gaging stations P1 and P2. Computed-river seepage between gages P1 and P2 is significantly smaller (-0.63 ft^3/s; negative indicating streamflow loss and potential aquifer recharge) than the observed arithmetic mean of the difference between 13 coupled measurements of streamflow (-5.5 ft^3/s). The procedure for computing river leakage from coupled streamflow measurements is discussed in detail in Harte and others (1997). The nine-fold difference between simulated and observed is not attributed to uniform increases in riverbed conductance or aquifer hydraulic conductivity because these parameters were varied by factors of 10 and 3, respectively, with only minor differences in computed river seepage (less than several tenths of ft^3/s). Rather, the large difference is

attributed to (1) the inducement of large river leakage during short-term (less than 24 hours) hydrologic conditions that are not adequately simulated under average annual steady-state conditions, and (2) vertical heterogeneity of aquifer hydraulic conductivity. For example, with regard to the former, discrete hydrologic events such as sharp increases in river stage during high streamflow conditions, will induce large amounts of river leakage into the aquifer. Several of the coupled streamflow measurements were made during high streamflow (flow duration of 35 percent or less). These events are averaged and thus not represented in steady-state models nor in transient models with time discretizations greater than one day. Therefore, the impact of discrete hydrologic events on the ground-water system can not be assessed with this model. The effect of vertical heterogeneity on river leakage is discussed in the section on the transient-seasonal model.

Steady-state advective transport of ground-water particles were tracked forward from the 1,000 ppb line of equal concentration distribution of tetrachloroethylene (PCE) from 1989 (fig. 10) for 5 years and compared to the 1994 distribution of PCE. During this period, increases in withdrawals at the State Fish Hatchery wells and decreases in withdrawals at wells along the southern part of the plume have caused a northward shifting of ground-water pathlines (Harte and Willey, 1997). Comparing advective transport of particles to the plume during this period helps constrain average interstitial velocities of the flow model and also helps to identify the role advective transport plays in contaminant transport. For example, if advective-transport velocities in the flow model were too slow, pathlines would be significantly slower than the observed plume. Tracked ground-water particles started in 1989 shifted about 2 times the distance after 5 years than the observed 1,000 ppb line-of-equal concentration did in 1994 (fig. 21). It appears that the computed advective transport pathlines respond quicker than the observed plume suggesting some retardation of contaminants.

Transient Seasonal

Seasonal ranges in the volumetric budget for the final-calibrated transient model of seasonal conditions are significant and show a lag effect between aquifer recharge and discharge of ground water to the river (table 10). Largest amounts of recharge occur in the fall and winter seasons for the simulated period (June 1994-95). In contrast, the largest amounts of ground-water discharge to the rivers occurred in winter and spring. Therefore, the increases in fall recharge appear to affect aquifer discharge the most in the following season. The lag effect reflects the ability of the aquifer to store recharge and is most evident in the fall because recharge in the fall replenishes the low storage of ground water in the aquifer caused by the preceding low rates of recharge in the summer. As a result, maximum increases in storage occur in the fall.

Summation of components of the seasonal volumetric budget shows there is a small change in aquifer storage during the simulated period of June 1994-95. The total for storage is 0.93 ft^3/s, which equals an average annual rate of 0.23 ft^3/s; therefore, water from storage is being released over the annual cycle at a rate of 0.23 ft^3/s. Compared to the summation products of the other budget components, water in storage represents a small part (only 5.5 percent) of available sources of water. Recharge, river leakage, and water from the eastern boundary are the primary sources of water and contribute 74, 9.5, and 11 percent of water respectively.

Results of the analysis of seasonal volumetric budgets suggests that a true average annual steady-state condition probably does not exist because a net storage change occurs over the annual cycle. The amount of storage change is relatively small and the system is in dynamic equilibrium. This is probably a typical storage response of this type of aquifer because the aquifer is permeable and recharge boundaries like the river supplement storage and force quick equilibration of the system.

Use of the seasonal-transient model adequately approximates[6] observed-head fluctuations from biweekly measurements of heads at observed wells (table 11). Seasonal comparisons of simulated and observed heads show that the largest average head difference between computed and observed occurs in the fall of 1994.

A statistical summary of variations in the direction and slope of simulated maximum ground-water hydraulic gradients from seasonal conditions (June 1994-95) is given in table 12. Model-computed and observed heads were analyzed by triangular grouping of wells (fig. 22) to allow for computation of direction and slope of maximum ground-water hydraulic gradients by three-point planar solution (Johnston and Harte, 1998).

[6]An example of head comparisons between computed and observed can be seen in appendix 5.

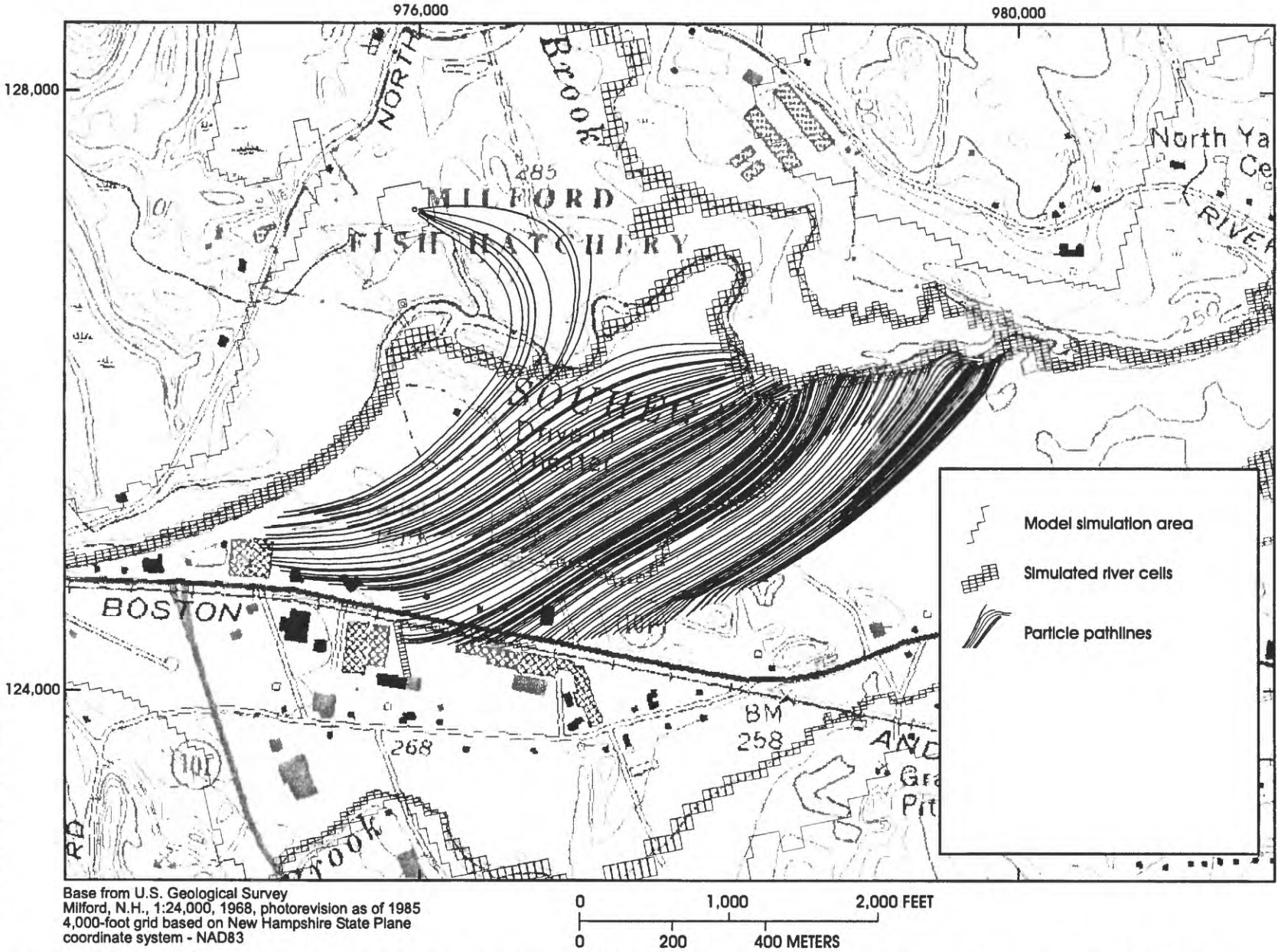

Figure 21. Steady-state advective transport of ground-water particles showing pathlines from 1,000 ppb line of equal concentration of PCE in 1989 (overlay A), and 1994 PCE concentrations (overlay B), to discharge locations in 1994, Milford-Souhegan glacial-drift aquifer, Milford, New Hampshire. (PCE = tetrachloroethylene; ppb = parts per billion)

Table 10. Volumetric budget from June 1994-95 from the transient-seasonal-model simulation of the Milford-Souhegan glacial-drift aquifer, Milford, New Hampshire

[Model area is 46, 011, 180 ft^2; ft^3/s, cubic foot per second; in/yr, inch per year; For conversion from ft^3/s to in/yr multiply by 8.2304; positive value means recharge to the aquifer; negative value means discharge of water from the aquifer; a positive value for storage means water coming out of storage while a negative value means water going into storage]

Budget components	Net volumetric budget, in ft^3/s				Cumulative budget, in ft^3/s
	Summer 1994	Fall 1994	Winter 1994-95	Spring 1995	
Storage	1.15	-2.93	0.84	1.87	0.93
Wells	-4.39	-4.39	-4.16	-4.05	-16.99
Recharge	1.21	4.71	4.25	2.38	12.55
River seepage	1.09	2.29	-0.95	-0.82	1.61
Eastern general-head boundary	0.93	0.32	0.03	0.57	1.85

Table 11. Differences between computed seasonal mean heads and observed seasonal mean heads from the transient-seasonal-model simulation of the Milford-Souhegan glacial-drift aquifer, Milford, New Hampshire

[All units are in feet. Negative numbers mean simulated heads are below observed heads in biweekly measurements of heads in observed wells, appendix 3]

Season	Standard head difference	Absolute head difference
Summer, 1994	0.03	0.55
Fall, 1994	0.29	0.62
Winter, 1994-95	-0.01	0.71
Spring, 1995	-0.10	0.62
Annual	0.05	0.63

Table 12. Statistics from model-computed and observed direction and slope of maximum ground-water hydraulic gradients from triangular grouping of wells, June 1994-June 1995, Milford, New Hampshire

[Triangle locations are shown in figure 22; to convert slope, in degrees, to slope in foot per foot, take the tangent of the value of slope in degrees; triangles listed in descending order of standard deviation]

Direction of maximum ground-water gradient					Triangle	Slope of maximum ground-water gradient			
	Observed		Model computed			Observed		Model computed	
Triangle	Mean direction, in degrees from true north	Standard deviation	Mean direction, in degrees from true north	Standard deviation		Mean slope, in degrees	Standard deviation	Mean slope, in degrees	Standard deviation
M	86.3	50.9	52.5	7.1	D	0.537	0.113	0.682	0.125
J	77.2	33.9	127.5	8.3	B	.429	.084	.360	.013
B	131.5	4.3	81.0	4.6	M	.206	.078	.137	.030
D	11.0	9.4	3.9	7.5	A	.401	.056	.287	.026
H	52.3	5.6	63.0	4.8	J	.131	.032	.181	.031
E	86.8	5.1	87.8	4.2	E	.207	.026	.188	.006
C	75.5	4.3	70.1	3.1	N	.223	.020	.184	.005
A	125.4	4.1	110.8	3.5	H	.258	.018	.173	.003
N	82.0	3.2	55.4	6.8	K	.184	.011	.183	.007
G	67.9	2.9	68.6	4.3	G	.142	.008	.235	.008
I	31.2	2.5	52.6	2.7	I	.177	.007	.244	.011
K	52.8	2.2	55.1	5.2	F	.196	.007	.223	.013
F	48.9	2.1	41.6	2.6	L	.191	.006	.202	.009
L	53.8	1.6	57.5	4.1	C	.273	.003	.252	.006

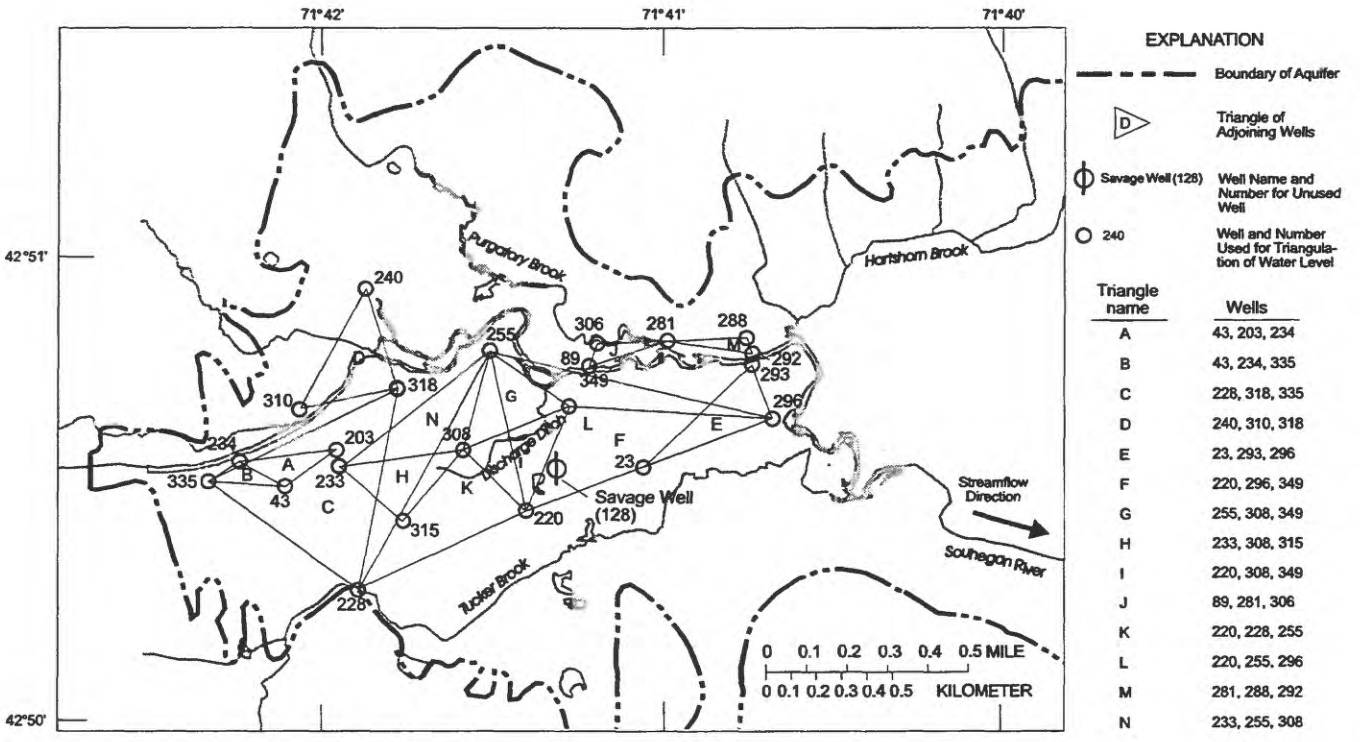

Figure 22. Triangular groupings of biweekly measured wells for determination of model-computed and observed ground-water hydraulic gradients, Milford-Souhegan glacial-drift aquifer, Milford, New Hampshire. (From Harte and others, 1992)

The transient-seasonal model adequately approximates the observed direction of maximum slope in most areas of the model except three: the area west and upgradient of the source area (triangle B), by the confluence of Purgatory Brook and the Souhegan River (triangles J and M), and the northcentral part of the contaminant plume (triangle N). The maximum difference between the model-computed and observed directions of maximum gradient occurs at triangle B (table 12). A possible explanation for the difference in direction is inadequate specification of river stage in the model, which linearly slopes between gaging stations P1 and P2 (plate 1). The presence of riffles and pools between P1 and P2 on the Souhegan River supports the fact that the river slope is not linear and that a non-linear slope of the river probably would produce a better match. At triangles J and M, two possible factors that could be attributed to the discrepancy are (1) inadequate specification of river stage along Purgatory Brook and (2) oversimplification or lack of aquifer heterogeneity. These factors cause the advective transport of ground water to completely discharge to the Souhegan River rather than be partially transported underneath the Souhegan River as indicated by the observed chemical data.

Simulated slopes of maximum gradients from triangular groupings of wells are fairly evenly split between being greater than or less than the observed maximum gradients and, therefore, show no strong deficiency of the model to approximate observed conditions. The maximum difference between model-computed and observed slope is located downgradient from the source area (triangle A). The computed gradient is -0.114 degrees (-0.002 ft/ft) less than the observed gradient (0.007 ft/ft), a difference of 29 percent.

The observed slope of maximum gradient at triangle A is negatively correlated (-0.88) with the height of the water table (fig. 23). Lowest gradients occur with the highest positioning of the water table

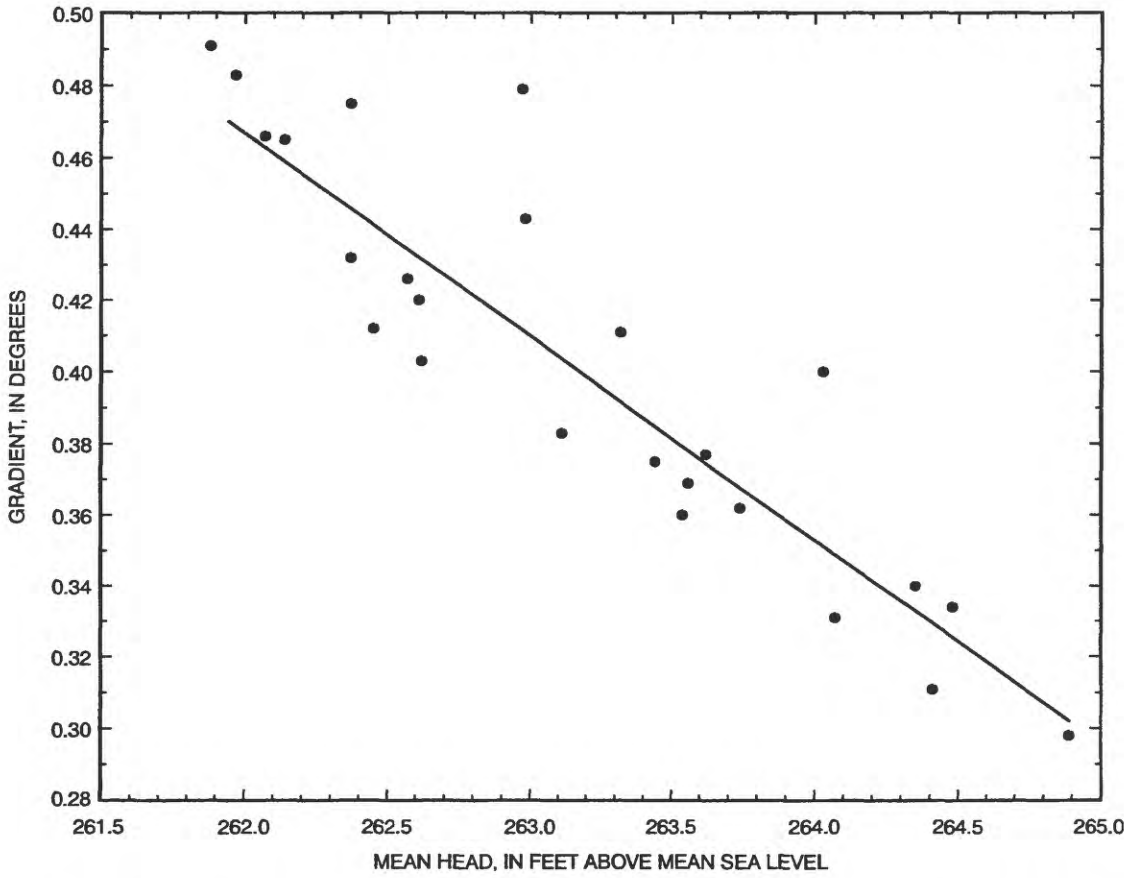

Figure 23. Ground-water gradients in relation to positioning of the water-table surface for triangle A, Milford-Souhegan glacial-drift aquifer, Milford, New Hampshire. (For location of triangle A, refer to figure 22.)

(the positioning of the water table was computed from the mean water level from the three wells comprising triangle A and is specified as the mean head in the abscissa of figure 23. Because the upper aquifer at the source area contains cobble deposits and these deposits are only partially saturated during conditions of average to below-average water levels, the degree of saturation of the cobble zone could control gradients. The lithologic evidence suggests the aquifer is vertically heterogeneous, with the greatest hydraulic conductivity near the top of the aquifer. With this type of hydraulic-conductivity distribution, the bulk transmissivity of the aquifer is highly sensitive to the position of the water table. As the water table rises, large increases may occur in the bulk transmissivity of the aquifer producing a decrease in hydraulic gradient.

Computed river seepage into the aquifer between gaging stations P1 and P2 ranges from 0.34 to 1.19 ft^3/s (fig. 24A). Maximum river seepage occurred in December of 1994 and minimum river seepage in January 1995. The computed range in river seepage is much lower than the observed-river leakage (measured) range. Whereas seepage is comprised only of ground-water recharge and discharge to the river, leakage can include other processes such as runoff and back storage. Field data indicate a minimum leakage of -6.6 ft^3/s (discharge to the river) and a maximum leakage of 23 ft^3/s (recharge to the aquifer) (fig. 24B). Time discretization, as well as vertical heterogeneity, also causes an underestimation of simulated variability in river leakage. A coarse time discretization with relatively large time steps, as used in the transient-seasonal model, reduces computed variability.

The transient-seasonal model simulates 15-day periods of time with constant monthly parameters and stresses (except in September 1994). This time step tends to average the effects of short-term responses in the aquifer to hydrological events. One of the most

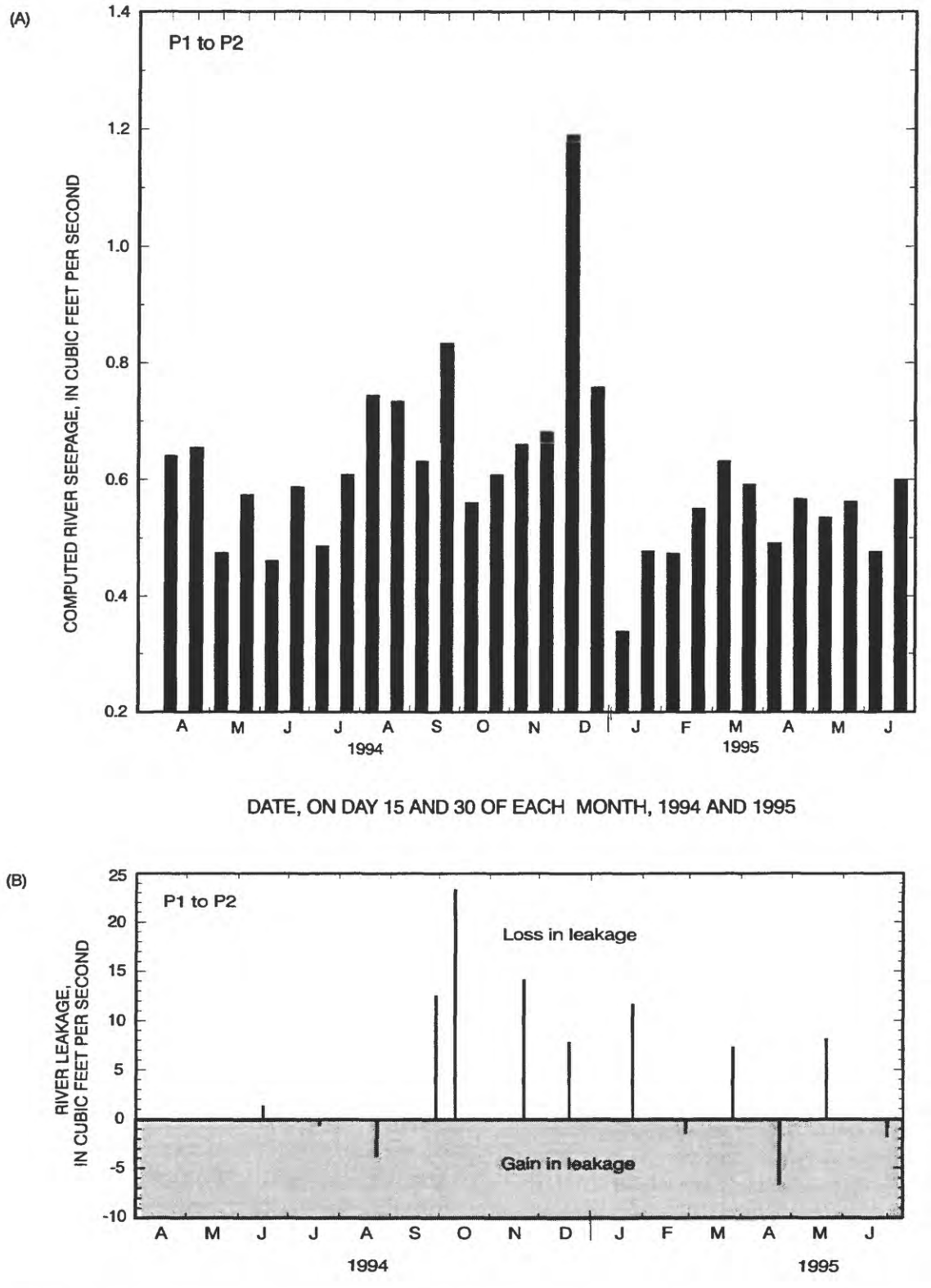

Figure 24. Model-computed river seepage between river gaging stations P1 and P2 for transient-seasonal simulation (A), and measured river leakage for the same reach (B), Milford, New Hampshire.

important factors in river seepage to the aquifer is the rate at which river stage increases relative to the rise of ground-water levels. High rates of river leakage into the aquifer will occur in losing river reaches when river stages increase quickly relative to ground-water levels. Because river stage is averaged over a monthly period and the minimum time step is 15 days, variations in river leakage are underestimated by the model. To test this hypothesis, time-discretization was increased in December of 1994 to simulate the observed rise in river stage over a single day, instead of a month. The increased time discretization alone resulted in a computed river seepage 3-times the 15-day rate of 1.19 ft^3/s. It is expected that further refinement of time steps would increase seepage.

SUMMARY AND CONCLUSIONS

The Milford-Souhegan glacial-drift aquifer (MSGD) aquifer is highly permeable with relatively rapid advective transport. The western half of the aquifer is contaminated by a plume of volatile-organic compounds (VOC's), primarily tetrachloroethylene (PCE), that covers a 0.5 mi^2 area. The primary source of contamination was from a discontinued tool company that discharged contaminants into the subsurface for many years until the early 1980's. Although these discharges have ceased, contaminants continue to desorb from the underlying sediments, and immiscible fluids continue to contaminant ground water flowing under the site.

This report summarizes construction and calibration of three-dimensional, steady-state and transient numerical ground-water flow models that will be used to help in the design of a remediation plan, and to monitor the VOC plume. The model area covers 1.65 mi^2, has more than 70,000 active cells with smallest cell sizes of 25 by 50 ft, and consists of 5 model layers of approximately 20-feet thick. The steady-state model closely approximates observed heads and river leakages throughout much of the aquifer. Most computed heads are within 1.0 ft of observed heads computed from the arithmetic mean of biweekly measured heads for one year. Steady-state river leakages also match observed river leakages fluxes from one round of measurements of river leakages. The calibrated transient model, which simulates seasonal conditions, showed that annual recharge to the aquifer is approximately 60 percent of precipitation. Recharge is nonuniformly distributed throughout the year and most recharge occurs when evapotranspiration is negligible. This causes large seasonal variations in recharge and discharge of ground waters. Seasonal variations in ground-water flow are also highly affected by variations in river stage, which cause large changes in the direction of ground-water flow and changes in the slope of maximum hydraulic gradients. Simulated flow (seepages and gradients) varied the most near the river.

The transient-seasonal model closely approximates the observed-head fluctuations in the aquifer. The largest differences between model-computed and observed heads were those for the fall of 1994 (standard-mean-head error of 0.29 ft). The transient model underestimates the observed variation in river leakages, partly because leakages incorporate other processes besides ground-water flow, but also because of the 15-day time step used in the transient model. Computed river seepages varied by a factor of 10 while the observed leakages varied by a factor of several hundred at one losing river reach where more than 13 coupled measurements of streamflow were made throughout the year. The unfavorable comparison suggests that the time discretization of the transient model can be used to estimate fluctuations in head, but cannot estimate the short-term dynamics of river-aquifer systems.

Ground-water flow and advective transport throughout most of the aquifer and contaminant plume area can be estimated using the transient-seasonal model. Several modeling deficiencies were detected that warrant further analysis; these are (1) a tendency for computed discharges to the Souhegan River in the area by the confluence between the Souhegan River and Purgatory Brook (see the area by triangle J in figure 22) to be greater than observed, (2) low computed heads in the State Fish Hatchery area could cause a more northerly trajectory of ground-water flow than observed in the northcentral part of the plume (see the area by triangle D in figure 22), and (3) the river stage and the vertical heterogeneity of the aquifer near the source area of the plume (see the area by triangle B in figure 22) is oversimplified. Possible solutions to reduce these discrepancies include (1) collecting additional river stage information in the areas near the source area and the confluence of the Souhegan River and Purgatory Brook to validate model input, and (2) incorporating spatially variable vertical heterogeneity into the model in the above mentioned areas.

SELECTED REFERENCES

Camp, Dresser, and McKee, Federal Programs Corporation, 1995, Final report of vertical contaminant profiling, Savage Municipal Supply Well, Superfund site-OU1, Milford, New Hampshire: Boston, Mass., Camp, Dresser, and McKee, Inc., Federal Programs Corporation, November 1995, 5 chaps., 5 apps.

Camp, Dresser, and McKee, Inc., 1996, Conceptual remedial design report for OK tool source area, Savage Municipal Supply Well, Superfund site-OU1, Milford, New Hampshire: Cambridge, Mass., Camp, Dresser, and McKee, Inc., March 1996, vol. 1, 5 chaps.

Chapelle, F.H., 1993, Ground-water microbiology and geochemistry: John Wiley and Sons, Inc., New York, 424 p.

Coakley, M.F., Keirstead, Chandlee, Brown, R.O., and Hilgendorf, G.S., 1997, Water resources data New Hampshire and Vermont water year 1996: U.S. Geological Survey Water-Data Report NH-VT-96-1, 189 p.

Environmental Science and Engineering, Inc., 1995, Results of vertical profiling program Savage Municipal Water Supply Superfund Site: Amherst, N.H., Environmental Science and Engineering, Inc., 3 chaps.

———1997a, Final results of vertical profiling program Savage Municipal Water Supply Superfund Site: Amherst, N.H., Environmental Science and Engineering, Inc., Feb. 1997, 25 p.

———1997b, Draft ground-water modeling report Savage municipal water supply well superfund site, Milford, New Hampshire: Nashua, N.H., QST Environmental, appendix E.

Harte, P.T., and Willey, R.E., 1997, Effects of historical withdrawals on advective transport of contaminated ground waters in a glacial-drift aquifer, Milford, New Hampshire: U.S. Geological Survey Fact Sheet 162-97, 6 p.

Harte, P.T., Flynn, R.H., Kiah, R.G., Severance, Timothy, and Coakley, M.F., 1997, Information on hydrologic and physical properties of water to assess transient hydrology of the Milford-Souhegan glacial-drift aquifer, Milford, New Hampshire: U.S. Geological Survey Open-File Report 97-414, 96 p.

Harte, P.T., and Mack, T.J., 1992, Geohydrology of, and simulation of ground-water flow in the Milford-Souhegan glacial-drift aquifer, Milford, New Hampshire: U.S. Geological Survey Water-Resources Investigations Report 91-4177, 90 p.

———1996, Effects of model discretization on zones of contribution to low pumping-rate wells in a hypothetical river-valley aquifer in hydrology and hydrogeology of urban and urbanizing areas: St. Paul, Minn., American Institute of Hydrology, p. GWQE42-GWQE56.

HMM Associates, Inc., 1989, Draft remedial investigation, Savage well site, Milford, New Hampshire: Concord, Mass., no. 2176 HAZ/2880, 218 p.

———1991, Remedial investigation, Savage well site, Milford, New Hampshire: Concord, Mass., no. 2176 HAZ/4814, 800 p.

Johnson, A.I., 1967, Specific yield-computations of specific yields for various materials: U.S. Geological Survey Water-Supply Paper 1662-D, 74 p.

Johnston, C.M., and Harte, P.T., 1998, Documentation and application example of a simple method to compute the maximum slope and direction of hydraulic head: U.S. Geological Survey Water-Resources Investigations Report 98-4021, 25 p.

Koteff, Carl, 1970, Surficial geologic map of the Milford quadrangle, Hillsborough County, New Hampshire: U.S. Geological Survey Geologic Quadrangle Map GQ-881, scale 1:62,500.

Lyons, J.B., Bothner, W.A., Moench, R.H., and Thompson, J.B., 1997, Bedrock geologic map of New Hampshire: U.S. Geological Survey State Geologic Map, 2 sheets, scale 1:250,000 and 1:500,000.

Mack, T.J., and Harte, P.T., 1996, Analysis of aquifer tests to determine hydrologic and water-quality conditions in stratified-drift and riverbed sediments near a former municipal well, Milford, New Hampshire: U.S. Geological Survey Water-Resources Investigations Report 96-4019, 77 p.

McDonald, M.G., and Harbaugh, A.W., 1988, A modular three-dimensional finite-difference ground-water flow model: U.S. Geological Survey Techniques of Water-Resources Investigations, chap. A1.

Moore, R.B., 1995, Geohydrologic setting, *in* Harte, P.T., and Johnson, W.P., Geohydrology and water quality of stratified-drift aquifers in the Contoocook River basin, south-central New Hampshire: U.S. Geological Survey Water-Resources Investigations Report 92-4154, p. 10-15.

New Hampshire Department of Environmental Services, 1985, Hydrogeological investigation of the Savage well site, Milford, New Hampshire: New Hampshire Water Supply and Pollution Control Division, Report 145, 91 p.

Olimpio, J.R., and Harte, P.T., 1994, Reassessment of geohydrologic data and refinement of a regional ground-water flow model of the Milford-Souhegan glacial-drift aquifer, Milford, New Hampshire: U.S. Geological Survey Water-Resources Investigations Report 95-281, 40 p.

Pollock, D.W., 1994, User's guide for MODPATH/MODPATH-PLOT, Version 3: A particle tracking post-processing package for MODFLOW the U.S. Geological Survey finite-difference ground-water flow model: U.S. Geological Survey Open-File Report 94-464, 220 p.

Rasmussen, W.C., and Andreason, G.E., 1959, Hydrologic budget of the Beaver Dam Creek basin, Maryland: U.S. Geological Survey Water-Supply Paper 1472, 106 p.

Trescott, P.C., and Pinder, G.F., and Larson, S.P., 1976, Finite-difference model for aquifer simulation in two dimensions with results of numerical experiments: U.S. Geological Survey Techniques of Water-Resources Investigations, book 7, chap. C1, 116 p.

U.S. Environmental Protection Agency, 1994a, The hydrologic evaluation of landfill performance (HELP) model; Users Guide for Version 3: Office of Research Development, Washington, D.C., Sept. 1994, 81 p.

———1994b, The hydrologic evaluation of landfill performance (HELP) model; Engineering Documentation for Version 3: Office of Research Development, Washington, D.C., Sept. 1994, 81 p.

APPENDIX 1: List and description of model-input files for the ground-water-flow models of the Milford-Souhegan glacial-drift aquifer, Milford, New Hampshire

Appendix 1. List and description of model-input files for the ground-water-flow models of the western half of the Milford-Souhegan glacial-drift aquifer, Milford, New Hampshire

[Model input files are for computer-modeling software MODFLOW-88 or MODFLOW-96]

Model run	File type	File name	Description of model input
			BASIC FILES
All steady-state models	Input,ascii	bas4.10796	Input file for basic package for steady-state model. Contains information on number of model cells and layers, and conditions to be simulated.The Milford model simulates 175 rows, 189 columns, and 5 layers.All model layers can simulate unconfined conditions.
Transient, seasonal analysis for 1994-95	Input, ascii	bas-48t.oc96	Basic file for transient input to basic package of MODFLOW. Total simulation is 2.5 years long. Contains 20 stress periods and simulates seasonal variations from April 1994 to June 1995. The period of January 1993 to April 1994 is used to insure starting heads are appropriate for seasonal analysis.
Transient, historical analysis for 1960-88	Input, ascii	bas-hist5	Basic file for transient input to basic package of MODFLOW. Total simulation is 29 years from 1960 - December 1988. Contains 8 stress periods and simulates historical changes in pumpage.
			IBOUND FILES
All steady-state and transient models	Input,ascii	Ib1noch.10796	Contains model cell ibound designation for layer one. Active cells where head is calculated are designated with a positive integer, specified-head cells are designated with a negative integer and inactive cells that are not simulated are designated with a zero.
All steady-state and transient models	Input,ascii	Ib2noch.10796	Contains model cell ibound designation for layer two.
All steady-state and transient models	Input,ascii	Ib3.797	Contains model cell ibound designation for layer three.
All steady-state and transient models	Input,ascii	Ib4.797	Contains model cell ibound designation for layer four.
All steady-state and transient models	Input,ascii	Ib5.797	Contains model cell ibound designation for layer five.
			REWETTING FILES
All steady-state and transient models	Input,ascii	wet1.10796	Contains model cell designation for layer one rewetting capabilities. A positive integer indicates cell can be rewetting if during iterative solution becomes dry. Rewetting option is invoked when calculated head is above the thickness criteria set in this array (positive integer) and wetness factor in bcf2 file. The Milford model activates rewetting when calculated head is 5 feet above base of cell.
All steady-state and transient models	Input,ascii	wet2.10796	Contains model cell designation for layer two rewetting capabilities.
All steady-state and transient models	Input,ascii	wet3.797	Contains model cell designation for layer three rewetting capabilities.
All steady-state and transient models	Input,ascii	wet4.797	Contains model cell designation for layer four rewetting capabilities.
All steady-state and transient models	Input,ascii	wet5.797	Contains model cell designation for layer five rewetting capabilities.

Appendix 1. List and description of model-input files for the ground-water-flow models of the western half of the Milford-Souhegan glacial-drift aquifer, Milford, New Hampshire--Continued

Model run	File type	File name	Description of model input
			BLOCK-CENTERED FILES
All steady-state models	Input,ascii	bcf.82696	Input file for bcf2 rewetting package for steady-state models. Contains information on model grid cell sizes, rewetting options, aquifer anisotropy (not invoked), and fortran unit numbers and formatting for aquifer hydraulic conductivity, vertical conductance, and model layer elevations.
Transient seasonal models for the period 1994-95	Input,ascii	bcf-48t.oc96	Input file for bcf2 rewetting package for transient seasonal models for the period 1994-95. Contains information on model grid cell sizes, rewetting options, aquifer anisotropy (not invoked), and fortran unit numbers and formatting for aquifer hydraulic conductivity, vertical conductance, and model-layer elevations.
Transient historical model for the period 1960-88	Input,ascii	bcf-hist2	Input file for bcf2 rewetting package for transient historical model.
			HYDRAULIC CONDUCTIVITY FILES
All steady-state and transient models	Input,ascii	K1okhigh.897	Hydraulic conductivity array for layer one.
All steady-state and transient models	Input,ascii	K2.5597	Hydraulic conductivity array for layer two.
All steady-state and transient models	Input,ascii	K3.797	Hydraulic conductivity array for layer three.
All steady-state and transient models	Input,ascii	K4.797	Hydraulic conductivity array for layer four.
All steady-state and transient models	Input,ascii	K5.797	Horizontal hydraulic conductivity array for layer five.
All steady-state and transient models	Input,ascii	vcon1okhigh.897	Vertical hydraulic conductance between layers one and two.
All steady-state and transient models	Input,ascii	vcon2.5597	Vertical hydraulic conductance between layers two and three.
All steady-state and transient models	Input,ascii	vcon3.797	Vertical hydraulic conductance between layers three and four.
All steady-state and transient models	Input,ascii	vcon4.797	Vertical hydraulic conductance between layers four and five.
			MODEL LAYER SURFACES
All steady-state and transient models	Input,ascii	bot1.ap98	Altitude of bottom of model cells in layer one, in feet above sea level. Also is used for top of model layer two.
All steady-state and transient models	Input,ascii	bot2.ap98	Altitude of bottom of model cells in layer two, in feet above sea level. Also is used for top of model layer three.
All steady-state and transient models	Input,ascii	bot3.sp98	Altitude of bottom of model cells in layer three, in feet above sea level. Also is used for top of model layer four.
All steady-state and transient models	Input,ascii	bot4.sp98	Altitude of bottom of model cells in layer four, in feet above sea level. Also is used for top of model layer five.
All steady-state and transient models	Input,ascii	bot5.sp98	Altitude of bottom of model cells in layer five, in feet above sea level.
			STRESS FILES
Steady-state model for 1994-95	Input,ascii	recharge.31897	Contains recharge rates to model cells for steady-state models. Valley edge cells receive higher rates than interior cells. Total recharge is 3.25 ft^3/s, which is about 26.2 in/yr.
Transient seasonal for 1994-95	Input, ascii	rech-caltt.897	Seasonal transient recharge for 1994-95.
Transient historical model for 1960-88	Input ascii	rech-hist5	Historical transient recharge for 1960-88.

Appendix 1. List and description of model-input files for the ground-water-flow models of the western half of the Milford-Souhegan glacial-drift aquifer, Milford, New Hampshire--Continued

Model run	File type	File name	Description of model input
			STRESS FILES--Continued
Steady-state 1983 conditions	Input,ascii	well83.897	Location of ground-water withdrawals and rates for 1983 conditions with Savage well pumping.
Steady-state 1988 conditions	Input,ascii	well88.897	Location of ground-water withdrawals and rates for October 1988, ground-water withdrawals.
Steady-state 1990 conditions	Input,ascii	well90.897	Location of ground-water withdrawals and rates for 1990 conditions.
Steady-state 1994 conditions	Input,ascii	well94.5597	Location of ground-water withdrawals and rates for 1994 conditions.
Steady-state 1996 conditions	Input,ascii	well96.55967	Location of ground-water withdrawals and rates for 1996 conditions.
Transient seasonal for 1994-95		well94-t.897	Transient seasonal well file.
Transient historical for 1960-88	Input, ascii	well-hist5	Transient historical well file.
			BOUNDARY CONDITION FILES
All steady-state files	Input, ascii	rivbas.112097	Steady-state model of altitude of river stage and riverbed, and riverbed conductances for the Souhegan River, Purgatory Brook, discharge ditch, Tucker Brook, and Hartshorn Brook.
Transient seasonal model for 1994-95	Input, ascii	river-61t.nv97	Transient seasonal river package.
Transient historical model for 1960-88	Input, ascii	rivbas.112097	Transient historical river package.
All steady-state models	Input, ascii	ghb.71697	Contains general-head boundary information including altitude of external head and conductances along column 181 of model.
			SOLUTION FILES
All steady-state and transient models	Input,ascii	pcg-nl4	Information on iterative solution options for the preconditioned-conjugate gradient solution. The Milford model uses non-linear solution techniques.
All steady-state models	Input,ascii	oc	Output control options for printing and saving heads and fluxes. The Milford model saves heads in ascii and binary form and fluxes in binary.
Transient seasonal model for 1994-95	Input, ascii	oc-47t	Output control for seasonal transient model.
Transient historical model for 1960-88	Input, ascii	oc-hist5	Output control for historical simulation.
Steady-state models and seasonal transient model	Input,ascii	hdl1-r94-44.in	Input array for starting steady-state heads for model layer 1.
Steady-state models and seasonal transient model	Input,ascii	hdl2-r94-44.in	Input array for starting steady-state heads for model layer 2.
Steady-state models and seasonal transient model	Input,ascii	hdl3-r94-44.in	Input array for starting steady-state heads for model layer 3.
Steady-state models and seasonal transient model	Input,ascii	hdl4-r94-44.in	Input array for starting steady-state heads for model layer 4.
Steady-state models and seasonal transient model	Input,ascii	hdl5-r94-44.in	Input array for starting steady-state heads for model layer 5.

APPENDIX 2: Information on well construction (sorted by well number) for selected wells in Milford, New Hampshire

Appendix 2. Information on well construction for selected wells in Milford, New Hampshire

[All units in feet; horizontal datum based on 2,000-foot grid New Hampshire State Plane coordinate system North American Datum 1983; vertical datum based on feet above National Geodetic Vertical Datum of 1929; depth in feet below land surface; some wells not shown on plate 1: --, no data; TPVC, top of polyvinyl casing (pvc); TSC, top of steel casing; CONC, concrete; TINRSC, top of inner steel casing; TCONC, top of concrete; WELLCVR, well cover; BOLT, top of bolt; PWMC, from metal cover; AHPUMP, air line reading at pump; SHELTER, labeled point inside wooden shelter; TOP REBAR, top of rebar]

Well number on plate 1	Well name	Easting	Northing	Description of measurement point	Altitude of		Depth to			
					Measurement point	Land surface	Top of screen or opening	Bottom of screen or opening	Refusal	Bedrock
5	LW-01D	984848.90	125391.90	--	--	264.80	100.00	110.00	--	114.3
6	LW-02D	984490.30	124835.40	--	245.66	243.10	45.00	55.00	--	62.5
7	LW-03D	984873.40	124642.50	--	251.14	247.30	44.50	54.50	--	80.2
8	LW-04D	985001.00	124601.20	--	246.43	243.40	40.00	50.00	--	80
9	MOW-33	976961.90	125149.30	--	--	260.00	60.00	70.00	--	56
10	GW-02D	983382.40	127459.90	--	--	255.40	19.00	29.00	--	34
11	GW-03D	984183.60	126015.00	--	--	252.40	28.00	38.00	--	23.5
12	GW-04D	983753.10	127211.90	--	--	255.60	21.50	31.50	--	19
13	GW-05D	984174.30	127024.90	--	--	261.00	23.00	33.00	--	33
14	RFW-1	980111.60	123484.10	--	--	255.70	8.00	28.00	28	--
15	RFW-2	980419.40	123831.60	--	253.87	253.80	10.00	35.00	35	--
16	RFW-3	980457.30	124035.20	--	253.51	253.50	13.00	43.00	43	--
17	RFW-4	980142.70	124069.50	--	252.15	251.60	6.00	16.00	16	--
18	PA-1	980332.10	123667.20	--	--	255.10	--	8.70	--	--
19	PA-2	980334.70	123737.30	--	--	254.90	--	8.70	--	--
20	PA-3	980388.40	123703.10	--	--	255.30	--	7.80	--	--
21	MI-7	978642.40	125263.60	TSC	256.68	253.20	--	31.00	--	--
22	MI-8	976549.90	125251.50	TINRSC	264.93	262.60	--	--	--	--
23	MI-10	979677.40	124853.90	TPVC	255.12	252.20	44.00	47.00	--	58.5
24	MI-11	979580.10	125310.70	TSC	254.52	252.10	40.00	56.00	63	--
25	MI-12	979476.40	125858.70	TSC	253.26	251.50	43.00	49.00	50	--
26	MI-15	976242.80	123624.90	TSC	265.17	264.70	--	--	--	--
27	MI-16	976813.60	123543.90	--	--	269.10	--	--	--	--
29	MI-18	977625.40	123963.10	TCONC	264.34	262.70	--	--	--	--
30	MI-19	974416.40	124870.30	TSC	277.99	275.60	65.00	80.00	--	63.5
31	MI-20	974416.40	124870.30	TSC	277.99	275.60	10.00	40.00	--	63.5
32	MI-20A	974565.10	124758.40	TPVC	--	274.70	--	14.80	--	--
33	MI-21	974566.70	125043.30	TPVC	274.95	272.10	15.00	40.00	--	53
34	MI-21A	974696.40	124790.30	TPVC	272.61	272.50	--	--	--	--
35	MI-22	975053.70	125123.50	TSC	272.08	269.10	99.00	114.00	--	94
36	MI-22A	974976.60	125182.60	--	--	270.10	--	11.70	--	--
37	MI-23	975053.70	125123.50	TSC	272.08	269.10	10.00	75.00	--	94
38	MI-24	975050.20	124966.30	TPVC	272.63	269.80	10.00	85.00	--	96
39	MI-24A	975092.10	124891.90	--	--	272.00	--	14.00	--	--
40	MI-25	975089.20	124821.70	TSC	271.41	269.30	101.80	111.00	--	105
41	MI-26	975089.20	124821.70	TSC	271.41	269.30	8.00	88.00	--	105
42	MI-27	975064.80	124731.30	TPVC	272.23	269.90	13.00	78.00	--	88
43	MI-28	974962.80	124603.60	TPVC	271.85	270.30	35.00	55.00	56	--
44	MI-30	975877.30	124347.00	TPVC	269.35	265.70	27.00	72.00	75	--
45	MI-31	975786.40	124591.90	TPVC	267.23	266.10	36.00	54.00	--	--
46	MI-32	975247.20	124933.70	TPVC	273.57	270.20	30.00	75.00	--	95

Appendix 2. Information on well construction for selected wells in Milford, New Hampshire--Continued

Well number on plate 1	Well name	Easting	Northing	Description of measurement point	Altitude of		Depth to			
					Measurement point	Land surface	Top of screen or opening	Bottom of screen or opening	Ref sal	Bedrock
47	MI-33	975651.30	124011.30	WELLCVR	265.90	268.00	50.00	60.00	60	--
48	MI-34	975833.60	122797.60	TPVC	278.84	278.80	--	17.70	--	--
49	MI-35	976578.50	124150.80	PWMC	263.20	262.20	--	55.00	--	--
50	MI-36	974900.80	123429.20	TPVC	270.51	269.90	--	12.50	--	--
51	MI-37	975299.50	123330.90	TPVC	272.60	270.40	--	12.50	--	--
52	MI-38	975116.90	123948.10	--	--	270.00	--	--	--	--
54	MI-41	977561.60	124774.20	TPVC	260.12	258.70	--	20.00	--	--
55	MI-42	977567.30	124958.10	TPVC	258.51	257.20	--	20.00	--	--
56	MI-43	977583.80	125123.00	TPVC	258.82	257.30	--	20.00	--	--
57	MOW-63	975248.20	125062.10	--	--	270.00	53.00	62.00	65	--
58	MI-44	977514.10	125199.40	TPVC	260.60	259.20	--	20.00	--	--
59	MI-45	975909.30	125772.40	--	--	264.90	--	--	--	--
60	MI-46	975970.80	125598.00	--	--	267.30	--	--	--	--
61	MI-47	975825.50	125094.20	--	--	270.00	--	--	--	--
62	MI-48	976556.30	124678.90	CONC	--	264.10	--	--	--	--
63	--	973226.90	124779.40	--	--	282.40	--	--	--	--
64	--	976086.60	124426.60	--	--	265.30	--	--	--	--
65	P-03	976979.60	124880.40	TSC	263.27	261.30	--	--	--	--
66	--	975354.00	124548.90	--	--	270.00	--	--	--	--
67	--	979957.10	124233.70	--	--	250.00	--	--	--	--
68	--	976054.90	124695.20	--	--	267.90	--	--	--	--
69	--	976146.70	124676.00	--	--	266.30	--	--	--	--
70	--	976282.60	124669.80	--	--	264.10	--	--	--	--
71	--	976275.60	124553.60	--	--	264.00	--	--	--	--
72	MI-62	977408.80	125554.80	--	--	260.00	17.00	58.00	--	60.7
73	MI-64	979161.50	123887.20	--	--	259.90	--	--	--	--
74	MOW-35	979010.10	124641.80	--	--	260.00	--	--	59	--
78	MOA-4	978318.20	124603.50	--	--	249.50	33.00	38.00	54	--
79	--	975782.30	119504.90	--	--	350.00	--	--	--	--
80	--	975917.30	119166.00	--	--	--	--	--	--	--
82	--	982214.80	125347.60	--	--	240.00	--	--	--	23
83	--	982062.20	125393.90	--	--	240.90	--	--	--	--
84	#226inSurvey	975999.60	127234.70	TSC	262.51	261.70	51.00	66.00	--	60
85	FH-15	976951.60	126886.40	AHPUMP	265.72	265.10	18.00	38.00	--	--
86	FH-13OBS	975717.70	126524.20	TPVC	269.03	260.00	33.00	43.00	--	--
87	FH-14	975867.00	126592.80	BOLT	263.53	262.20	32.00	42.00	--	--
88	FH-16	977174.80	126706.30	--	262.99	261.00	--	--	--	--
89	FH-27	978957.50	126176.80	TSC	253.41	251.30	36.00	41.00	--	--
90	FH-22	978953.00	126400.00	TPVC	255.10	253.10	24.00	29.00	--	--
91	FH-24	979035.90	126403.90	TPVC	253.27	251.60	24.00	29.00	--	--
92	FH-25	979102.50	126406.50	TPVC	251.63	252.10	23.00	28.00	--	--
93	FH-23	979002.60	126401.50	TPVC	253.70	252.00	22.00	25.00	--	--
94	FH-21	978928.60	126400.60	TPVC	251.63	252.10	21.00	26.00	--	--

Appendix 2. Information on well construction for selected wells in Milford, New Hampshire--Continued

Well number on plate 1	Well name	Easting	Northing	Description of measurement point	Altitude of		Depth to			
					Measurement point	Land surface	Top of screen or opening	Bottom of screen or opening	Refusal	Bedrock
95	FH85-8A	975813.90	126532.90	--	--	260.00	20.00	26.00	--	--
96	FH1974	978905.30	126519.50	--	--	254.50	--	--	--	--
97	B1	974473.70	125037.50	--	--	269.90	--	43.00	43	--
98	B3	974360.10	124970.20	--	--	269.30	--	33.80	33.8	--
99	B4	974211.60	124942.20	--	--	270.00	--	54.50	54.5	--
100	B6	974327.40	125036.10	--	--	269.00	--	--	25.2	--
101	B8	974392.90	125051.00	--	--	269.70	--	26.00	--	--
102	B9	974212.30	125172.50	--	--	275.30	--	--	--	--
103	B11	974370.30	125169.70	--	--	275.00	--	--	--	--
104	B12	974471.90	125190.80	--	--	275.40	--	--	--	--
105	--	972221.40	119573.10	--	--	--	--	--	--	--
106	--	969943.60	115997.70	--	--	--	--	--	--	--
107	--	982412.50	131350.50	--	--	349.20	--	--	--	--
108	--	969797.70	115772.40	--	--	--	--	--	--	--
109	--	982510.90	130710.20	--	--	349.30	--	--	--	--
111	--	976843.40	115878.60	--	--	--	--	--	--	--
117	--	977035.00	115723.00	--	--	--	--	--	--	--
118	--	974663.40	117151.10	--	--	--	--	--	--	--
119	--	975143.40	117530.10	--	--	--	--	--	--	--
120	--	974826.10	117243.00	--	--	--	--	--	--	--
121	--	976507.90	117660.40	--	--	--	--	--	--	--
122	WW-125	975152.70	129134.80	--	--	269.00	--	--	--	--
123	GW-01S	982781.10	127851.50	--	--	256.10	6.00	16.00	--	--
124	GW-01D	982862.30	127876.40	--	--	256.50	60.00	70.00	--	56
125	GW-01M	982953.40	127904.30	--	--	256.70	30.00	40.00	--	--
127	HAYWOOD	981163.80	124370.30	--	--	256.30	--	--	--	--
128	SavageWell	978473.20	124848.00	--	--	261.00	35.00	45.00	--	--
148	LW-01M	984856.90	125418.50	--	--	265.10	42.60	52.60	--	--
149	LW-01S	984856.90	125419.50	--	--	265.20	25.60	35.60	--	--
150	LW-02S	984495.90	124860.80	--	245.91	243.40	4.00	14.00	--	--
151	LW-03S	984876.20	124673.40	--	250.44	250.00	9.00	19.00	--	--
152	LW-04S	985003.80	124625.30	--	246.46	244.80	5.00	15.00	--	--
153	MOW-38	975574.20	128320.70	--	--	262.70	30.00	40.00	41	--
154	MOW-32	976679.80	124466.70	--	--	261.80	6.00	16.00	20	--
155	GW-02S	983400.80	127487.90	--	--	255.10	6.00	16.00	--	--
156	GW-03S	984191.20	126042.60	--	--	252.40	8.40	18.40	--	--
157	GW-04S	983770.60	127239.50	--	--	255.60	5.40	15.40	--	--
158	GW-05S	984189.90	127055.10	--	--	264.20	7.00	17.00	--	--
163	MI-2	978827.60	124764.70	TSC	253.94	252.90	42.00	47.00	--	--
164	MI-3	978692.70	124915.00	TSC	257.28	254.50	44.00	49.00	--	--
165	MI-4	978596.40	124892.50	TSC	257.49	255.00	39.00	49.00	--	--
166	MI-5	978717.70	124920.50	TSC	255.89	255.20	39.00	49.00	--	--
167	MI-6	978717.10	124918.60	TSC	255.66	255.10	--	--	--	--

Appendix 2. Information on well construction for selected wells in Milford, New Hampshire--Continued

Well number on plate 1	Well name	Easting	Northing	Description of measurement point	Altitude of		Depth to			
					Measurement point	Land surface	Top of screen or opening	Bottom of screen or opening	Refusal	Bedrock
168	MI-6A	978830.10	124812.80	--	--	259.50	--	--	--	--
169	MI-9	976255.70	125936.00	TCONC	265.05	263.80	--	--	--	--
170	MI-14	977619.80	123760.40	--	--	260.00	--	--	--	--
171	MI-29	975306.90	123808.10	TPVC	269.93	268.50	31.50	51.50	51.5	--
172	MI-40	977391.30	124739.20	TPVC	257.40	256.10	--	--	--	--
173	H12-71	981352.50	124815.30	--	--	250.00	36.00	36.00	--	36
174	H11-71	981478.20	125561.40	--	--	241.60	25.00	35.00	--	39
175	H9-71	981665.10	126217.40	--	--	250.80	20.00	25.00	--	28.5
176	H8-71	981881.90	126202.30	--	--	250.00	20.00	25.00	--	32
177	H6-71	981885.60	126032.00	--	--	249.50	16.00	16.00	--	16
178	H7-71	981841.00	125953.90	--	--	246.90	15.00	15.00	--	15
179	H10-71	981819.40	126331.60	--	--	250.90	18.00	28.00	--	34
180	H5-71	981751.40	126415.00	--	--	250.50	23.00	28.00	--	31
188	MOA-25	975839.70	125937.00	--	--	262.00	50.00	60.00	72	--
189	MOA-35	975554.90	125804.90	--	--	265.20	--	--	12	--
190	MOA-37	975737.60	126314.60	--	--	260.00	--	--	13	--
191	MOA-38	975295.40	125590.60	--	--	270.00	--	--	14	--
192	--	984005.20	123305.50	--	--	266.70	--	--	--	12
193	MOW-15	977255.80	127892.70	--	--	260.00	--	--	--	--
194	MOW-58	975647.00	125574.50	--	--	268.70	54.00	63.00	76	--
195	MOW-64	976832.40	126380.50	--	--	260.00	41.00	49.00	76	--
196	MOW-65	976555.40	126488.70	--	--	260.00	54.00	62.00	73	--
197	MOW-66	982904.60	124297.20	--	--	252.80	27.00	33.00	37	--
198	MOW-67	983164.50	124318.20	--	--	249.80	37.00	43.00	45	--
199	MOW-68	983417.40	124322.20	--	--	245.00	36.00	42.00	53	--
200	MOW-25	977668.80	122997.30	--	--	259.70	--	--	4	--
201	MOW-26	977661.40	122551.60	--	--	260.00	--	--	14	--
202	MOW-19	976722.50	125725.60	--	--	260.80	--	--	--	--
203	MI-63	975636.80	125076.60	TSC	267.75	265.10	24.00	64.00	--	--
204	MI-13	984325.50	123765.20	--	251.42	249.60	12.00	18.00	33	--
208	FH-5 (pump)	975988.30	127199.90	TINRSC	267.89	268.00	50.00	65.00	--	--
209	MW-1C	974922.80	122726.70	TPVC	281.28	279.50	51.10	61.10	--	62
210	MW-2B	975151.80	125599.90	TSC	269.19	266.40	70.70	80.70	--	--
212	MW-4B	975303.50	123583.80	TPVC	268.59	266.70	45.80	55.80	--	43.2
213	MW-5B	975408.30	123982.60	TPVC	269.61	267.60	50.40	60.40	--	61.35
214	MW-6B	975521.20	124486.80	TPVC	268.95	267.10	56.80	66.80	--	69.4
215	MW-7B	976263.30	123908.40	TPVC	264.29	262.50	45.60	55.60	--	58.6
216	MW-8B	976524.90	124151.40	TPVC	263.80	261.80	57.00	67.00	--	90
217	MW-9C	976503.30	124473.60	TPVC	268.09	266.30	79.00	90.00	--	94
218	MW-10C	976215.00	124930.60	TPVC	264.74	262.80	81.50	91.50	--	91.6
219	MW-11R	976435.00	125881.60	TSC	263.30	261.00	52.00	64.00	--	65
220	MW-12A	978133.30	124280.70	TPVC	265.96	264.00	25.00	35.00	--	--
221	MW-13B	977300.60	125081.10	TPVC	259.35	257.90	48.00	58.00	--	64

Appendix 2. Information on well construction for selected wells in Milford, New Hampshire--Continued

Well number on plate 1	Well name	Easting	Northing	Description of measurement point	Altitude of		Depth to			
					Measurement point	Land surface	Top of screen or opening	Bottom of screen or opening	Refusal	Bedrock
222	MW-14R	978696.00	125647.00	TSC	255.75	253.80	50.00	60.00	--	60
223	MW-15A	982006.40	125915.30	TPVC	258.53	256.80	12.50	27.50	--	--
225	MW-26	975206.20	123141.40	TPVC	271.11	268.70	3.00	13.00	--	--
226	MW-25	975168.90	123046.50	TPVC	273.12	270.50	4.00	12.00	--	--
228	MW-3	975915.60	123237.10	TPVC	270.54	268.70	11.50	21.50	--	21.5
231	MW-18A	975824.80	124273.40	TPVC	269.78	267.90	44.50	54.50	--	--
233	MW-16A	975671.20	124863.10	SHELTER	270.39	267.50	16.90	26.90	--	--
234	MW-28	974374.90	124929.30	TPVC	275.42	275.60	5.00	15.00	--	--
235	MW-27	974728.20	125049.90	TPVC	275.36	273.80	5.00	15.00	--	--
237	MW-23A	975835.10	125944.30	TPVC	267.51	265.40	20.00	30.00	--	--
240	FH-10(OBS)	975991.40	127198.40	TSC	268.01	267.30	58.00	63.00	--	--
242	FH-9	975997.30	127233.10	TSC	269.83	268.30	--	52.00	--	--
244	RW6	974672.70	126362.00	--	--	--	--	--	--	--
245	RW3	974864.40	126779.80	--	--	-2.00	111.00	420.00	--	--
247	RW1	975397.40	127471.00	--	--	-2.00	59.00	340.00	--	--
248	RW2	975425.10	127514.80	--	--	--	--	--	--	--
249	Cassarino	975491.40	127480.10	--	--	267.90	--	12.50	--	--
250	SP-1	976415.40	128176.90	TPVC	259.17	257.40	2.00	7.00	--	--
251	SP-7	977551.40	127255.90	TPVC	258.66	258.20	4.50	9.50	--	--
252	SP-6	976792.40	126621.20	TPVC	261.05	260.00	3.00	8.00	--	--
255	MW-24A	977644.90	126373.30	TPVC	259.67	257.10	19.50	29.50	--	--
258	MW-17A	976216.50	124754.00	TPVC	263.29	264.40	19.80	29.80	--	--
262	MW-29	977125.30	124080.30	TPVC	260.90	261.00	2.50	12.50	--	--
264	MW-20A	977472.90	124629.10	TPVC	263.23	260.80	15.20	25.20	--	--
267	SP-4	977995.70	127200.00	--	258.63	257.10	2.50	7.50	--	--
268	SP-3	978256.80	126568.90	--	256.30	255.30	4.50	9.50	--	--
269	P-9A	978624.20	126009.90	--	254.73	253.10	7.00	8.00	--	--
270	P-9B	978624.00	126015.80	--	255.01	252.60	9.20	10.20	--	--
271	P-15	978953.70	126170.90	TPVC	252.08	251.40	7.00	8.00	--	--
273	HP-1	978832.70	125303.40	--	254.51	252.30	1.00	6.00	--	--
274	HP-2	979099.70	125374.20	--	253.24	251.00	1.50	6.50	--	--
275	HP-3	979343.90	125403.50	--	253.53	251.10	1.50	6.50	--	--
276	P-10	979466.80	125859.00	--	252.70	250.40	7.50	8.50	--	--
277	P-11	979689.20	126100.90	--	254.54	252.50	7.50	8.50	--	--
278	MW-21A	979001.30	124463.60	TPVC	261.27	259.20	3.80	13.80	--	--
279	SPZ-2	979817.20	126368.50	TPVC	251.94	249.90	1.00	6.00	--	--
280	P-16	979986.60	126500.00	TPVC	260.43	258.30	12.00	13.00	--	--
281	MW-34	979987.00	126490.70	TPVC	260.91	258.50	9.50	19.50	--	20.5
282	P-17A	980125.10	126109.10	--	252.54	250.60	8.00	9.00	--	--
283	P-17B	980124.10	126110.10	--	253.66	252.60	12.00	13.00	--	--
284	RW4	980479.80	126905.00	--	280.08	278.30	--	23.00	--	--
285	SPZ-1	980666.60	126449.90	TPVC	259.17	257.40	3.50	8.50	--	--
287	RW9	981114.80	127599.20	--	271.45	270.40	--	22.00	--	--

Appendix 2. Information on well construction for selected wells in Milford, New Hampshire--Continued

Well number on plate 1	Well name	Easting	Northing	Description of measurement point	Altitude of		Depth to			
					Measurement point	Land surface	Top of screen or opening	Bottom of screen or opening	Refusal	Bedrock
288	FH-28	981031.70	126543.60	TSC	248.85	248.10	--	23.00	--	--
289	FH-29	981063.30	126519.20	TSC	250.07	247.80	--	33.90	--	--
290	SP-18	981032.50	126481.60	--	250.17	248.20	4.50	7.50	--	--
291	SP-11	981256.90	126375.40	--	249.67	247.70	8.50	9.50	--	--
292	FH-30	981104.80	126341.00	TSC	250.69	248.30	--	23.00	--	--
293	MW-22A	981102.30	126204.00	TPVC	252.52	250.20	13.80	23.80	--	--
294	MW-22B	981098.70	126201.30	TPVC	252.77	250.10	33.50	43.50	--	47
295	P-13	981806.60	126346.10	--	250.84	248.30	7.50	8.50	--	--
296	MW-32A	981366.60	125490.00	TPVC	250.46	247.90	7.00	17.00	--	--
297	MW-32B	981369.80	125487.10	TPVC	251.23	248.30	31.80	41.80	--	43.5
299	HM-1	975363.00	125252.30	TPVC	268.14	269.20	3.00	83.00	--	--
301	FH-11	975989.90	127199.80	TSC	268.08	267.40	--	62.00	--	--
302	FH-19	978898.80	126408.40	TSC	256.17	--	--	--	--	--
304	SP-5	977271.90	126837.80	--	257.07	255.30	2.50	7.50	--	--
305	FH-18	978724.80	126549.20	--	255.01	--	--	--	--	--
306	MW-33	979070.90	126468.10	TPVC	253.89	251.80	41.50	51.50	--	52.5
307	MW-1A	974929.80	122712.20	TPVC	281.26	279.70	5.00	17.00	--	--
308	MW-13A	977298.80	125084.80	TSC	259.85	257.90	23.90	33.90	--	--
309	MW-1B	974926.70	122718.30	TPVC	281.38	279.50	35.40	45.40	--	--
310	MW-2A	975148.90	125591.30	SHELTER	270.08	266.60	29.00	39.00	--	--
311	MW-2R	975145.00	125587.70	TSC	267.67	266.20	134.00	164.00	--	115.5
312	MW-4A	975307.90	123586.40	TPVC	268.34	266.50	19.70	29.70	--	--
313	MW-5A	975414.60	123981.80	TPVC	269.71	267.60	28.00	38.00	--	--
314	MW-7A	976267.60	123912.60	TPVC	264.40	262.30	3.20	13.20	--	--
315	MW-8A	976511.80	124151.80	TPVC	263.91	262.00	4.50	16.50	--	--
316	MW-10A	976221.50	124928.60	TPVC	263.77	262.20	19.00	29.00	--	--
317	MW-10B	976218.50	124928.40	TPVC	263.55	262.20	44.00	54.00	--	--
318	MW-11A	976433.30	125888.70	TPVC	262.78	260.90	20.50	30.50	--	--
319	MW-11B	976435.20	125885.30	TPVC	262.83	261.00	52.30	64.30	--	65
320	MW-12B	978134.30	124287.40	TPVC	265.61	264.00	56.00	66.00	--	66
321	MW-16B	975671.00	124868.60	TPVC	269.85	267.60	39.60	49.60	--	--
322	MW-17B	976212.00	124755.50	TPVC	263.34	264.60	52.40	62.40	--	--
323	MW-17C	976212.80	124757.90	TPVC	263.36	264.70	85.00	95.00	--	99.3
324	MW-18B	975824.10	124279.10	TPVC	270.30	268.00	72.00	82.00	--	82
326	MW-19A	977289.20	124123.20	TSC	264.30	261.60	23.50	33.50	--	--
327	MW-19B	977294.80	124124.80	TSC	263.88	260.90	39.00	49.00	30	35
328	MW-20B	977476.10	124622.30	TPVC	263.03	260.70	35.00	45.00	--	47.5
329	MW-21B	979001.20	124469.80	TPVC	261.77	259.30	20.00	30.00	--	--
330	MW-21C	979001.50	124474.00	TPVC	261.34	259.40	44.10	54.10	--	63.75
331	MW-23B	975802.80	125947.10	TPVC	267.40	265.30	48.00	58.00	--	--
332	MW-23C	975840.80	125954.00	TPVC	267.34	265.30	84.30	94.30	--	106
333	MW-24B	977649.70	126372.30	TPVC	259.39	256.80	31.00	41.00	--	40.5
334	MW-31	978979.10	126191.90	TSC	251.87	250.10	--	--	--	50.5

Appendix 2. Information on well construction for selected wells in Milford, New Hampshire--Continued

Well number on plate 1	Well name	Easting	Northing	Description of measurement point	Altitude of		Depth to			
					Measurement point	Land surface	Top of screen or opening	Bottom of screen or opening	Refusal	Bedrock
335	P-1	974088.30	124847.50	TPVC	278.95	276.60	13.90	14.90	--	--
336	P-2	975100.90	125281.90	TPVC	271.32	268.60	17.00	18.00	--	--
337	WLR4	978297.60	125583.70	SHELTER	257.38	251.30	4.00	5.00	--	--
338	P-14	981843.10	124952.70	--	248.69	246.70	7.00	8.00	--	--
339	SP-9	976276.60	126593.00	--	261.16	259.40	1.50	6.50	--	--
340	SP-10	975407.80	126569.50	--	263.92	262.40	1.00	6.00	--	--
341	MW-14B	978696.60	125651.10	TPVC	255.13	253.30	50.00	60.00	--	60
342	MW-15B	982001.40	125914.50	TPVC	258.61	257.00	29.40	36.40	--	27.5
344	MW-16C	975678.10	124877.10	TSC	269.70	267.40	73.20	83.20	--	87.5
345	MW-16R	975670.80	124875.20	TSC	268.92	266.50	88.00	138.00	--	87.5
347	MW-4R	975299.90	123581.50	TINRSC	267.94	266.40	64.00	98.00	--	45
348	MW-6A	975521.40	124481.80	TPVC	269.11	267.00	8.00	20.00	--	--
349	MW-14A	978695.90	125654.90	TPVC	254.65	253.40	19.00	29.00	--	--
351	MW-9A	976502.90	124485.80	TPVC	267.76	266.10	30.70	40.70	--	--
352	MW-9B	976503.60	124479.10	TPVC	267.87	266.10	58.20	68.20	--	--
353	FH-17	978711.30	127671.80	BOLT	272.44	--	--	--	--	--
354	PFHprodWell	981195.60	126601.60	--	251.68	249.20	30.00	40.00	--	--
356	--	981217.30	126573.60	--	250.05	247.40	--	--	--	--
357	--	981218.60	126572.10	--	249.97	247.40	--	--	--	--
358	--	981191.10	126524.60	TSC	250.03	247.20	--	20.50	--	--
359	FH-?	981138.80	126516.30	TSC	249.86	248.50	--	24.80	--	--
360	--	981136.40	126667.90	TSC	251.03	247.10	--	34.50	--	--
361	P-12	980380.20	125709.40	--	252.03	252.00	9.00	10.00	--	--
362	USGS-DISK	978965.10	126138.80	--	250.02	--	--	--	--	--
364	--	976295.60	125521.00	--	264.93	262.50	--	--	--	--
366	MW-30	975228.80	125893.30	TSC	267.96	--	--	--	--	--
367	M261942	973138.90	124764.60	--	--	--	--	--	--	--
369	FHwoods	976854.10	127069.30	TSC	266.46	266.10	--	--	--	--
374	FH-26	979100.80	126405.40	TPVC	254.35	--	--	--	--	--
375	nearFH19	978900.70	126413.00	--	--	--	--	--	--	--
376	2ftHitchPW1	975620.10	124005.90	--	--	--	--	--	--	--
377	3ftHitchPW1	975608.90	124010.10	--	--	--	--	--	--	--
380	HitchWlHs	975651.60	124010.80	--	--	--	--	--	--	--
396	B95-01	975177.38	124917.10	--	--	269.83	--	--	--	107
397	B95-02	975120.69	125077.40	--	--	269.67	--	--	--	99.8
398	B95-03	974985.31	125214.80	TPVC	272.41	269.65	61.50	71.50	--	86
399	B95-04	974848.69	125108.90	--	--	270.35	--	--	--	69
400	B95-05	974688.19	125027.70	TPVC	275.10	273.05	37.00	47.00	--	73.5
401	B95-06	974669.00	124826.00	TPVC	272.12	272.75	41.50	51.50	--	--
402	B95-07	974914.31	124802.50	TPVC	273.64	271.71	46.00	56.00	--	58
403	B95-08	975035.38	124825.80	TPVC	276.12	270.08	72.00	82.00	--	88
404	B95-09	975039.81	124825.60	TPVC	273.34	270.31	10.00	20.00	--	--
405	B95-10	974816.69	124997.50	TPVC	274.68	272.14	61.00	66.00	--	--

Appendix 2. Information on well construction for selected wells in Milford, New Hampshire--Continued

Well number on plate 1	Well name	Easting	Northing	Description of measurement point	Altitude of		Depth to			
					Measurement point	Land surface	Top of screen or opening	Bottom of screen or opening	Refusal	Bedrock
406	B95-11	974969.13	124987.00	TPVC	274.58	272.38	73.00	78.00	--	80
407	B95-12	975343.81	124724.70	TPVC	272.01	269.45	55.00	60.00	--	76
408	B95-13	975490.63	125002.00	TPVC	266.26	267.01	60.00	65.00	--	90.5
409	B95-15	975254.00	125149.40	TPVC	267.90	269.61	85.00	95.00	--	96.5
410	B95-16	974827.31	124995.70	TPVC	274.48	272.04	10.00	20.00	--	--
411	B95-17	974980.38	124985.10	TPVC	274.50	272.07	40.00	50.00	--	--

APPENDIX 3: Observed ground-water levels for selected wells in the Milford-Souhegan glacial-drift aquifer, Milford, New Hampshire

Appendix 3. Observed ground-water levels from selected wells in the Milford-Souhegan Glacial-Drift Aquifer, Milford, New Hampshire

[All units in feet; aquifer code: S&G= sand and gravel, over=overburden; water level datum is NGVD 1929; horizontal datum 2000 foot grid New Hampshire State Planar coordinates; --, no data available]

Well number on plate 1	Well name	Easting	Northing	Model row	Model column	Model layer	Aquifer code	Synoptic water level, October 1988	Synoptic water-level October 1990	Mean biweekly water level, June 1994-95
21	MI-7	978642.4	125263.6	103	104	1	S&G	250.16	251.19	250.77
29	MI-18	977625.4	123963.1	146	79	1	S&G	254.32	255.27	255.88
223	MW-15A	982006.4	125915.3	103	172	1	S&G	--	--	242.08
280	P-16	979986.6	126500	65	135	1	--	--	249.32	246.31
281	MW-34	979987	126490.7	65	135	1	S&G	--	245.53	245.67
285	SPZ-1	980666.6	126449.9	72	148	1	S&G	--	245.81	244.81
288	FH-28(OBS6)	981031.7	126543.6	71	156	1	S&G	--	--	243.39
292	FH-30	981104.8	126341	80	156	1	S&G	--	243.43	243.39
296	MW-32A	981366.6	125490	115	158	1	Sand	--	243.6	242.71
31	MI-20 (M-1b)	974416.4	124870.3	85	19	1	S&G	265.14	--	265.84
233	MW-16A	975671.2	124863.1	95	44	1	S&G	--	258.48	259.34
234	MW-28	974374.9	124929.3	82	19	1	S&G	--	267.14	266.89
235	MW-27	974728.2	125049.9	80	26	1	S&G	--	264.5	265.25
250	SP-1 (SP-8)	976415.4	128176.9	13	72	1	S&G	--	252.55	253.35
314	MW-7A	976267.6	123912.6	137	52	1	S&G	--	258.38	259.18
315	MW-8A	976511.8	124151.8	130	58	1	S&G	--	257.56	258.29
335	P-1	974088.3	124847.5	83	13	1	S&G	--	268.06	267.6
336	P-2	975100.9	125281.9	74	35	1	S&G	--	261.42	261.61
348	MW-6A	975521.4	124481.8	109	40	1	S&G	--	--	260
228	MW-3	975915.6	123237.1	161	43	1	S&G	--	261.14	261.43
307	MW-1A	974929.8	122712.2	169	21	1	S&G	--	272.51	273.62
220	MW-12A	978133.3	124280.7	137	90	2	Sand	--	253.51	253.7
326	MW-19A	977289.2	124123.2	137	73	2	S&G	--	255.9	256.56
255	MW-24A	977644.9	126373.3	52	89	2	S&G	--	250.56	250.93
297	MW-32B	981369.8	125487.1	115	158	2	Sand	--	243.67	242.79
318	MW-11A	976433.3	125888.7	61	63	2	S&G	--	255.99	255.98
333	MW-24B	977649.7	126372.3	52	89	2	Till	--	250.62	250.95
349	MW-14A	978695.9	125654.9	88	107	2	S&G	--	--	249.18
258	MW-17A	976216.5	124754	104	54	2	S&G	--	257.72	258.53
264	MW-20A	977472.9	124629.1	118	79	2	Sand	--	254.98	255.13
351	MW-9A	976502.9	124485.8	116	59	2	S&G	--	--	257.91
33	MI-21 (M-2)	974566.7	125043.3	81	21	2	S&G	264.53	--	265.35
308	MW-13A	977298.8	125084.8	99	77	2	S&G	--	254.65	254.74
310	MW-2A	975148.9	125591.3	62	37	2	S&G	--	260.3	260.06
316	MW-10A	976221.5	124928.6	97	55	2	S&G	--	257.57	258.43
293	MW-22A	981102.3	126204	85	156	2	S&G	--	243.82	243.53
309	MW-1B	974926.7	122718.3	169	21	2	S&G	--	272.39	271.62
312	MW-4A	975307.9	123586.4	142	32	2	S&G	--	260.77	261.63
294	MW-22B	981098.7	126201.3	85	156	2,3	S&G	--	243.82	243.5
341	MW-14B	978696.6	125651.1	88	107	3	S&G	--	248.78	249.42

Appendix 3. Observed ground-water levels from selected wells in the Milford-Souhegan Glacial-Drift Aquifer, Milford, New Hampshire--Continued

Well number on plate 1	Well name	Easting	Northing	Model row	Model column	Model layer	Aquifer code	Synoptic water level, October 1988	Synoptic water-level, October 1990	Mean biweekly water level, June 1994-95
43	MI-28 (H-1)	974962.8	124603.6	100	29	3	S&G	260.56	260.91	262.24
209	MW-1C	974922.8	122726.7	169	21	3	S&G	--	267.95	268.46
23	MI-10	979677.4	124853.9	127	123	3	S&G	--	248.66	248.9
89	FH-27	978957.5	126176.8	69	114	3	S&G	--	245.9	247.64
306	MW-33	979070.9	126468.1	59	117	3	S&G	--	246.54	247.37
320	MW-12B	978134.3	124287.4	137	90	3	Sand	--	253.61	253.7
25	MI-12	979476.4	125858.7	86	123	3	S&G	--	247.46	247.5
165	MI-4	978596.4	124892.5	117	102	3	Sand	--	251.99	251.98
203	MI-63	975636.8	125076.6	86	44	3	Over	--	--	260.38
215	MW-7B	976263.3	123908.4	137	52	3	S&G	257.16	258.34	259.27
221	MW-13B	977300.6	125081.1	99	77	3	Sand	--	254.67	254.79
240	FH-10(OBS)	975991.4	127198.4	28	59	3	S&G	--	240.76	244.64
317	MW-10B	976218.5	124928.4	97	55	3	S&G	--	257.55	258.4
319	MW-11B	976435.2	125885.3	61	63	3	S&G	--	255.83	255.87
321	MW-16B	975671	124868.6	95	44	3	S&G	--	258.57	259.46
322	MW-17B	976212	124755.5	104	54	3	S&G	--	257.82	258.53
328	MW-20B	977476.1	124622.3	119	79	3	S&G	--	255.01	255.11
38	MI-24 (M-4)	975050.2	124966.3	86	32	3	Over	259.86	--	261.33
42	MI-27 (M-6)	975064.8	124731.3	96	32	3	Over	259.98	--	261.57
46	MI-32	975247.2	124933.7	88	38	3	S&G	259.16	259.94	260.96
86	FH-13OBS	975717.7	126524.2	40	51	3	S&G	--	249.88	252.65
299	HM-1	975363	125252.3	76	39	3	Over	--	--	260
210	MW-2B	975151.8	125599.9	62	37	4	S&G	--	260.06	260.54
216	MW-8B	976524.9	124151.4	130	58	4	S&G	255.25	257.53	258.13
352	MW-9B	976503.6	124479.1	117	59	4	S&G	--	--	257.92
214	MW-6B	975521.2	124486.8	109	40	4	S&G	257.24	259.01	259.82
344	MW-16C	975678.1	124877.1	95	44	4	S&G	--	258.67	259.5
217	MW-9C	976503.3	124473.6	117	59	5	S&G	255.9	--	257.78
218	MW-10C	976215	124930.6	97	55	5	S&G	--	257.4	258.01
323	MW-17C	976212.8	124757.9	103	54	5	S&G	--	257.69	258.46

APPENDIX 4: Information on well construction (sorted by easting location) for selected wells in Milford, New Hampshire

Appendix 4. Information on well construction (sorted by easting location) for selected wells in Milford, New Hampshire

[Some wells are not shown on plate; all units in feet; horizontal datum based on 2,000-foot grid New Hampshire State Plane coordinate system North American Datum 1983; vertical datum based on feet above National Geodetic Vertical Datum of 1929; depth in feet below land surface; --, no data; TPVC, top of polyvinyl casing (pvc); TSC, top of steel casing; CONC, concrete; TINRSC, top of inner steel casing; TCONC, top of concrete; WELLCVR, well cover; BOLT, top of bolt; PWMC, from metal cover; AHPUMP, air line reading at pump; SHELTER, labeled point inside wooden shelter; TOP REBAR, top of rebar]

Well number on plate 1	Well name	Easting	Northing	Description of measurement point	Altitude of		Depth to			
					Measurement point	Land surface	Top of screen or opening	Bottom of screen or opening	Refusal	Bedrock
108	--	969797.70	115772.40	--	--	--	--	--	--	--
106	--	969943.60	115997.70	--	--	--	--	--	--	--
105	--	972221.40	119573.10	--	--	--	--	--	--	--
367	M261942	973138.90	124764.60	--	--	--	--	--	--	--
63	--	973226.90	124779.40	--	--	282.40	--	--	--	--
391	WLR-1	973834.40	124843.10	SHELTER	282.80	--	--	--		
335	P-1	974088.30	124847.50	TPVC	278.95	276.60	13.90	14.90	--	--
99	B4	974211.60	124942.20	--	--	270.00	--	54.50	54.5	--
102	B9	974212.30	125172.50	--	--	275.30	--	--	--	--
100	B6	974327.40	125036.10	--	--	269.00	--	--	26.2	--
98	B3	974360.10	124970.20	--	--	269.30	--	33.80	33.8	--
103	B11	974370.30	125169.70	--	--	275.00	--	--	--	--
234	MW-28	974374.90	124929.30	TPVC	275.42	275.60	5.00	15.00	--	--
101	B8	974392.90	125051.00	--	--	269.70	--	26.00	--	--
31	MI-20	974416.40	124870.30	TSC	277.99	275.60	10.00	40.00	--	63.5
30	MI-19	974416.40	124870.30	TSC	277.99	275.60	65.00	80.00	--	63.5
104	B12	974471.90	125190.80	--	--	275.40	--	--	--	--
97	B1	974473.70	125037.50	--	--	269.90	--	43.00	43	--
32	MI-20A	974565.10	124758.40	TPVC	--	274.70	--	14.80	--	--
33	MI-21	974566.70	125043.30	TPVC	274.95	272.10	15.00	40.00	--	53
118	--	974663.40	117151.10	--	--	--	--	--	--	--
401	B95-06	974669.00	124826.00	TPVC	272.12	272.75	41.50	51.50	--	--
244	RW6	974672.70	126362.00	--	--	--	--	--	--	--
400	B95-05	974688.19	125027.70	TPVC	275.10	273.05	37.00	47.00	--	73.5
34	MI-21A	974696.40	124790.30	TPVC	272.61	272.50	--	--	--	--
235	MW-27	974728.20	125049.90	TPVC	275.36	273.80	5.00	15.00	--	--
405	B95-10	974816.69	124997.50	TPVC	274.68	272.14	61.00	66.00	--	--
120	--	974826.10	117243.00	--	--	--	--	--	--	--
410	B95-16	974827.31	124995.70	TPVC	274.48	272.04	10.00	20.00	--	--
399	B95-04	974848.69	125108.90	--	--	270.35	--	--	--	69
245	RW3	974864.40	126779.80	--	--	-2.00	111.00	420.00	--	--
50	MI-36	974900.80	123429.20	TPVC	--	269.90	--	12.50	--	--
402	B95-07	974914.31	124802.50	TPVC	--	271.71	46.00	56.00	--	58
209	MW-1C	974922.80	122726.70	TPVC	281.28	279.50	51.10	61.10	--	62
309	MW-1B	974926.70	122718.30	TPVC	281.38	279.50	35.40	45.40	--	--
307	MW-1A	974929.80	122712.20	TPVC	281.26	279.70	5.00	17.00	--	--
43	MI-28	974962.80	124603.60	TPVC	271.85	270.30	35.00	55.00	56	--
406	B95-11	974969.13	124987.00	TPVC	274.58	272.38	73.00	78.00	--	80
36	MI-22A	974976.60	125182.60	--	--	270.10	--	11.70	--	--
411	B95-17	974980.38	124985.10	TPVC	274.50	272.07	40.00	50.00	--	--

Appendix 4. Information on well construction (sorted by easting location) for selected wells in Milford, New Hampshire --Continued

Well number on plate 1	Well name	Easting	Northing	Description of measurement point	Altitude of		Depth to			
					Measurement point	Land surface	Top of screen or opening	Bottom of screen or opening	Refusal	Bedrock
398	B95-03	974985.31	125214.80	TPVC	272.41	269.65	61.50	71.50	--	86
403	B95-08	975035.38	124825.80	TPVC	276.12	270.08	72.00	82.00	--	88
404	B95-09	975039.81	124825.60	TPVC	273.34	270.31	10.00	20.00	--	--
38	MI-24	975050.20	124966.30	TPVC	272.63	269.80	10.00	85.00	--	96
35	MI-22	975053.70	125123.50	TSC	272.08	269.10	99.00	114.00	--	94
37	MI-23	975053.70	125123.50	TSC	272.08	269.10	10.00	75.00	--	94
42	MI-27	975064.80	124731.30	TPVC	272.23	269.90	13.00	78.00	--	88
41	MI-26	975089.20	124821.70	TSC	271.41	269.30	8.00	88.00	--	105
40	MI-25	975089.20	124821.70	TSC	271.41	269.30	101.80	111.00	--	105
39	MI-24A	975092.10	124891.90	--	--	272.00	--	14.00	--	--
336	P-2	975100.90	125281.90	TPVC	271.32	268.60	17.00	18.00	--	--
52	MI-38	975116.90	123948.10	--	--	270.00	--	--	--	--
397	B95-02	975120.69	125077.40	--	--	269.67	--	--	--	99.8
119	--	975143.40	117530.10	--	--	--	--	--	--	--
311	MW-2R	975145.00	125587.70	TSC	267.67	266.20	134.00	164.00	--	115.5
310	MW-2A	975148.90	125591.30	SHELTER	270.08	266.60	29.00	39.00	--	--
210	MW-2B	975151.80	125599.90	TSC	269.19	266.40	70.70	80.70	--	--
122	WW-125	975152.70	129134.80	--	--	269.00	--	--	--	--
226	MW-25	975168.90	123046.50	--	273.12	270.50	4.00	12.00	--	--
396	B95-01	975177.38	124917.10	--	--	269.83	--	--	--	107
225	MW-26	975206.20	123141.40	--	271.11	268.70	3.00	13.00	--	--
366	MW-30	975228.80	125893.30	TSC	267.96	--	--	--	--	--
46	MI-32	975247.20	124933.70	TPVC	273.57	270.20	30.00	75.00	--	95
57	MOW-63	975248.20	125062.10	--	--	270.00	53.00	62.00	65	--
409	B95-15	975254.00	125149.40	TPVC	267.90	269.61	85.00	95.00	--	96.5
191	MOA-38	975295.40	125590.60	--	--	270.00	--	--	14	--
51	MI-37	975299.50	123330.90	TPVC	272.60	270.40	--	12.50	--	--
347	MW-4R	975299.90	123581.50	TINRSC	267.94	266.40	64.00	98.00	--	45
212	MW-4B	975303.50	123583.80	TPVC	268.59	266.70	45.80	55.80	--	43.2
171	MI-29	975306.90	123808.10	TPVC	269.93	268.50	31.50	51.50	51.5	--
312	MW-4A	975307.90	123586.40	TPVC	268.34	266.50	19.70	29.70	--	--
407	B95-12	975343.81	124724.70	TPVC	272.01	269.45	55.00	60.00	--	76
66	--	975354.00	124548.90	--	--	270.00	--	--	--	--
299	HM-1	975363.00	125252.30	TPVC	268.14	269.20	3.00	83.00	--	--
247	RW1	975397.40	127471.00	--	--	-2.00	59.00	340.00	--	--
340	SP-10	975407.80	126569.50	--	263.92	262.40	1.00	6.00	--	--
213	MW-5B	975408.30	123982.60	TPVC	269.61	267.60	50.40	60.40	--	61.35
313	MW-5A	975414.60	123981.80	TPVC	269.71	267.60	28.00	38.00	--	--
248	RW2	975425.10	127514.80	--	--	--	--	--	--	--
408	B95-13	975490.63	125002.00	TPVC	266.26	267.01	60.00	65.00	--	90.5
249	Cassarino	975491.40	127480.10	--	--	267.90	--	12.50	--	--
214	MW-6B	975521.20	124486.80	TPVC	268.95	267.10	56.80	66.80	--	69.4
348	MW-6A	975521.40	124481.80	TPVC	269.11	267.00	8.00	20.00	--	--

Appendix 4. Information on well construction (sorted by easting location) for selected wells in Milford, New Hampshire --Continued

Well number on plate 1	Well name	Easting	Northing	Description of measure-ment point	Altitude of		Depth to			
					Measure-ment point	Land surface	Top of screen or opening	Bottom of screen or opening	Refusal	Bedrock
189	MOA-35	975554.90	125804.90	--	--	265.20	--	--	12	--
153	MOW-38	975574.20	128320.70	--	--	262.70	30.00	40.00	41	--
377	3ftHitchPW1	975608.90	124010.10	--	--	--	--	--	--	--
376	2ftHitchPW1	975620.10	124005.90	--	--	--	--	--	--	--
203	MI-63	975636.80	125076.60	TSC	267.75	265.10	24.00	64.00	--	--
194	MOW-58	975647.00	125574.50	--	--	268.70	54.00	63.00	76	--
47	MI-33	975651.30	124011.30	WELLCVR	265.90	268.00	50.00	60.00	60	--
380	HitchWlHs	975651.60	124010.80	--	--	--	--	--	--	--
345	MW-16R	975670.80	124875.20	TSC	268.92	266.50	88.00	138.00	--	87.5
321	MW-16B	975671.00	124868.60	TPVC	269.85	267.60	39.60	49.60	--	--
233	MW-16A	975671.20	124863.10	SHELTER	270.39	267.50	16.90	26.90	--	--
344	MW-16C	975678.10	124877.10	TSC	269.70	267.40	73.20	83.20	--	87.5
86	FH-13OBS	975717.70	126524.20	TPVC	269.03	260.00	33.00	43.00	--	--
190	MOA-37	975737.60	126314.60	--	--	260.00	--	--	13	--
79	--	975782.30	119504.90	--	--	350.00	--	--	--	--
45	MI-31	975786.40	124591.90	TPVC	267.23	266.10	36.00	54.00	--	--
331	MW-23B	975802.80	125947.10	TPVC	267.40	265.30	48.00	58.00	--	--
381	MW23-SG1	975803.80	125915.30	SG1	257.74	--	--	--	--	--
382	MW23-SG2	975805.70	125912.70	SG2	257.74	--	--	--	--	--
95	FH85-8A	975813.90	126532.90	--	--	260.00	20.00	26.00	--	--
324	MW-18B	975824.10	124279.10	TPVC	270.30	268.00	72.00	82.00	--	82
231	MW-18A	975824.80	124273.40	TPVC	269.78	267.90	44.50	54.50	--	--
61	MI-47	975825.50	125094.20	--	--	270.00	--	--	--	--
48	MI-34	975833.60	122797.60	TPVC	278.84	278.80	--	17.70	--	--
237	MW-23A	975835.10	125944.30	TPVC	267.51	265.40	20.00	30.00	--	--
188	MOA-25	975839.70	125937.00	--	--	262.00	50.00	60.00	72	--
332	MW-23C	975840.80	125954.00	TPVC	267.34	265.30	84.30	94.30	--	106
87	FH-14	975867.00	126592.80	BOLT	263.53	262.20	32.00	42.00	--	--
44	MI-30	975877.30	124347.00	TPVC	269.35	265.70	27.00	72.00	75	--
59	MI-45	975909.30	125772.40	--	--	264.90	--	--	--	--
228	MW-3	975915.60	123237.10	TPVC	270.54	268.70	11.50	21.50	--	21.5
80	--	975917.30	119166.00	--	--	--	--	--	--	--
60	MI-46	975970.80	125598.00	--	--	267.30	--	--	--	--
208	FH-5 (pump)	975988.30	127199.90	TINRSC	267.89	268.00	50.00	65.00	--	--
301	FH-11	975989.90	127199.80	TSC	268.08	267.40	--	62.00	--	--
240	FH-10(OBS)	975991.40	127198.40	TSC	268.01	267.30	58.00	63.00	--	--
242	FH-9	975997.30	127233.10	TSC	269.83	268.30	--	52.00	--	--
84	#226inSurv	975999.60	127234.70	TSC	262.51	261.70	51.00	66.00	--	60
68	--	976054.90	124695.20	--	--	267.90	--	--	--	--
64	--	976086.60	124426.60	--	--	265.30	--	--	--	--
69	--	976146.70	124676.00	--	--	266.30	--	--	--	--
322	MW-17B	976212.00	124755.50	TPVC	263.34	264.60	52.40	62.40	--	--
323	MW-17C	976212.80	124757.90	TPVC	263.36	264.70	85.00	95.00	--	99.3

Appendix 4. Information on well construction (sorted by easting location) for selected wells in Milford, New Hampshire --Continued

Well number on plate 1	Well name	Easting	Northing	Description of measurement point	Altitude of		Depth to			
					Measurement point	Land surface	Top of screen or opening	Bottom of screen or opening	Refusal	Bedrock
218	MW-10C	976215.00	124930.60	TPVC	264.74	262.80	81.50	91.50	--	91.6
258	MW-17A	976216.50	124754.00	TPVC	263.29	264.40	19.80	29.80	--	--
317	MW-10B	976218.50	124928.40	TPVC	263.55	262.20	44.00	54.00	--	--
316	MW-10A	976221.50	124928.60	TPVC	263.77	262.20	19.00	29.00	--	--
26	MI-15	976242.80	123624.90	TSC	265.17	264.70	--	--	--	--
169	MI-9	976255.70	125936.00	TCONC	265.05	263.80	--	--	--	--
215	MW-7B	976263.30	123908.40	TPVC	264.29	262.50	45.60	55.60	--	58.6
314	MW-7A	976267.60	123912.60	TPVC	264.40	262.30	3.20	13.20	--	--
71	--	976275.60	124553.60	--	--	264.00	--	--	--	--
339	SP-9	976276.60	126593.00	--	261.16	259.40	1.50	6.50	--	--
70	--	976282.60	124669.80	--	--	264.10	--	--	--	--
364	--	976295.60	125521.00	--	264.93	262.50	--	--	--	--
250	SP-1	976415.40	128176.90	TPVC	259.17	257.40	2.00	7.00	--	--
318	MW-11A	976433.30	125888.70	TPVC	262.78	260.90	20.50	30.50	--	--
219	MW-11R	976435.00	125881.60	TSC	263.30	261.00	52.00	64.00	--	65
319	MW-11B	976435.20	125885.30	TPVC	262.83	261.00	52.30	64.30	--	65
351	MW-9A	976502.90	124485.80	TPVC	267.76	266.10	30.70	40.70	--	--
217	MW-9C	976503.30	124473.60	TPVC	268.09	266.30	79.00	90.00	--	94
352	MW-9B	976503.60	124479.10	TPVC	267.87	266.10	58.20	68.20	--	--
121	--	976507.90	117660.40	--	--	--	--	--	--	--
315	MW-8A	976511.80	124151.80	TPVC	263.91	262.00	4.50	16.50	--	--
216	MW-8B	976524.90	124151.40	TPVC	263.80	261.80	57.00	67.00	--	90
22	MI-8	976549.90	125251.50	TINRSC	264.93	262.60	--	--	--	--
196	MOW-65	976555.40	126488.70	--	--	260.00	54.00	62.00	73	--
62	MI-48	976556.30	124678.90	CONC	--	264.10	--	--	--	--
49	MI-35	976578.50	124150.80	PWMC	263.20	262.20	--	55.00	--	--
154	MOW-32	976679.80	124466.70	--	--	261.80	6.00	16.00	20	--
202	MOW-19	976722.50	125725.60	--	--	260.80	--	--	--	--
252	SP-6	976792.40	126621.20	TPVC	261.05	260.00	3.00	8.00	--	--
27	MI-16	976813.60	123543.90	--	--	269.10	--	--	--	--
195	MOW-64	976832.40	126380.50	--	--	260.00	41.00	49.00	76	--
111	--	976843.40	115878.60	--	--	--	--	--	--	--
369	FHwoods	976854.10	127069.30	TSC	266.46	266.10	--	--	--	--
85	FH-15	976951.60	126886.40	AHPUMP	265.72	265.10	18.00	38.00	--	--
9	MOW-33	976961.90	125149.30	--	--	260.00	60.00	70.00	--	56
65	P-03	976979.60	124880.40	TSC	263.27	261.30	--	--	--	--
117	--	977035.00	115723.00	--	--	--	--	--	--	--
262	MW-29	977125.30	124080.30	TPVC	260.90	261.00	2.50	12.50	--	--
88	FH-16	977174.80	126706.30	--	262.99	261.00	--	--	--	--
193	MOW-15	977255.80	127892.70	--	--	260.00	--	--	--	--
304	SP-5	977271.90	126837.80	--	257.07	255.30	2.50	7.50	--	--
326	MW-19A	977289.20	124123.20	TSC	264.30	261.60	23.50	33.50	--	--
327	MW-19B	977294.80	124124.80	TSC	263.88	260.90	39.00	49.00	30	35

Appendix 4. Information on well construction (sorted by easting location) for selected wells in Milford, New Hampshire --Continued

Well number on plate 1	Well name	Easting	Northing	Description of measurement point	Altitude of		Depth to			
					Measurement point	Land surface	Top of screen or opening	Bottom of screen or opening	Refusal	Bedrock
308	MW-13A	977298.80	125084.80	TSC	259.85	257.90	23.90	33.90	--	--
221	MW-13B	977300.60	125081.10	TPVC	259.35	257.90	48.00	58.00	--	64
172	MI-40	977391.30	124739.20	TPVC	257.40	256.10	--	--	--	--
72	MI-62	977408.80	125554.80	--	--	260.00	17.00	58.00	--	60.7
264	MW-20A	977472.90	124629.10	TPVC	263.23	260.80	15.20	25.20	--	--
328	MW-20B	977476.10	124622.30	TPVC	263.03	260.70	35.00	45.00	--	47.5
58	MI-44	977514.10	125199.40	TPVC	260.60	259.20	--	20.00	--	--
251	SP-7	977551.40	127255.90	TPVC	258.66	258.20	4.50	9.50	--	--
54	MI-41	977561.60	124774.20	TPVC	260.12	258.70	--	20.00	--	--
55	MI-42	977567.30	124958.10	TPVC	258.51	257.20	--	20.00	--	--
56	MI-43	977583.80	125123.00	TPVC	258.82	257.30	--	20.00	--	--
170	MI-14	977619.80	123760.40	--	--	260.00	--	--	--	--
29	MI-18	977625.40	123963.10	TCONC	264.34	262.70	--	--	--	--
255	MW-24A	977644.90	126373.30	TPVC	259.67	257.10	19.50	29.50	--	--
333	MW-24B	977649.70	126372.30	TPVC	259.39	256.80	31.00	41.00	--	40.5
201	MOW-26	977661.40	122551.60	--	--	260.00	--	--	14	--
200	MOW-25	977668.80	122997.30	--	--	259.70	--	--	4	--
267	SP-4	977995.70	127200.00	--	258.63	257.10	2.50	7.50	--	--
220	MW-12A	978133.30	124280.70	TPVC	265.96	264.00	25.00	35.00	--	--
320	MW-12B	978134.30	124287.40	TPVC	265.61	264.00	56.00	66.00	--	66
268	SP-3	978256.80	126568.90	--	256.30	255.30	4.50	9.50	--	--
337	WLR4	978297.60	125583.70	SHELTER	257.38	251.30	4.00	5.00	--	--
78	MOA-4	978318.20	124603.50	--	--	249.50	33.00	38.00	54	--
368	BMc821934	978403.90	123964.90	--	--	--	--	--	--	--
128	SavageWell	978473.20	124848.00	--	--	261.00	35.00	45.00	--	--
165	MI-4	978596.40	124892.50	TSC	257.49	255.00	39.00	49.00	--	--
270	P-9B	978624.00	126015.80	--	255.01	252.60	9.20	10.20	--	--
269	P-9A	978624.20	126009.90	--	254.73	253.10	7.00	8.00	--	--
21	MI-7	978642.40	125263.60	TSC	256.68	253.20	--	31.00	--	--
164	MI-3	978692.70	124915.00	TSC	257.28	254.50	44.00	49.00	--	--
349	MW-14A	978695.90	125654.90	TPVC	254.65	253.40	19.00	29.00	--	--
222	MW-14R	978696.00	125647.00	TSC	255.75	253.80	50.00	60.00	--	60
341	MW-14B	978696.60	125651.10	TPVC	255.13	253.30	50.00	60.00	--	60
353	FH-17	978711.30	127671.80	BOLT	272.44	--	--	--	--	--
167	MI-6	978717.10	124918.60	TSC	255.66	255.10	--	--	--	--
166	MI-5	978717.70	124920.50	TSC	255.89	255.20	39.00	49.00	--	--
305	FH-18	978724.80	126549.20	--	255.01	--	--	--	--	--
163	MI-2	978827.60	124764.70	TSC	253.94	252.90	42.00	47.00	--	--
168	MI-6A	978830.10	124812.80	--	--	259.50	--	--	--	--
273	HP-1	978832.70	125303.40	--	254.51	252.30	1.00	6.00	--	--
302	FH-19	978898.80	126408.40	TSC	256.17	--	--	--	--	--
375	nearFH19	978900.70	126413.00	--	--	--	--	--	--	--
96	FH1974	978905.30	126519.50	--	--	254.50	--	--	--	--

Appendix 4. Information on well construction (sorted by easting location) for selected wells in Milford, New Hampshire --Continued

Well number on plate 1	Well name	Easting	Northing	Description of measurement point	Altitude of		Depth to			
					Measurement point	Land surface	Top of screen or opening	Bottom of screen or opening	Refusal	Bedrock
94	FH-21	978928.60	126400.60	TPVC	251.63	252.10	21.00	26.00	--	--
90	FH-22	978953.00	126400.00	TPVC	255.10	253.10	24.00	29.00	--	--
271	P-15	978953.70	126170.90	TPVC	252.08	251.40	7.00	8.00	--	--
89	FH-27	978957.50	126176.80	TSC	253.41	251.30	36.00	41.00	--	--
379	FH27-SG2	978965.00	126143.60	SG2	245.48	--	--	--	--	--
362	USGS-DISK	978965.10	126138.80	--	250.02	--	--	--	--	--
378	FH27-SG1	978965.10	126137.30	SG1	245.48	--	--	--	--	--
334	MW-31	978979.10	126191.90	TSC	251.87	250.10	--	--	--	50.5
329	MW-21B	979001.20	124469.80	TPVC	261.77	259.30	20.00	30.00	--	--
278	MW-21A	979001.30	124463.60	TPVC	261.27	259.20	3.80	13.80	--	--
330	MW-21C	979001.50	124474.00	TPVC	261.34	259.40	44.10	54.10	--	63.75
93	FH-23	979002.60	126401.50	TPVC	253.70	252.00	22.00	25.00	--	--
74	MOW-35	979010.10	124641.80	--	--	260.00	--	--	59	--
91	FH-24	979035.90	126403.90	TPVC	253.27	251.60	24.00	29.00	--	--
306	MW-33	979070.90	126468.10	TPVC	253.89	251.80	41.50	51.50	--	52.5
274	HP-2	979099.70	125374.20	--	253.24	251.00	1.50	6.50	--	--
374	FH-26	979100.80	126405.40	TPVC	254.35	--	--	--	--	--
92	FH-25	979102.50	126406.50	TPVC	251.63	252.10	23.00	28.00	--	--
73	MI-64	979161.50	123887.20	--	--	259.90	--	--	--	--
275	HP-3	979343.90	125403.50	--	253.53	251.10	1.50	6.50	--	--
276	P-10	979466.80	125859.00	--	252.70	250.40	7.50	8.50	--	--
25	MI-12	979476.40	125858.70	TSC	253.26	251.50	43.00	49.00	50	--
24	MI-11	979580.10	125310.70	TSC	254.52	252.10	40.00	56.00	63	--
23	MI-10	979677.40	124853.90	TPVC	255.12	252.20	44.00	47.00	--	58.5
277	P-11	979689.20	126100.90	--	254.54	252.50	7.50	8.50	--	--
279	SPZ-2	979817.20	126368.50	TPVC	251.94	249.90	1.00	6.00	--	--
67	--	979957.10	124233.70	--	--	250.00	--	--	--	--
280	P-16	979986.60	126500.00	TPVC	260.43	258.30	12.00	13.00	--	--
281	MW-34	979987.00	126490.70	TPVC	260.91	258.50	9.50	19.50	--	20.5
14	RFW-1	980111.60	123484.10	--	--	255.70	8.00	28.00	28	--
283	P-17B	980124.10	126110.10	--	253.66	252.60	12.00	13.00	--	--
282	P-17A	980125.10	126109.10	--	252.54	250.60	8.00	9.00	--	--
17	RFW-4	980142.70	124069.50	--	252.15	251.60	6.00	16.00	16	--
18	PA-1	980332.10	123667.20	--	--	255.10	--	8.70	--	--
19	PA-2	980334.70	123737.30	--	--	254.90	--	8.70	--	--
361	P-12	980380.20	125709.40	--	252.03	252.00	9.00	10.00	--	--
20	PA-3	980388.40	123703.10	--	--	255.30	--	7.80	--	--
15	RFW-2	980419.40	123831.60	--	253.87	253.80	10.00	35.00	35	--
16	RFW-3	980457.30	124035.20	--	253.51	253.50	13.00	43.00	43	--
284	RW4	980479.80	126905.00	--	280.08	278.30	--	23.00	--	--
393	WLR-5	980644.90	126283.60	SHELTER	254.27	--	--	--	--	--
285	SPZ-1	980666.60	126449.90	TPVC	259.17	257.40	3.50	8.50	--	--
288	FH-28	981031.70	126543.60	TSC	248.85	248.10	--	23.00	--	--

Appendix 4. Information on well construction (sorted by easting location) for selected wells in Milford, New Hampshire --Continued

Well number on plate 1	Well name	Easting	Northing	Description of measurement point	Altitude of		Depth to			
					Measurement point	Land surface	Top of screen or opening	Bottom of screen or opening	Refusal	Bedrock
290	SP-18	981032.50	126481.60	--	250.17	248.20	4.50	7.50	--	--
289	FH-29	981063.30	126519.20	TSC	250.07	247.80	--	33.90	--	--
294	MW-22B	981098.70	126201.30	TPVC	252.77	250.10	33.50	43.50	--	47
293	MW-22A	981102.30	126204.00	TPVC	252.52	250.20	13.80	23.80	--	--
292	FH-30	981104.80	126341.00	TSC	250.69	248.30	--	23.00	--	--
287	RW9	981114.80	127599.20	--	271.45	270.40	--	22.00	--	--
360	--	981136.40	126667.90	TSC	251.03	247.10	--	34.50	--	--
359	FH-?	981138.80	126516.30	TSC	249.86	248.50	--	24.80	--	--
127	HAYWOOD	981163.80	124370.30	--	--	256.30	--	--	--	--
358	--	981191.10	126524.60	TSC	250.03	247.20	--	20.50	--	--
354	PFHprodWell	981195.60	126601.60	--	251.68	249.20	30.00	40.00	--	--
356	--	981217.30	126573.60	--	250.05	247.40	--	--	--	--
357	--	981218.60	126572.10	--	249.97	247.40	--	--	--	--
291	SP-11	981256.90	126375.40	--	249.67	247.70	8.50	9.50	--	--
173	H12-71	981352.50	124815.30	--	--	250.00	36.00	36.00	--	36
296	MW-32A	981366.60	125490.00	TPVC	250.46	247.90	7.00	17.00	--	--
297	MW-32B	981369.80	125487.10	TPVC	251.23	248.30	31.80	41.80	--	43.5
174	H11-71	981478.20	125561.40	--	--	241.60	25.00	35.00	--	39
175	H9-71	981665.10	126217.40	--	--	250.80	20.00	25.00	--	28.5
180	H5-71	981751.40	126415.00	--	--	250.50	23.00	28.00	--	31
295	P-13	981806.60	126346.10	--	250.84	248.30	7.50	8.50	--	--
179	H10-71	981819.40	126331.60	--	--	250.90	18.00	28.00	--	34
178	H7-71	981841.00	125953.90	--	--	246.90	15.00	15.00	--	15
338	P-14	981843.10	124952.70	--	248.69	246.70	7.00	8.00	--	--
176	H8-71	981881.90	126202.30	--	--	250.00	20.00	25.00	--	32
177	H6-71	981885.60	126032.00	--	--	249.50	16.00	16.00	--	16
342	MW-15B	982001.40	125914.50	TPVC	258.61	257.00	29.40	36.40	--	27.5
223	MW-15A	982006.40	125915.30	TPVC	258.53	256.80	12.50	27.50	--	--
83	--	982062.20	125393.90	--	--	240.90	--	--	--	--
82	--	982214.80	125347.60	--	--	240.00	--	--	--	23
107	--	982412.50	131350.50	--	--	349.20	--	--	--	--
109	--	982510.90	130710.20	--	--	349.30	--	--	--	--
123	GW-01S	982781.10	127851.50	--	--	256.10	6.00	16.00	--	--
124	GW-01D	982862.30	127876.40	--	--	256.50	60.00	70.00	--	56
197	MOW-66	982904.60	124297.20	--	--	252.80	27.00	33.00	37	--
125	GW-01M	982953.40	127904.30	--	--	256.70	30.00	40.00	--	--
198	MOW-67	983164.50	124318.20	--	--	249.80	37.00	43.00	45	--
10	GW-02D	983382.40	127459.90	--	--	255.40	19.00	29.00	--	34
155	GW-02S	983400.80	127487.90	--	--	255.10	6.00	16.00	--	--
199	MOW-68	983417.40	124322.20	--	--	245.00	36.00	42.00	53	--
12	GW-04D	983753.10	127211.90	--	--	255.60	21.50	31.50	--	19
157	GW-04S	983770.60	127239.50	--	--	255.60	5.40	15.40	--	--
192	--	984005.20	123305.50	--	--	266.70	--	--	--	12

Appendix 4. Information on well construction (sorted by easting location) for selected wells in Milford, New Hampshire --Continued

Well number on plate 1	Well name	Easting	Northing	Description of measurement point	Altitude of		Depth to			
					Measurement point	Land surface	Top of screen or opening	Bottom of screen or opening	Refusal	Bedrock
13	GW-05D	984174.30	127024.90	--	--	261.00	23.00	33.00	--	33
11	GW-03D	984183.60	126015.00	--	--	252.40	28.00	38.00	--	23.5
158	GW-05S	984189.90	127055.10	--	--	264.20	7.00	17.00	--	--
156	GW-03S	984191.20	126042.60	--	--	252.40	8.40	18.40	--	--
204	MI-13	984325.50	123765.20	--	251.42	249.60	12.00	18.00	33	--
6	LW-02D	984490.30	124835.40	--	245.66	243.10	45.00	55.00	--	62.5
150	LW-02S	984495.90	124860.80	--	245.91	243.40	4.00	14.00	--	--
5	LW-01D	984848.90	125391.90	--	--	264.80	100.00	110.00	--	114.3
148	LW-01M	984856.90	125418.50	--	--	265.10	42.60	52.60	--	--
149	LW-01S	984856.90	125419.50	--	--	265.20	25.60	35.60	--	--
7	LW-03D	984873.40	124642.50	--	251.14	247.30	44.50	54.50	--	80.2
151	LW-03S	984876.20	124673.40	--	250.44	250.00	9.00	19.00	--	--
8	LW-04D	985001.00	124601.20	--	246.43	243.40	40.00	50.00	--	80
152	LW-04S	985003.80	124625.30	--	246.46	244.80	5.00	15.00	--	--

APPENDIX 5: Ground-water-level hydrographs showing an example of the comparison between model-computed head and observed head from wells MW14B (well number 341) and MW10A (well number 316). (Location of wells is shown on plate 1)

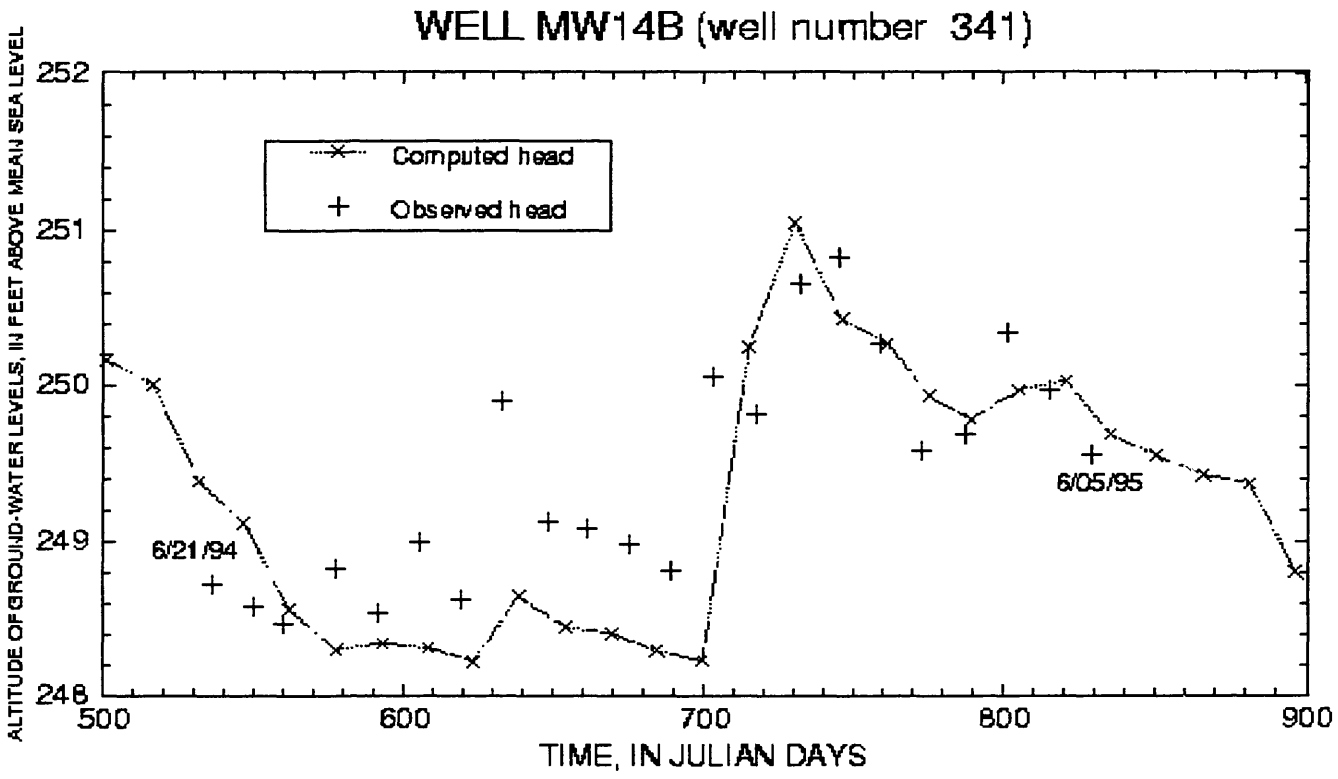
WELL MW14B (well number 341)
ALTITUDE OF GROUND-WATER LEVELS, IN FEET ABOVE MEAN SEA LEVEL
252
251
250
249
248
500
600
700
800
900
TIME, IN JULIAN DAYS
Computed head
Observed head
6/21/94
6/05/95

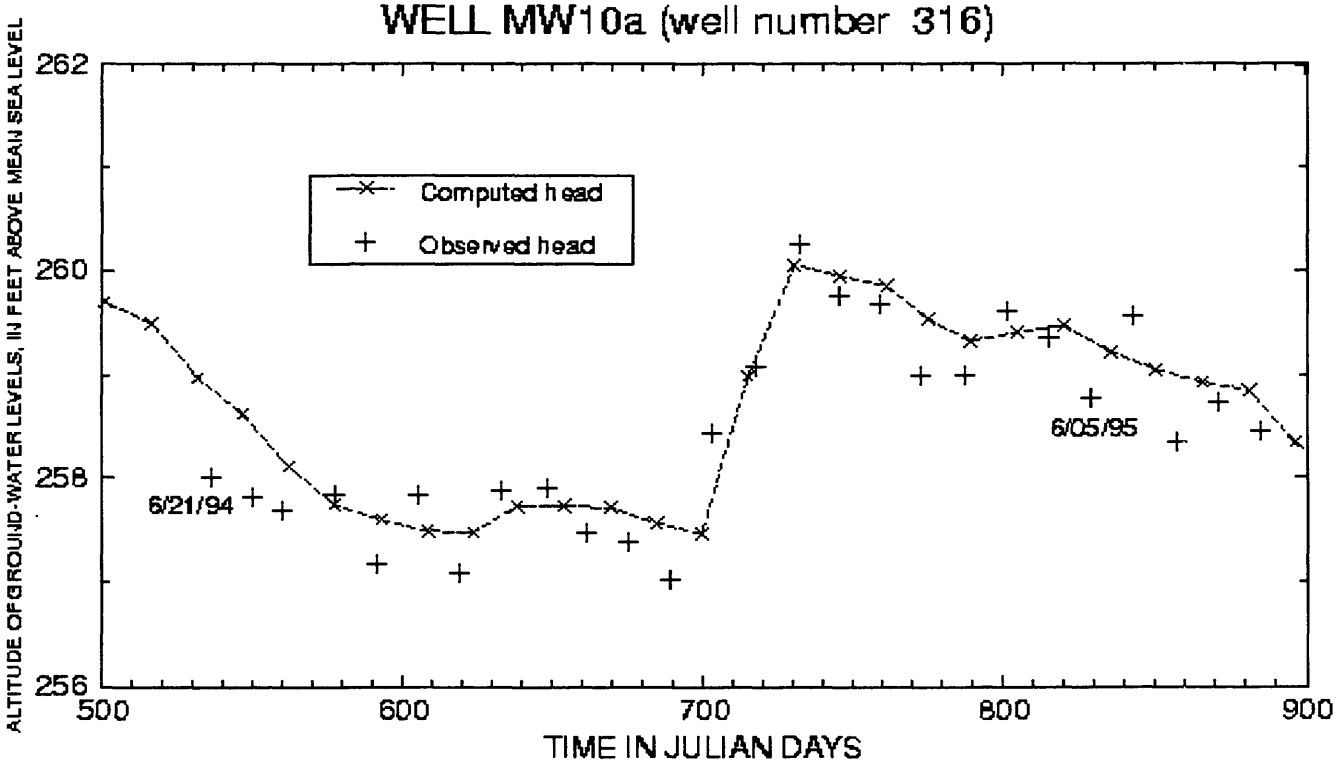
WELL MW10a (well number 316)
ALTITUDE OF GROUND-WATER LEVELS, IN FEET ABOVE MEAN SEA LEVEL
262
260
258
256
500
600
700
800
900
TIME IN JULIAN DAYS
Computed head
Observed head
6/21/94
6/05/95